Study of reversal behavior and chemotaxis in *Caenorhabditis elegans*

Nagesh Yadavrao Kadam

A thesis submitted for the partial fulfillment of
the degree of Doctor of Philosophy

Department of Biological Sciences
Indian Institute of Science Education and Research Mohali
Knowledge city, Sector 81, SAS Nagar, Manauli PO, Mohali 140306, Punjab, India.

August 2019

Declaration

The work presented in this thesis has been carried out by me under the guidance of Dr. Kavita Babu at the Indian Institute of Science Education and Research Mohali. This work has not been submitted in part or in full for a degree, a diploma, or a fellowship to any other university or institute. Whenever contributions of others are involved, every effort is made to indicate this clearly, with due acknowledgement of collaborative research and discussions. This thesis is a bona fide record of original work done by me and all sources listed within have been detailed in the bibliography.

Nagesh Yadavrao Kadam

In my capacity as the supervisor of the candidate's thesis work, I certify that the above statements by the candidate are true to the best of my knowledge.

Dr. Kavita Babu

Table of Contents

List of Figures

List of Tables

List of appendix Tables

Acknowledgements

The last six year has been the challenging and learning phase of my life. Many people met during this time and directly or indirectly influence my professional and personal life. Firstly, I would like to thanks to my supervisor Dr. Kavita Babu for providing me opportunity to work in her lab with full freedom. I am very thankful to her for supporting and guiding me through my doctoral studies. Her guidance helps me during all the time of research and writing this work. I thanks to her for helping me in preparing presentation, seminars and research article.

I express my immense gratitude to my doctoral committee members, Dr Sudip Mandal and Dr Samarjit Bhattacharyya for their timely review of my work, suggestions and showing continued interest in my different projects. Their scientific inputs and encouragements help me a lot to complete my work. I am immensely thankful to them for their time and continuous involvement with my work.

I would like to thanks to the Dr Thomas Pucadyil from IISER Pune for the great collaboration. It allows me to work on different topic and to learn the new techniques. I am also thankful to his lab members for continuously helping me out in the project.

I also thankful to the entire IISER family, administration, library, instrumentation, store and purchase section, canteen staff, mess staff, sports facility, gym facility and hostel caretakers for their continuous cooperation's and maintenance of the facility which helps in the smooth running of my Ph.D. and personal time

I am very lucky to have wonderful lab members; they help me a lot in my scientific and personal journey. I am very thankful for their valuable inputs and thoughtful discussion on my changing project. I am extremely thankful to have Dr. Yogesh Dahiya, who is always there to help me out. And all the help from critically discussing the project to designing the new project, he is always there to guide me. I would like to thanks to Dr Pratima Pandey for her continuous suggestions, discussion, support and love from the last six year and now towards the end. My sincere thanks to the Dr Pallavi Sharma, Dr Ashwani Bhardwaj, for being my wonderful seniors. All gossips and outing we had with Dr. kuldeep will be missed. I would like to thanks to Dr Shruti Thapliyal and Dr Vina Tikiyani for all their helps and leg pulling activities in

the lab. It was really nice to have you guys as my colleagues; in the last days of my Ph.D. missed you guys a lot. I am also thankful to my juniors Anuradha and Umer for helping me whenever I needed.

I would like to thank Sukanta Behra for his help in the work and all healthy and technical discussions. Also, I would like to thanks to Saurabh, Anupreet, Varun, Ambey, Shubham, Kuldeep, Sohit, Vedant, Sujata, Nandini, for their helps and cooperation whenever needed. I feel lucky to have great friend circle outside the lab. I am very thankful to Bhupinder, Bhisham, Anup, Mayank, Devshish, Simran, Harleen, Amol, Vijay, Vishal, Shakti, Datta and Kiran being there for always help.

Words are never enough to describe the gratitude I feel towards my family. As always, I fell short of words to describe what I fell for them. They have been my strong pillar of support understanding and encouraging during all my trails in life. All my achievements in life till date have been and always are because of their prayers, love, support, encouragements, sacrifices and the values instilled in me.

Thanks to my BABA for his unconditional support both financially and emotionally. Thanks to my parents for their advice, support and encouragements. You voluntarily missed out on so many opportunities just to allow me, to get the best education and future possible. You mean more to me than I could possible express in words. Thanks for everything!

I am very thankful to my brother, sister, and sister in law for their endless encouragement and love throughout my journey. Above all I am grateful to the almighty God, whose grace and blessings permeate each and every aspects of my life.

List of Publications

1. Deo, R., Kushwah, M.S., Kamerkar, S.C., **Kadam, N.Y.,** Dar, S., Babu, K., Srivastava, A., and Pucadyil, T.J. (2018). ATP-dependent membrane remodeling links EHD1 functions to endocytic recycling. Nat Commun *9*, 5187.

2. **Kadam N.Y**., Behara Sukant, and Kavita Babu. Role of the SRX-97 GPCR in modulating *C. elegans* behavior. (**Manuscript is under preparation)**

ABBREVITATIONS

Weights and measures	
%	Percent
µmol, nmoles, mmoles	Micromol, nanomol, millimoles
°C	Degree centigrade
bp, kb, mb	Base pair, kilobase, Megabase
O.D.	Optical density
Psi	Pounds per square inch
Rpm	Revolutions per minute
RT	Room temperature
Sec, min, h	Second, minute, hour
µg, mg, g	Microgram, milligram, gram
µl, ml, L	Microliter, milliliter, liter
µM, mM ,M	Micromolar, millimolar, molar
mV, V	Millivolt, Volt
Symbols	
~	Approximately
=	Equal to
α	Alpha
β	Beta
γ	Gamma
Δ	Delta
Techniques	
PCR	Polymerase Chain Reaction
RNAi	RNA Interference
qPCR	Quantitative PCR
Chemicals	
Amp	Ampicillin
ATP	Adenosine Triphosphate
BSA	Bovine Serum Albumin
dNTPs	2'-deoxyadenosine 5'-triphosphate
DTT	Dithiothreitol; Cleland's reagent
EDTA	Ethylenediamine-tetra-acetic acid
SDS	Sodium Dodecyl Sulphate
Tris	[Tris(hydroxymethyl)amino methane]
DA	Diacetyl
BDM	2, 3-butanedione monoxamine
Bz	Benzaldehyde
Miscellaneous	
aa	amino acids
ACh	Acetylcholine

AMPA	α-amino-3-hydroxy-5-methyl-4-isoxazolepropionic acid
CGC	*C. elegans* Genetics Centre
CIP	Calf Intestinal Phosphatase
CRISPR	Clustered Regularly Interspaced Short Palindromic Repeat
C-terminal	Carboxy- terminal
DNA	Deoxyribonucleic acid
FP	Forward primer
GFP	Green Fluorescent Protein
GPCR	G-protein-coupled receptor
LB	Lysogeny Broth
NGM	Nematode Growth Medium
NMDA	N-methyl-D-aspartate
EE	Early endosomes
REs	Recycling endosomes
LE	Late endosomes
NMJ	Neuro-Muscular Junction
LS	lysosome
PS	Phosphatidyl choline
N-terminal	Amino- terminal
ORF	Open Reading Frame
RNA	Ribonucleic acid
ROI	Region of interest
RP	Reverse primer
SEM	Standard error mean
SNB	Synaptobrevin
SP	Signal Peptide
SV	Synaptic vesicle
TBS	Tris-Buffered Saline
TE	Tris chloride and EDTA
TMD	Transmembrane domain
TRP	Transient Receptor Potential
VNC	Ventral Nerve Cord
WT	Wild-type

Abstract

The free living nematode *C. elegans* is an important yet simple animal to study various behaviours and their underlying neuronal circuits. Having just 302 neurons and a transparent body allows researchers to study and trace new molecules and pathways in the nervous system

In First half, I will talk about how the level of AMPA type glutamate receptor (GLR-1) on neuronal cells is regulated through the endocytic pathways. In case of endocytic pathways different organelles are involved in trafficking; one such organelle is the endocytic recycling compartment (ERC) which plays important role in recycling of trafficked cargos. AMPA/GLR-1 receptors are also maintained through the ERC pathways, any defect in the pathway leads to decrease in the active receptors on the membrane. In case of *C. elegans,* decrease in active amounts of AMPA/GLR-1 receptors on neuronal membranes results in behavioural consequences such as altered reversals. Further, the mechanism of such molecules that are involved in recycling of these cargos in the ERC will be discussed.

In second part, I will talk about newly identified G-protein Coupled receptor (GPCR) and its role in chemosensory neurons of *C. elegans*. Chemosensation is the only way to navigate the surrounding for a blind animal like *C. elegans*. Through chemosensation *C. elegans* searches for food, mates and successfully escapes danger. Majority of the chemosensory neurons are present in the head and a few are found in the tail. These chemosensory neurons express numerous GPCRs which act as receptors for the surrounding cues and activate downstream signalling pathways that help the animal to modulate behaviours. Some GPCR enable *C. elegans* to sense lower and higher concentrations of chemicals. We have found an as yet undescribed GPCR which specifically senses higher concentrations of chemical and the loss of which results in aberrant animal behaviour.

Synopsis

General Introduction

Caenorhabditis elegans is widely used to study development and various other functional aspects of the nervous system. Completely mapped neural network with just 302 neurons, transparent body and ease of genetic manipulation makes *C. elegans* an ideal model to study neuronal circuits. *C. elegans* exhibits various simplistic behaviors in response to external stimuli. These simplistic behaviors can be studied in conjunction with the well-mapped neurons to investigate various aspects of the nervous system. In *C. elegans,* locomotion one of the main behavior, includes forward movement punctuated with abrupt short reverse movements called reversals. Diverse receptors expressed in the interneurons play an important role in regulating the locomotory behavior of *C. elegans.* Endocytosis and recycling of these receptors through cellular trafficking pathways plays an important role in regulation of reversal behavior. Locomotion strategy of the worm is dictated by its surrounding environment. Worms sense various chemical cues in their immediate environment through a specific set of receptor molecules e.g. GPCRs expressed in the sensory neurons. Thus, these different sets of receptors expressed in both interneuron and chemosensory neurons of *C. elegans* modulate their locomotory behavior.

In this thesis we aimed at understanding the mechanism of trafficking pathways which controls the reversal behavior in *C. elegans.* We also investigated the function of a GPCR in regulating the chemosensory behavior of the worm. These undertakings have been described in this thesis in two parts:

- To explore the mechanism and endocytic role of EHD1/RME-1, an EH domain containing protein, in intestine and interneurons of *C. elegans*
- To explore the role of SRX-97, a G-protein coupled receptor, in chemosensory neurons of *C. elegans*

To explore the mechanism and endocytic role of EHD1/RME-1, an EH domain containing protein in intestine and interneurons of *C. elegans*

Introduction:

Multiple endocytic and recycling pathways generate vesicles from various membrane surfaces for sorting different types of cargo to their destined locations. These pathways play an important role in various cellular physiological processes. Macromolecules like several receptors in the cell membrane are pinched off as vesicles by a process called endocytosis. During endocytosis, Dynamin, a well-known GTPase, plays an important role in pinching off vesicles budding from the plasma membrane. Depending upon the nature of cargo, the endocytosed vesicles are either destined for degradation or recycling by various dedicated sub-cellular compartments. The recycling of cargo vesicles is managed by a dynamic organelle containing endocytosed network of membrane tubules and vesicles known as Endocytic Recycling Compartment (ERC) (Grant and Donaldson, 2009). Similar to endocytosis, vesicles are pinched off from ERC membrane and carried to cell membrane for fusion. An EH domain containing molecule has been proposed to generate recycled vesicles from the ERC membrane.

The C-terminal Eps15 Homology Domain (EHD)–family proteins are membrane-binding ATPases with structural similarity to dynamin. Screening of mutants defective in Receptor Mediated Endocytosis (RME) led to identification of an EHD domain containing protein called RME-1 in *C. elegans* (Grant et al., 2001). The human and mouse genomes encode for four Eps15-homology domain-containing proteins (EHD1-4), of which EHD1 shows 67% percent identity with *C. elegans* RME-1 (Ying et al., 2007). A study showed that mutation in *rme-1* results in defective vesicle recycling leading to formation of enlarged vacuoles in the intestinal cells of *C. elegans* (Grant et al., 2001). Cross-species complementation of EHD1 rescued the vacuolated intestinal phenotype of *rme-1* mutants, suggesting the functional similarity between RME-1 and EHD1 (Ying et al., 2007). The EH domain plays an important role in interaction of EHD1 with NPF motif containing proteins involved in recycling of cargo from endosomes to the plasma membrane (Braun et al., 2005; Pant et al., 2009). A previous report showed that depletion of EHD1 leads to enlargement of ERC while addition of purified EHD1 restores its normal

tubular morphology (Giridharan et al., 2013). Thus, EHD1 was proposed to be involved in membrane fission at ERC, although the underlying mechanism is not yet fully understood. Here we used an *in vivo* complementation assay in *C. elegans* to show that EHD1/RME-1 works in an ATP hydrolysis dependent manner to cut and form the vesicles from the endocytic recycling compartment.

Similar to EHD1, RME-1 has been shown to function at the ERC in receptor or cargo recycling events in *C. elegans* (Fares and Grant, 2002). Mutation in *rme-1* was found to cause a delayed recycling of several important receptors like MHC, transferrin and β1 integrin *etc* in mammalian cells (Grant and Caplan, 2008). Importantly, in another study, mutation in Rme1 (mouse ortholog of *rme-1*), was shown to cause sluggish recycling of AMPA-type GluR1 receptors in the hippocampal neurons (Park et al, 2004). On similar lines, RME-1 has been shown to play an important role in recycling of several other important molecules in neurons (Bhattacharyya et al., 2016; Koles et al., 2015; Lasiecka et al., 2010). Here we investigated the role of RME-1 in endocytosis of an AMPA-type glutamate receptor (GLR-1) in *C. elegans*. We show that *rme-1* mutants exhibit impaired recycling of GLR-1 receptors resulting in defective reversal behavior of *C. elegans.*

Results and Discussion

To understand the mechanism of EHD1 in membrane fission at ERC, we cloned the WT EHD1 under the VHA-6 promoter which is expressed specifically in the intestine of *C. elegans*. We exploited the vacuolated intestinal phenotype of *rme-1* mutants to investigate the role of different domains of EHD1 in the ERC trafficking pathway. In this direction, we first verified that EHD1 rescues the vacuolated intestinal phenotype as shown previously (Ying et al., 2007). We found that EHD1 carrying T72A mutation in the ATP binding domain failed to rescue the vacuolated phenotype suggesting that both ATP binding and hydrolysis are important for the functioning of EHD1. Further, EHD1 mutant either lacking 2-8 amino acid residues of N-domain or carrying a F322A mutation in second helical domain of EHD1 could not rescue the vacuolated intestine phenotype signifying the role of the EHD1 N-domain and second helical domain in binding to the membrane (Possibly allowing for enhanced ATPase activity required for membrane fission). Along with the *in vitro* assays performed by Dr. Pucadyil's laboratory, we propose that two

scaffolds of EHD1 bind the membrane adjacently and using its ATP hydrolyzing activity expand the intervening tube ultimately leading to scission of the membrane between the scaffolds (Deo et al., 2018).

To investigate the role RME-1 in endocytic recycling of receptors in *C. elegans*, we first investigated the expression of mCherry under the control of *rme-1* promoter. As shown previously, P*rme-1::mCherry* was found to be expressed ubiquitously in *C. elegans* (Grant et al., 2001). However, RME-1 has been shown to have a punctate localization in the ventral nerve cord of *C. elegans* (Glodowski et al., 2007). As mentioned previously, Rme-1 (mouse ortholog of RME-1) regulates recycling of AMPA-type receptors in the hippocampal neurons (Park, 2004). Moreover, GLR-1, an AMPA-type glutamate receptor known to be highly expressed in the interneurons of the ventral nerve cord, have been reported to regulate the reversal behavior of *C. elegans* (Glodowski et al., 2007; Rongo et al., 1998). We found that the mutation of *rme-1* significantly reduces the reversal frequency of the worm. Further, expression of *rme-1* under its native (P*rme-1*) or glutamate neuron specific promoter (P*glr-1*) restored the reversal behavior. Thus, we show that RME-1 is possibly involved in controlling the reversal behavior of *C. elegans*.

We used P*glr-1*::GLR-1::GFP transgenic line to verify whether RME-1 is involved in recycling of GLR-1 receptor (Glodowski et al., 2007; Juo et al., 2007; Rongo et al., 1998). We found that the size of GLR-1::GFP puncta in the posterior ventral nerve cord were larger in *rme-1* mutants in comparison to wild type. Further, we checked the functionality of the increased punctal size by using a pHluorin transgenic line (P*glr-1::*GLR-1::mCherry::SEP) (Hoerndli et al., 2013). The decreased ratio of pHluorin/mCherry indicated a significant reduction in the number of functional GLR1 receptors on the plasma membrane. Collectively, these data suggest that RME-1 modulates the reversal behavior of *C. elegans* by regulating the endocytic recycling of AMPA-type GLR-1 receptors (Park, 2004).

To explore the role of SRX-97, a G-protein coupled receptor in chemosensory neurons of *C. elegans*

Introduction:

In *C. elegans*, the well-developed chemosensory system allows the worms to sense a wide range of chemicals through olfaction and gustation. *C. elegans* can relate these cues with food, availability of mates and potent threat in the surroundings (Bargmann, 2006). These chemical cues are mainly sensed by the amphid chemosensory neurons in the head and the phasmid chemosensory neurons in the tail region of the worm. The amphid organ contains 11 pairs of chemosensory neurons. Each pair of chemosensory neuron expresses a subset of GPCRs that detects numerous chemical cues including pheromones and various other attractive and putrid molecules (Bargmann, 2006).Chemosensory GPCRs are classified into nine different classes on the basis of their sequence homology with the Rhodopsin class of GPCRs (Vidal et al., 2018). *C. elegans* harbors 1341 genes encoding functional GPCRs and among these the expression pattern of only 320 genes is known at a single cell resolution (Vidal et al., 2018). Here we investigate the role of a previously unknown GPCR, SRX-97 in chemosensation. The SRX-97 is a member of the Serpentine Receptor (SRX) family belonging to the SRG super family of chemosensory GPCRs. The role and ligand of most GPCRs are still unknown (Robertson, 2006). Our results suggest that SRX-97 is expressed in the ASH neurons and possibly involved in sensing benzaldehyde.

Results and Discussion:

To determine the expression pattern of SRX-97, a 2 kb upstream region including a few bases of first exon from *srx-97* was amplified and used to generate a mCherry reporter line (P*srx-97::mCherry*). In the transgenic animals, mCherry was found to be expressed specifically in a single pair of head amphid and single pair of tail phasmid neurons. We crossed the P*srx-97::mCherry* transgenic lines with the known reporter lines, to confirm that SRX-97 shows expression in the head ASH and tail PHB chemosensory neurons. Lack of expressions in any other parts of the body; suggest that SRX-97 may be involved in chemosensation

The ASH, a polymodal neuron, is involved in avoidance behavior of *C. elegans* towards noxious stimuli like high osmolarity, heavy metals, detergents and volatile organic compounds (Aoki et al., 2011; Bargmann, 2006; Nuttley et al., 2001). To understand the function of SRX-97 in

chemosensation, we made the deletion mutant of *srx-97* using the CRISPR/Cas9 system (Dickinson et al., 2015, 2013; Dickinson and Goldstein, 2016).We tested chemotaxis behavior of *srx-97* mutants towards a variety of noxious and volatile compounds. Of all these tested chemicals, we found that *srx-97* mutants show attraction towards the higher concentration of benzaldehyde. Suggesting that SRX-97 expressed in ASH neurons is responsible for sensing higher concentrations of benzaldehyde.

References:

Aoki R, Yagami T, Sasakura H, Ogura K -i., Kajihara Y, Ibi M, Miyamae T, Nakamura F, Asakura T, Kanai Y, Misu Y, Iino Y, Ezcurra M, Schafer WR, Mori I, Goshima Y (2011) A Seven-Transmembrane Receptor That Mediates Avoidance Response to Dihydrocaffeic Acid, a Water-Soluble Repellent in *Caenorhabditis elegans*. Journal of Neuroscience 31:16603–16610.

Bargmann C (2006) Chemosensation in *C. elegans*. WormBook.

Bhattacharyya S, Rainey MA, Arya P, Dutta S, George M, Storck MD, McComb RD, Muirhead D, Todd GL, Gould K, Datta K, Waes JG, Band V, Band H (2016) Endocytic recycling protein EHD1 regulates primary cilia morphogenesis and SHH signaling during neural tube development. Scientific Reports 6.

Braun A, Pinyol R, Dahlhaus R, Koch D, Fonarev P, Grant BD, Kessels MM, Qualmann B (2005) EHD proteins associate with syndapin I and II and such interactions play a crucial role in endosomal recycling. Molecular biology of the cell 16:3642–3658.

Deo R, Kushwah MS, Kamerkar SC, Kadam NY, Dar S, Babu K, Srivastava A, Pucadyil TJ (2018) ATP-dependent membrane remodeling links EHD1 functions to endocytic recycling. Nat Commun 9:5187.

Dickinson DJ, Goldstein B (2016) CRISPR-Based Methods for *Caenorhabditis elegans* Genome Engineering. Genetics 202:885–901.

Dickinson DJ, Pani AM, Heppert JK, Higgins CD, Goldstein B (2015) Streamlined Genome Engineering with a Self-Excising Drug Selection Cassette. Genetics 200:1035–1049.

Dickinson DJ, Ward JD, Reiner DJ, Goldstein B (2013) Engineering the *Caenorhabditis elegans* genome using Cas9-triggered homologous recombination. Nature Methods 10:1028–1034.

Fares H, Grant B (2002) Deciphering endocytosis in *Caenorhabditis elegans*. Traffic 3:11–19.

Giridharan SSP, Cai B, Vitale N, Naslavsky N, Caplan S (2013) Cooperation of MICAL-L1, syndapin2, and phosphatidic acid in tubular recycling endosome biogenesis. Mol Biol Cell 24:1776–1790.

Glodowski DR, Chen CC-H, Schaefer H, Grant BD, Rongo C (2007) RAB-10 regulates glutamate receptor recycling in a cholesterol-dependent endocytosis pathway. Molecular biology of the cell 18:4387–4396.

Grant B, Zhang Y, Paupard M-C, Lin SX, Hall DH, Hirsh D (2001) Evidence that RME-1, a conserved *C. elegans* EH-domain protein, functions in endocytic recycling. Nature cell biology 3:573–579.

Grant BD, Caplan S (2008) Mechanisms of EHD/RME-1 protein function in endocytic transport. Traffic 9:2043–2052.

Grant BD, Donaldson JG (2009) Pathways and mechanisms of endocytic recycling. Nature Reviews Molecular Cell Biology 10:597–608.

Hoerndli FJ, Maxfield DA, Brockie PJ, Mellem JE, Jensen E, Wang R, Madsen DM, Maricq AV (2013) Kinesin-1 regulates synaptic strength by mediating the delivery, removal, and redistribution of ampa receptors. Neuron 80:1421–1437.

Juo P, Harbaugh T, Garriga G, Kaplan JM (2007) CDK-5 regulates the abundance of GLR-1 glutamate receptors in the ventral cord of *Caenorhabditis elegans*. Molecular biology of the cell 18:3883–3893.

Koles K, Messelaar EM, Feiger Z, Crystal JY, Frank CA, Rodal AA (2015) The EHD protein Past1 controls postsynaptic membrane elaboration and synaptic function. Molecular biology of the cell 26:3275–3288.

Lasiecka ZM, Yap CC, Caplan S, Winckler B (2010) Neuronal Early Endosomes Require EHD1 for L1/NgCAM Trafficking. Journal of Neuroscience 30:16485–16497.

Nuttley WM, Harbinder S, van der Kooy D (2001) Regulation of Distinct Attractive and Aversive Mechanisms Mediating Benzaldehyde Chemotaxis in *Caenorhabditis elegans*. Learn Mem 8:170–181.

Pant S, Sharma M, Patel K, Caplan S, Carr CM, Grant BD (2009) AMPH-1/Amphiphysin/Bin1 functions with RME-1/Ehd1 in endocytic recycling. Nature Cell Biology 11:1399–1410.

Park M (2004) Recycling Endosomes Supply AMPA Receptors for LTP. Science 305:1972–1975.

Robertson H (2006) The putative chemoreceptor families of *C. elegans*. WormBook.

Rongo C, Whitfield CW, Rodal A, Kim SK, Kaplan JM (1998) LIN-10 is a shared component of the polarized protein localization pathways in neurons and epithelia. Cell 94:751–759.

Vidal B, Aghayeva U, Sun H, Wang C, Glenwinkel L, Bayer EA, Hobert O (2018) An atlas of *Caenorhabditis elegans* chemoreceptor expression. PLOS Biology 16:e2004218.

Ying G, Rainey MA, Solomon A, Parikh PT, Gao Q, Band V, Band H (2007) Shared as well as distinct roles of EHD proteins revealed by biochemical and functional comparisons in mammalian cells and *C. elegans*. BMC cell biology 8:3.

Chapter 1

Review of Literature

1.1 Part 1 General Introduction

Caenorhabditis elegans is a microscopic nematode, which flourishes in moist soil environments. It is a transparent organism that is around 1 mm in length. A single brood consists of around 350 *C. elegans*, with most of the worms being hermaphrodites and less than 1% being males. Males can be differentiated by hook-like appendages in the tail region as well as a smaller body size when compared to hermaphrodite animals. In 1963 Sydney Brenner introduced this organism in the field of developmental biology and neurobiology (Brenner, 1974). After that, *C. elegans* have been used as a model system to study the different aspects of developmental biology, cell biology, neurobiology, and aging studies.

Owing to the simple nervous system, consisting of just 302 neurons with 52 glial and supporting cells, *C. elegans* has proved to be an excellent model system for neurobiological studies. Furthermore, the neurons are entirely mapped out, and their neural network (Connectome) is well-defined (Emmons, 2015; White et al., 1986). The other attractive feature of this tiny worm includes (i) A transparent body, which allows the researchers to trace the localization of fluorescent-tagged proteins, to do optogenetic studies and also to track down the neuronal activity in live worms through calcium imagining (ii) the self-fertilization of hermaphrodites, which mostly used in the high throughput genetic studies, and the existence of males is used to quickly transfer the mutations which allow making multiple genetic manipulations (iii) It is the first multicellular organism, whose whole genome sequence and well defined neural network (Connectome) is available (Bargmann, 1998; White et al., 1986) (iv) Finally, *C. elegans* is easy to handle and can be stored by freezing in liquid nitrogen for decades.

The studies of neurobiology in *C. elegans* start with the study of locomotion, which is a robust and multidimensional behavior, which is thoroughly studied to understand the functioning of the nervous system. Here, we will discuss the endocytic pathways that regulate the trafficking of receptors on the plasma membrane and the role of a chemotaxis receptor, which is involved in detecting the surrounding cues and allows for changes in the behavior of *C. elegans*.

1.2 Part II. To explore the mechanism and endocytic role of EHD1/RME-1, an EH domain-containing protein in intestine and interneurons of *C. elegans*

1.2.1 Endocytosis

Endocytosis is a cellular process where membrane proteins or particles and macromolecules from the surrounding medium are taken into the cell. During endocytosis, the material which gets internalized is surrounded by a plasma membrane, which further buds from the membrane-forming vesicles.

The term endocytosis was coined by Christian de Duve in 1963. It was also used for the ingestion of large molecules like bacteria called phagocytosis (cell eating), which occurs using specialized cells like neutrophils and macrophages and drinking of fluid or macromolecules through vesicles called pinocytosis (cell drinking). The pinocytosis process occurs regularly in eukaryotic cells and is widely studied (Doherty and McMahon, 2009). Here we will talk about the different modes of the pinocytosis process.

Endocytosis plays an essential role in maintaining the normal physiology of a cell, which includes maintenance of receptor numbers at the membrane, plasma membrane composition, and cell size and shape. Through the help of various proteins complexes involved in the transport and sorting of different vesicles at different endocytic organelles, these endocytic organelles play an important role in the degradation or recycling of different endocytosed cargoes.
Endocytosis pathways are primarily classified into Clathrin-dependent and clathrin-independent, which are discussed below.

1.2.2 Clathrin-dependent and Clathrin-independent endocytosis

Clathrin-dependent endocytosis (CDE) is a well-characterized mechanism for mediating the internalization of cargo such as membrane receptors, viruses, and toxins in cells. In this process, the endocytic vesicles carrying the cargo coated with a lattice consisting of polymerized clathrin, which further distorts the membrane into a bud. The clathrin assembles into triskelia composed of three clathrin heavy chains (CHCs) and three clathrin light chains (CLCs), whose three-dimensional arrangement forms the clathrin coat. The formation of clathrin-coated pits initiates

with the recruitment of adaptors and accessory proteins that interact with short peptide motifs in cargo proteins and membrane lipids and subsequently recruit clathrin from the cytoplasm to the initiation site at the plasma membrane. There are different types of adaptors present near the plasma membrane (AP-1, AP-2, AP-3, AP-4, and AP-5). AP-2 is the main adaptor protein present at the plasma membrane and plays a vital role in the formation of clathrin-coated vesicles during endocytosis (Traub, 2009). As AP-2 or other adaptor proteins recognize cargo, clathrin triskelia recruited from the cytosol, and the clathrin coat starts to assemble. So, the Clathrin-mediated endocytosis is often mentioned as "receptor-mediated endocytosis" because it is started by membrane receptors that bind and recruit adaptor complexes (AP-2 in particular) and clathrin. After cargo selection and clathrin coat assembly, dynamin-dependent membrane scission occurs at the neck of the nascent vesicle to release the vesicle into the cytoplasm. Dynamin is a large GTPase that assembles into multimeric helical groups, wrapping the necks of clathrin-coated pits, and its GTP hydrolysis is necessary for membrane fission, releasing the Clathrin-coated vesicles into the cell interior (Kaksonen and Roux, 2018). After detachment from the plasma membrane, the clathrin-coated vesicle loses its coat and fuses with early endosomes (Doherty and McMahon, 2009).

In comparison to the clathrin-dependent pathway, Clathrin independent endocytosis (CIE) is comparatively less understood. The CIE pathways utilize lateral heterogeneity of lipids and proteins in the plasma membrane composition to choose cargo into dynamic membrane microdomains that bud into the cell. Based on this, CIE pathways are classified into the caveolae-dependent endocytosis, Flotillin-dependent endocytosis, CLIC/GEEC pathway, and Arf6 associated pathways (Doherty and McMahon, 2009; Sandvig et al., 2018). Likewise, CDE, vesicles released from the CIE fuse to the early endosomes and further transported to the different compartments of the endosomal system (Doherty and McMahon, 2009).

1.2.3 Endomembranes in endocytic pathways

The endocytosed vesicles once they bud from the plasma membrane then travel through different irregularly closed membrane systems called the endosomal compartment. The endosomal system categorized as early endosomes, recycling endosomes, and late endosomes (Mellman, 1996). The classification based upon the time taken for the cargo internalization, morphology, and the different RAB proteins, which act as molecular markers of the endosomes.

The endocytosed vesicles first fuse with the early endosomes (EEs) composed of a dynamic network of tubules and vesicles that are present near the peripheral cytoplasm. The ATP driven proton pump generates a slightly acidic pH (pH~6-6.8) environment in EEs due to which there is a dissociation of many receptor-ligand complexes (Jovic et al., 2010). The free receptors accumulate in a tubular extension, which buds off to make recycling vesicles and further directly or indirectly through recycling endosomes travel back to the plasma membrane. The ligands travel to the vesicular structure of EEs, then the transport vesicles pinch off and will go and fuse with the late endosome, which further transported into lysosome (pH~5) (Van Dyke, 1996). The late endosome and lysosomes with the help of different lysosomal enzymes and acidic pH are accountable for the accumulation and degradation of molecules from extrinsic or intrinsic pathways. The molecular markers which are present on EEs are Rab4 and Rab5, and the late endosomes express Rab7, Rab9 and mannose-6 phosphate receptor (Zerial and McBride, 2001).

The recycling endosomes play an important role in the reuptake of membrane constituents from the cytoplasm towards the membrane. Their role in receptors recycling and mechanism of RV generation are the topics studied in this thesis.

1.2.4 Recycling endosomes

The recycling endosomes (REs) are composed of heterogeneous tubulovesicular membranes that represent the dynamic and intense trafficking activity of membranes for conducting transport of internalized membrane constituents (Goldenring, 2015; IJzendoorn, 2006). The REs have slightly more acidic pH (pH~6.4), and the small GTPase Rab11 is a prominent marker (IJzendoorn, 2006). Apart from maintaining the plasma membrane composition and receptor numbers, REs plays a vital role in maintaining polarity in polar cells like epithelial and neuronal cells **(Figure. 1)**.

The *C. elegans* intestine is widely used to study different mechanistic aspects of REs. The epithelial cells form a ring beneath the cuticle of worms, forming a simple polarized epithelial tube called the intestine. The intestine has two plasma membrane domains; apical and basolateral. These two domains are separated by the apical junction, which prevents the lateral diffusion of lipids and proteins among the apical and basolateral membranes. The apical domain

forms the intestinal lumen, and the basolateral domain opens into the body cavity (pseudocoelom). So, anything ingested and produced by the intestine will go to other cells through the basolateral membrane. If markers or dyes like fluid-phase endocytic marker Texas Red-BSA (bovine serum albumin) injected into the body cavity, it would accumulate and mark the basolateral endosomal compartment (Sato et al., 2014).

Several proteins are reported to function in the basolateral trafficking process in the intestine (**Figure 1.1**). The RAB-10 is one of the crucial regulators of basolateral endocytosis, a mutation in *rab-10* causes vacuoles in the intestine of the worms and these vacuoles can be visualized under a microscope using the basolateral dye or marker. Likewise, the RME-1 (Receptor-mediated endocytosis) initially found in a basolateral yolk defective endocytic screen, mutant version of *rme-1* animals, shows large intestinal vacuoles (Grant et al., 2001). Consequent work rectifies that there is no effect on an early endosomal marker (RAB-5) and the vacuoles are not able to fill with the apical endocytosed dye indicating that the RME-1 is involved in a later step of basolateral endocytosis (Grant et al., 2001; Shi et al., 2012). Other reports confirm that the RME-1 homolog EHD1 shows localization on REs in mammalian cell lines (Grant et al., 2001; Lin et al., 2001a; Shi et al., 2012).

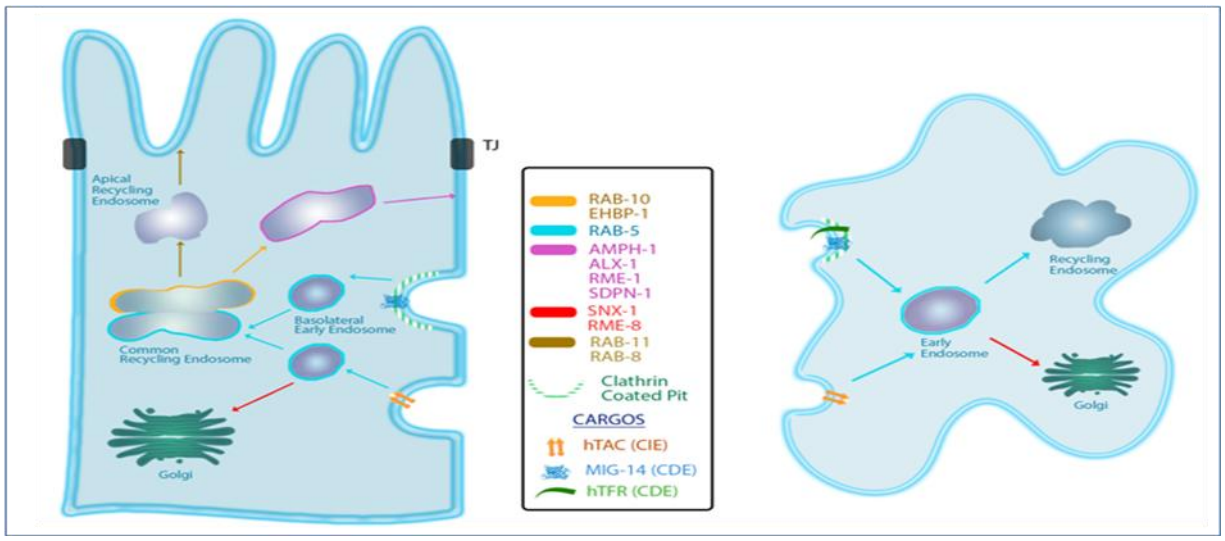

Figure 1.1 Recycling of Cargos in polar intestinal cells and non-polar cells.

The transport pathways are showing different compartment connecting the common recycling pathway. The different colour represents the different transport pathways with their known regulators. The model cargo internalized through CDE and CIE pathways are indicted. In case of the non-polarised cell, the cargos from both CDE and CIE pathways are destined to recycling endosome or Golgi complex from the common early endosomes [Adapted from (Sato et al., 2014)].

1.2.5 The role of RME-1/EHD1 molecules in recycling endosome

A number of cellular processes are carried out by protein complex, where multiple proteins are assembled through specific protein-protein interaction module (PIMs). Like ubiquitin: ubiquitin-binding domains, phosphotyrosine: SH2 domains, etc. In these cases hundreds of proteins interact with each other and form the PIMs, this network of a protein involved in the various aspects of cell regulation (Grabbe and Dikic, 2009; Pawson, 2004).The one such PIMs called EH (Eps15 homology) domain containing proteins plays an important role in the endocytic process. The EH domain firstly reported in the three copies at N- terminal of epidermal growth factor receptor substrate 15 (Eps15) (Wong et al., 1995). The proteins, which contain this domain, are called Eps15 homology domain (EHD) containing proteins. The EH domain recognizes an NPF (asparagine-proline-phenylalanine) motif within target proteins and forms a network of protein-protein interactions (Grant and Caplan, 2008). This EH domain network has various roles in endocytic route and synaptic vesicle recycling. Some EH domain proteins are also reported to be involved in intracellular trafficking, organization of the actin cytoskeleton, and in the regulation of transcription and other nuclear events (Tsushima et al., 2013). On the basis of the position and number of EH domains, proteins are classified into five families, these are Intesectin, Eps15, EHD, Reps and Synergin (Polo et al., 2003; Tsushima et al., 2013). The human genome encodes for 11 EH domain-containing proteins from five families, however the *C. elegans* genome encodes only five proteins, one representative of each family and most of the proteins are conserved between human and *C. elegans* (Tsushima et al., 2013).

The EHD, a family of EH domain-containing proteins is distinct from the rest having a C-terminus EH domain. The structure of EHD proteins contains a single EH domain which is present at the C-terminus, central coiled-coil region to form hetero or homo-oligomers and a phosphate binding loop capable of binding to a nucleotide at the N-terminus region (**Figure 1.2**) (Grant et al., 2001; Wong et al., 1995). The presence of the EH domain indicates a possible role for these proteins in receptor-mediated endocytosis (Tsushima et al., 2013). The human genome encodes four paralogs of EHD (EHD1-4) each having different functions in the endocytic pathway (George et al., 2007). The *C. elegans* genome encodes one gene for the EHD family i.e. *rme-1*. The RME-1 protein shows the highest identity (67%) over its entire length to the mammalian EHD1 ortholog (Grant et al., 2001). Studies have also shown that the increased

number of vacuoles in *rme-1* mutant animals could be rescued by the expression of EHD1 ortholog under the intestine-specific promoter (Deo et al., 2018; George et al., 2007). Suggesting, functional conservation of this protein across different species.

RME-1/EHD1 localizes to the recycling endosome, mutations in *rme-1/ehd1* cause the size of the recycling endosome to increase due to incoming vesicles continually fuse with the ERC which further can be visualized as vacuoles in the intestine of worms (George et al., 2007; Grant et al., 2001). A previous report showed that depletion of EHD1 leads to enlargement of ERC while the addition of purified EHD1 restores its normal tubular morphology (Giridharan et al., 2013). The EHD1 ATPase structure shows similarity with the Dynamin GTPase domain (Naslavsky and Caplan, 2005a). It was proposed that the dynamin-like molecule could be involved in pinching off the endosomal membrane from ERC (Grant and Donaldson, 2009; Melo et al., 2017), the EHD1 which is present on ERC and having the ATPase domain like dynamin may be a potential molecule in generating transport vesicle from the ERC. Thus, EHD1 was proposed to be involved in membrane fission at ERC, although the underlying mechanism is not yet fully understood. Our results confirm that it is the main molecule invoking scission like activity at ERC.

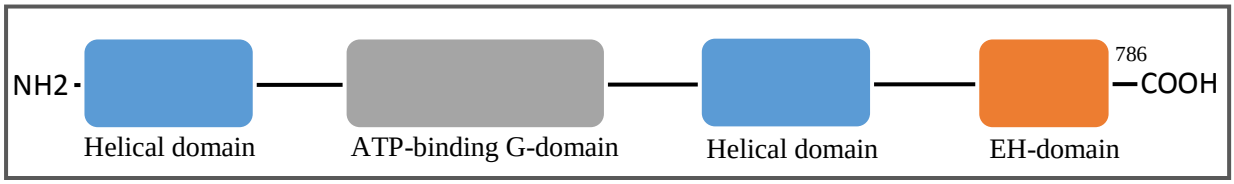

Figure 1.2 Structure of EHD1/RME-1

The EHD1/RME-1 consists of an N-terminal helical domain, ATP binding domain, and a C-terminal single EH domain [Adapted from (Grant and Caplan, 2008)].

1.2.6 Role of Recycling Endosomes in neuronal cells

The neurons are highly polarized cells having an axonal and somatodendritic membrane, which are morphologically and functionally very different from each other. The endocytic machinery plays a key role in generating and maintaining the neuronal polarity by selective endocytic and recycling activity of the synaptic and other plasma membrane cargos in neurons. The early endosome recycles back the vesicles in the same place while recycling from the REs is slower

and returns internalized cargos to several locations on the plasma membrane (Yap and Winckler, 2012). It was also reported that the REs are dispersed at different location in neurons and regulate the local recycling and degradation of receptors at specific domains like synapses, axons, and dendrites (**Figure 1.3**). The controlled transport through these various endosomal compartments allows endosomes with the capacity to fine-tune the delivery of receptors and the amount of signaling (Huotari and Helenius, 2011). So recycling endosomes are involved in the maintaining cell polarity, synaptic plasticity as well as axonal pathfinding during development and synaptic vesicle recycling in neuronal cells (Yap and Winckler, 2012).

The recycling endosomal proteins have a different role in the neuron. For example, EHD1 and EHD4 were involved in endocytosis in neurons (Shao et al., 2002), despite trafficking through early and recycling endosomes in epithelial cells (Fares and Grant, 2002; Grant and Caplan, 2008; Sharma et al., 2008). The EHD4 also involved in endocytosis of Nogo-A, a repulsive cue for axonal growth cones (Joset et al., 2010). EHD1/EHD4 hetero-oligomer complex mediates transcytotic L1/NgCAM endocytosis in hippocampal neuronal cells (Yap et al., 2010). In sympathetic neurons, Rab11 is involved in anterograde axonal trafficking of tropomyosin-related kinase (Trk) receptors (Ascaño et al., 2009). Besides, EHD family proteins are involved in unidirectional transport of the β-secretase (BACE1) (Buggia-Prévot et al., 2013). Furthermore, EHD1/RME-1, a ubiquitous regulator of endosomes, plays an essential role in regulating the local AMPA receptors recycling at the postsynaptic sites in hippocampal neurons (Park, 2004). However, the role of RME-1 or recycling endosome is in *the C. elegans* nervous system is not yet known. To look at the role of RME-1 molecule in *C. elegans*, we started looking at the command interneurons, which express the abundant amount of the AMPA/GLR-1 receptor.

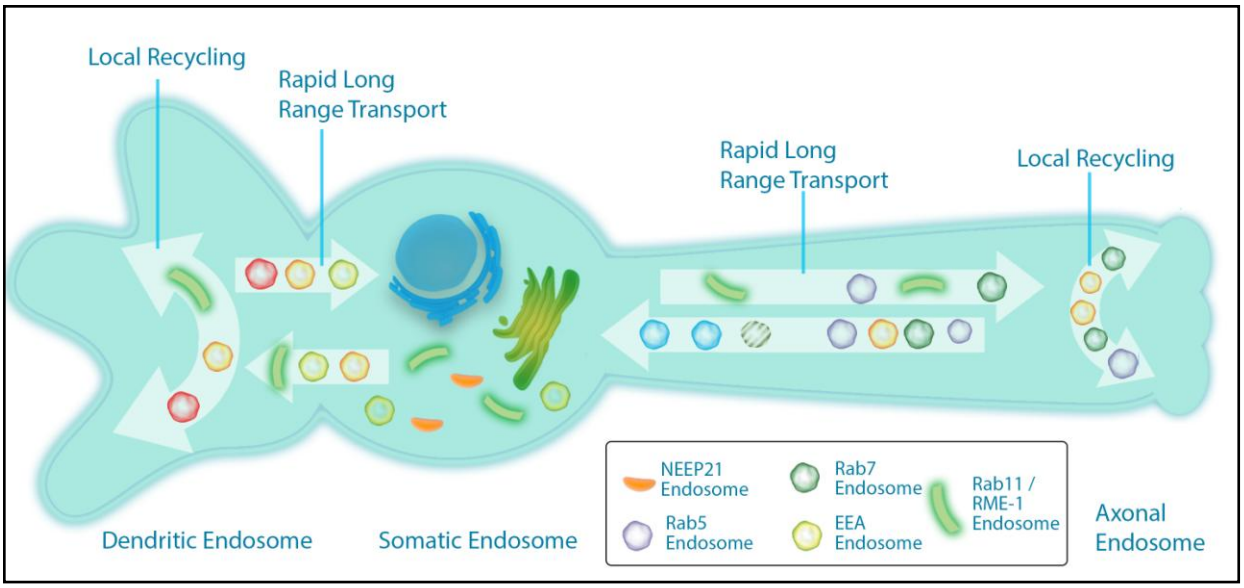

Figure 1.3 Endosomes in neurons

The large size and sub-cellular complexity make necessary for a different endosomal system in neurons when compared to a polarized cell. The different somatic, dendritic, axonal and synaptic regions have different endosomal regulators and show dissimilar motility profile [Adapted from (Yap and Winckler, 2012)]

1.2.7 Command interneurons and glutamatergic signaling in *C. elegans*

The sinusoidal movement of worms called locomotion, which includes forward and reversal movement. The command interneurons are known to regulate forward and reverse movements, act as caretakers of locomotion. There are five command interneurons, which divided into two classes; forward movement regulator (PVC and AVB) and other the three (AVA, AVD, and AVE) are involved in the regulation of reverse movement (Chalfie et al., 1985; Gray et al., 2005; Piggott et al., 2011) The AVA neuron has been reported to be involved in the initiation of reversal movement (Piggott et al., 2011). These different command interneurons are postsynaptic to most of sensory neurons and interneurons and give synaptic inputs to several motor neurons, which further control the movement of the worm. In reversal movement controlling neurons, glutamatergic signaling is crucial (Brockie et al., 2001; Wang et al., 2008). defect in glutamatergic signaling shows a reduced number of reversals behavior in the worm (Burbea et al., 2002; Juo and Kaplan, 2004; Zheng et al., 1999)

Glutamate is an excitatory neurotransmitter used by vertebrates and invertebrates in the nervous system (Bredt and Nicoll, 2003). Glutamatergic signaling is crucial for synaptic transmission and plasticity. In the case of *C. elegans*, reversal behavior controlled through glutamatergic signaling. For example, a gain of function mutation in GLR-1 receptor, shows increased reversal behavior and loss of function mutations in GLR-1 receptor decrease the reversal behavior to a significant extent (Burbea et al., 2002; Juo and Kaplan, 2004; Zheng et al., 1999). Likewise, the command interneurons AVA, AVD, and AVE are glutamatergic neurons (Chalfie et al., 1985; Piggott et al., 2011) and shows expression of an AMPA (α-amino-3-hydroxy-5-methyl-4-isoxazole propionic acid) type, ionotropic glutamate receptor GLR-1, responsible for rapid glutamate-gated currents (Mellem et al., 2002).

1.2.8 Glutamate receptors in *C. elegans*

The ionotropic glutamate receptors (iGluRs) are the primary class of receptors that mediate excitatory neurotransmission through interneurons. There are ten iGluR subunits in *C. elegans* 8 subunits (GLR-1- GLR-8) shows similarity with AMPA/kainate type receptor subunit, while the other two belongs to the NMDA type of receptors, i.e., NMR-1 and NMR-2 (Brockie et al., 2001). A large number of subunits suggest that glutamate can carry diverse functions in *C. elegans*. The AMPA subunits usually form a heteromeric receptor in combination with other subunits. The detailed expression of all iGluRs very well mapped in *C. elegans* (Brockie et al., 2001; Hart et al., 1999; Maricq et al., 1995). Most of the subunits expressed in command interneurons (GLR-1, GLR-2, GLR-4, GLR-5, NMR-1, and NMR-2) interneuron RIA (GLR-3 and GLR-6) and pharyngeal interneurons (GLR-7 and GLR-8) (Brockie et al., 2001). Out of these subunits, GLR-1 is known to be very important in regulating the reversal behavior and mechanosensation in worms (Burbea et al., 2002; Juo and Kaplan, 2004; Rongo and Kaplan, 1999; Zheng et al., 1999).

Studies from over several decades have tried to understand the various aspects of synapse development and maintenance. The glutamate receptors are mostly present in postsynaptic sites of command interneurons that form a synapse with presynaptic neurons. A GLR-1::GFP fusion protein has proven to be useful in studying the localization, organization, and trafficking of glutamate receptors at the subcellular level. LIN-10, a PDZ domain-containing protein, regulates the punctate localization of GLR-1 receptors (Rongo et al., 1998). Interestingly this protein also

reported regulating AMPA receptor trafficking and localization in vertebrates (Sheng and Sala, 2001; Stricker and Huganir, 2003). During development, UNC-43, a calcium and calmodulin-dependent protein kinase II (CaMKII), is required for the trafficking of GLR-1 receptors from the cell body to form a new synapse (Rongo and Kaplan, 1999). Further, the Anaphase-promoting complex (APC) is a multiunit ubiquitin ligase, regulates the ubiquitination or further degradation of its substrate. Any mutation in its subunits results in the accumulation of GLR-1 in the ventral nerve cord (Davis et al., 2002; Furuta et al., 2000; Juo and Kaplan, 2004).

The AMPA levels are never stable at the synapse; they keep recycling with the sub-cellular pool. This activity is important in regulating synaptic plasticity, allowing worms to change their synaptic strength according to the requirements and modulate the signaling through those particular circuits. Various molecules like LIN-10, UNC-11, an AP180 clathrin adaptor protein, RAB-10, a clathrin-independent endocytosis GTPase and ITSN-1, an intersectin adaptor protein are known to involve in regulating the punctate localization of GLR-1 receptors in the command interneurons (Burbea et al., 2002; Glodowski et al., 2007; Rongo et al., 1998). Any defect in these molecules causes an increase in accumulation or size of the synaptic GLR-1::GFP puncta and compromised reversal frequency. Here we show that *rme-1* mutants also show increased GLR-1::GFP punta size and reduction in reversal frequency.

1.2.9 Locomotion and reversal behavior in *C. elegans*

In *C. elegans*, locomotion means crawling behavior (sinusoidal) and is the basic foundation of many other behaviors (Croll, 1975). Locomotion consists of the forward movement, backward movement or reversals, and the turning movement of the worms. Reversals are a vital component of locomotion, which determine the angle of turn and allows the worm to change its direction. Each aspect of locomotion has its importance in *C. elegans* behavior.

In this study, reversal behavior studied in relation to local search behavior, also known as spontaneous reversals. Worms that are off food explore their environment in search of the food, executing local search behavior (Gray et al., 2005). There are different ways to read out the reversal behavior; here, we are looking at the reversal frequency, which represents the number of spontaneous reversals during particular time duration (Croll, 1975; Rankin et al., 1990). It will

allow understanding the change in the direction (frequency) of moving worms that are exploring their environment.

The cholinergic and GABAergic motor neurons coordinate the contraction and relaxation of dorsal and ventral longitudinal muscle rows and mediate the sinusoidal movement of the worm. There are two classes of cholinergic neurons, type A motor neurons control the backward movement, and type B motor neurons control the forward movement. The five command interneurons control the motor neurons activity. Mutations in the glutamatergic receptors affect the reversal movement of the worms, which is controlled by the AVA, AVD, and AVE command interneurons.

1.3 Part III. To explore the role of SRX-97, a G-protein coupled receptor in chemosensory neurons of *C. elegans*

1.3.1 Introduction

Caenorhabditis elegans mainly use chemosensation to navigate their surroundings. This involves searching for food, running away from danger or predators, finding its mate, and checking the population density to develop suitable survival mechanisms. To convey these events, the chemosensory nervous system of this tiny nematode is very well developed. Chemosensory neurons are present near the head and tail regions, where they sense the surrounding by expressing numerous GPCRs (Bargmann, 2006). These chemicals from surrounding activate the GPCR sensory transduction, which inferred into a neuronal signal by the organism through interneurons. Further, these interneurons signal to motor neurons and carry out the appropriate locomotory behavior in worms. Thus detection, recognition, and processing of these environmental signs are critical to fine-tuning fitness-related behaviors in these animals.

1.3.2 Chemosensory Neurons

Adult *C. elegans* contains 302 neurons; out of these, 32 are assumed to be chemosensory neurons. Chemosensory neurons are located in the amphid, inner labial, and phasmid organs and directly or indirectly exposed to the environment through cilium opening in the sheath or socket cells that are a type of glial cells (**Figure 1.4**) (Bargmann, 2006).

The *C. elegans* nervous system encodes for support cells: 24 sheath cells, 26 socket cells, and 6 GLR cells. GLR cells are present inside the nerve ring (NR) and help in the development of muscle arms. The sensory neurons with their sheath and socket cells mainly present in the head and tail region, making a sensory organ called sensilla. The sensilla comprise of dendrites of one or more chemosensory neurons, which is enclosed by a channel-shaped by a single sheath cell and one or more socket cells. In some neurons, dendrites form sensory cilia, a primary site for signal transduction where the stimuli converted into receptor potential. The receptor potential is a graded response to a stimulus that might be depolarizing or hyperpolarizing.

The members of the chemosensory neuron form right and left bilaterally symmetric pairs in the head and tail region of the worms. The amphid (head) contains a pair of neuronal cell bodies, which sense the environment through the cilium opening created by sheath and socket cells in the mouth. The amphid region is thought to be the largest chemosensory organ containing 12 pairs of chemosensory neurons, on the basis of their cilium morphology, axon morphology, and the synaptic targets each pair of a neuron can be distinguished (**Figure 1.4**). These are ADF, ADL, AFD, ASE, ASG, ASH, ASI, ASJ, ASK, AWA, AWB, and AWC with one sheath and socket cell. The cilia of odor sensing amphid neurons AWA, AWB, and AWC fixed within the sheath cell. The ADL, ASE, ASG, ASH, ASI, ASJ, and ASK cilia are perceptible to the external environment through the socket cells and regulate chemotaxis, mechanosensation, osmotaxis, and pheromone sensation in worms (Scholey, 2007). The cilia of AFD neurons are fixed within the sheath cells with many villi and help in the detection of adjacent temperature. The Phasmid is a unicellular sensilium which is present in the lateral tail of the worm. It contains a pair of PHA, PHB, and a single PQR neuron (Hall and Russell, 1991). PHA and PHB sense the surrounding through the cilium opening created by socket cells in the tail (**Figure 1.4**). The PQR neuron directly exposed to the pseudocoelomic (internal) body fluid of the worm. The role of all chemosensory neurons given in the **Table 1.**

Besides, the inner labial (IL) neurons (IL1 and IL2) together are arranged symmetrically in 6 sets of cells, ending with a lip like structure around the mouth of the worms (**Figure 1.4**). The two lateral outer labial (OLL) and four cephalic (CEP) neurons originate near the IL neurons and terminate the same way near the mouth of the worms (Scholey, 2007).

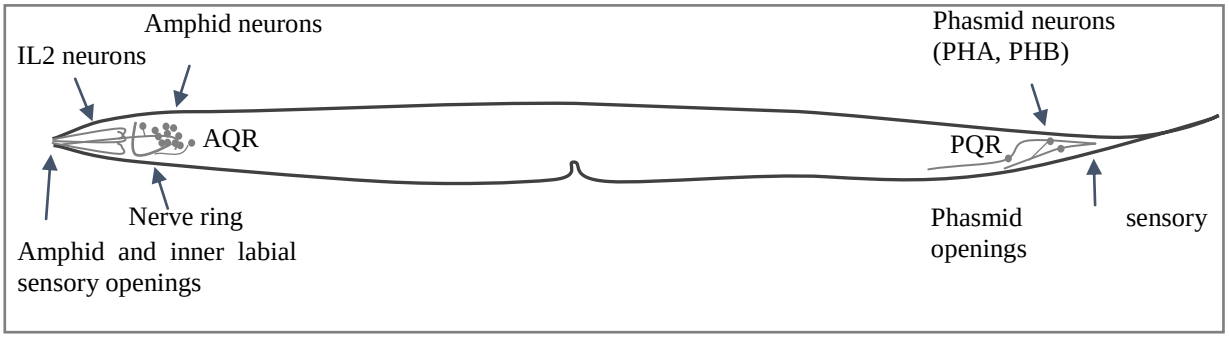

Figure 1.4 Location of Amphid and Phasmid neurons

Amphid contains 12 pairs of chemosensory neurons; phasmid contains a pair of PHA and PHB chemosensory neurons. The six Inner labial organs contain one IL1 mechanosensory and IL2

chemosensory neurons. The AQR and PQR neurons are present with their ending within the animal. Amphid and Phasmid chemosensory neurons open to outside through sensory openings [Adapted from (Bargmann, 2006)].

These chemosensory neurons express different sets of GPCRs to communicate with the outside environments

Table 1 list of chemosensory neurons with their function and expression of receptors or G-proteins.

[Adapted from (Bargmann, 2006)]

Sr. No	Neuron	Functions	Receptors; G-proteins
1	ASE	Water-soluble chemotaxis	Receptor Guanylate Cyclases; *gpa-3*
2	AWC	Volatile chemotaxis, Lifespan, Navigation	GPCRs *(str-2); odr-3, gpa-3, gpa-5, gpa-6 and gpa-13*
3	AWA	Volatile chemotaxis, Lifespan (minor)	GPCRs *(odr-10); odr-3 (major), gpa-3, gpa-5; gpa-13; gpa-6*
4	AWB	Volatile avoidance	GPCRs; *odr-3*
5	ASH	Nociception: Osmotic avoidance, Nose touch avoidance, Chemical avoidance, Social feeding	GPCRs; *odr-3 (major), gpa-3 (major), gpa-11, gpa-1, gpa-13, gpa-14, gpa-15*
6	ASI	Dauer formation, Chemotaxis(minor), Navigation	GPCRs; *gpa-1, gpa-3, gpa-4, gpa-5, gpa-6, gpa-10, gpa-14*
7	ADF	Dauer formation, Chemotaxis (minor)	GPCRs; *odr-3, gpa-3, gpa-10, gpa-13*
8	ASG	Dauer formation (minor), Lifespan, Chemotaxis (minor)	GPCRs; *gpa-3*
9	ASJ	Dauer formation and recovery, Chemotaxis (minor), Lifespan	GPCRs; *gpa-1, gpa-3, gpa-9, gpa-10, gpa-14*

10	ASK	Avoidance (minor), Chemotaxis (minor), Lifespan, Navigation	GPCRs; *gpa-2, gpa-3, gpa-14, gpa-15*
11	ADL	Avoidance (minor), Social feeding	GPCRs; *gpa-1, gpa-3, gpa-11, gpa-15*
12	URX, AQR, PQR	Oxygen/aerotaxis, Social feeding	Soluble guanylate cyclases *(gcy-35, gcy-36); gpa-8*
13	PHA, PHB	Avoidance (antagonistic)	GPCRs; *gpa-1, gpa-2, gpa-3, gpa-6, gpa-9, gpa-13, gpa-14, gpa-15*

1.3.3 GPCRs in chemosensory neurons

G protein-coupled receptors (GPCRs) is the most prominent family of signaling proteins which embrace a wide range of functions, including various autocrine, paracrine and endocrine processes (Latek et al., 2012).

GPCRs are also known as seven-transmembrane domain receptors; these transmembrane domains associated with heterotrimeric guanine nucleotide-binding proteins (G proteins). Ligand binding causes conformational changes to GPCRs, which activates the G protein, and the activated G protein initiates various biochemical reactions in the cell. These biochemical changes regulate different physiological functions like taste, smell, vision, secretion, neurotransmission, growth, and metabolism of the animal (Hu et al., 2017). The GPCRs classified into six different classes (A-F) based on similarity at the sequence and functional level (Attwood and Findlay, 1994). The Rhodopsin-like GPCRs also called Class A, and the other classes include the Secretin-like GPCRs (Class B), Metabotropic glutamate receptor family (Class C), fungal mating pheromone receptors (Class D), cAMP receptors (Class E) and frizzled/smoothened (Class F) receptors (Attwood and Findlay, 1994). The rhodopsin class A is the largest group having 80% of the GPCRs consisting of deeply conserves neurotransmitter receptors (acetylcholine, biogenic amines, and neuropeptides) and non-conserved chemosensory GPCRs (csGPCRs) (Katritch et al., 2013). The csGPCR has distinctly progressed with evolution and respond to diverse and phylogenetically related external as well as internal signals in different phyla (Vidal et al., 2018)

. In the case of nematodes, The *C. elegans* genome encodes around 1,341 csGPCR proteins; most of the proteins are unique for the nematode phylum. Altogether with pseudogenes (~400), csGPCRs encompass approximately 7% of the genes of the whole genome of this small animal (Robertson, 2006). These csGPCR coding genes signify the fact that just 302 neurons with 118 structurally defined neuronal classes respond to multiple cues (Robertson, 2006; Vidal et al., 2018).

The csGPCR are further classified into super-families and families on the basis of their similarities in protein sequence and shared intron location in the genes (Robertson, 2006). These include four super-families and 23 families (**Table 2**). The possible role of csGPCRs was determined by groups or pairs of chemosensory neurons that showed the expression of the csGPCR transgene (**Table 1**). The ligand and function of many of the csGPCRs remain unknown.

Table 2 Classification and expression of csGPCRs in *C. elegans*

[Adapted from (Robertson, 2006; Vidal et al., 2018)]

Classification		Gene counts	Reporters	Overview of expression		
Super family	family	New counts	Total examined reporters	Neurons only	Neurons + non neurons	Non-neurons only
Str	srh	223	43 (14)	24	16	3
	str	196	42 (16)	21	16	5
	sri	60	21 (7)	11	8	2
	srd	67	13 (6)	10	2	1
	srj	39	14 (1)	7	6	1
	srm	6	6 (-)	3	3	-

	srn	1	1 (-)	1	-	-
	all Str	591	140 (44)	77	51	12
Sra	sre	51	31 (20)	13	13	5
	sra	32	22 (11)	15	6	1
	srab	22	18 (6)	10	7	-
	srb	14	10 (4)	4	4	2
	all Sra	119	81 (41)	42	30	8
Srg	srx	105	20 (6)	12	7	1
	srt	67	16 (6)	13	2	1
	srg	61	23 (9)	15	7	1
	sru	40	12 (5)	6	6	-
	srv	30	12 (1)	10	2	-
	srxa	17	8 (4)	6	1	1
	all Srg	320	91 (31)	62	25	4
Solo	srw	115	11 (7)	8	1	2
Solo	srx	68	23 (1)	15	5	3
Solo	srbc	72	5 (2)	4	1	-
Solo	srsx	37	14 (4)	11	2	1
Solo	srr	9	9 (-)	4	5	1
Solo	sro	1	1 (1)	1	-	-
Total		1,341	375 (131)	224	120	31

1.3.4 Structure of GPCRs in *C. elegans*

G-protein coupled receptors bind to a tremendous diversity of signaling molecules, yet they share a structural design that has preserved over the progress of evolution.

GPCRs are made up of a single polypeptide chain, which is folded into a spherical shape and entrenched in the plasma membrane. In the folded form, seven segments of the GPCR protein span the entire width of the membrane (In and Out of the cell), making it a seven-transmembrane receptor. The extracellular loop of the polypeptide forms a pocket for ligand binding. Once the ligand binds to it, which causes structural change, as the name suggests, GPCRs interact with the nearby G proteins in the cell. The G proteins are heterotrimeric proteins made up of an alpha subunit (α), a beta subunit (β), and gamma subunit (γ) (Robertson, 2006). These G proteins are unique proteins having the ability to bind guanine triphosphate (GTP) or guanine diphosphate (GDP) and activate downstream signaling pathways, as shown in (**Figure 1.5)**. Thus, the signals transduce from the plasma membrane in a cycle of guanine nucleotide exchange and hydrolysis pathways and activate further signaling. The *C. elegans* genome encodes for 21 Gα, 2 Gβ, and 2 Gγ genes (Cuppen et al., 2003; Jansen et al., 1999). Most of these G proteins show expression in the chemosensory neurons along with some other parts of the worm body (Bastiani, 2006; Robertson, 2006).

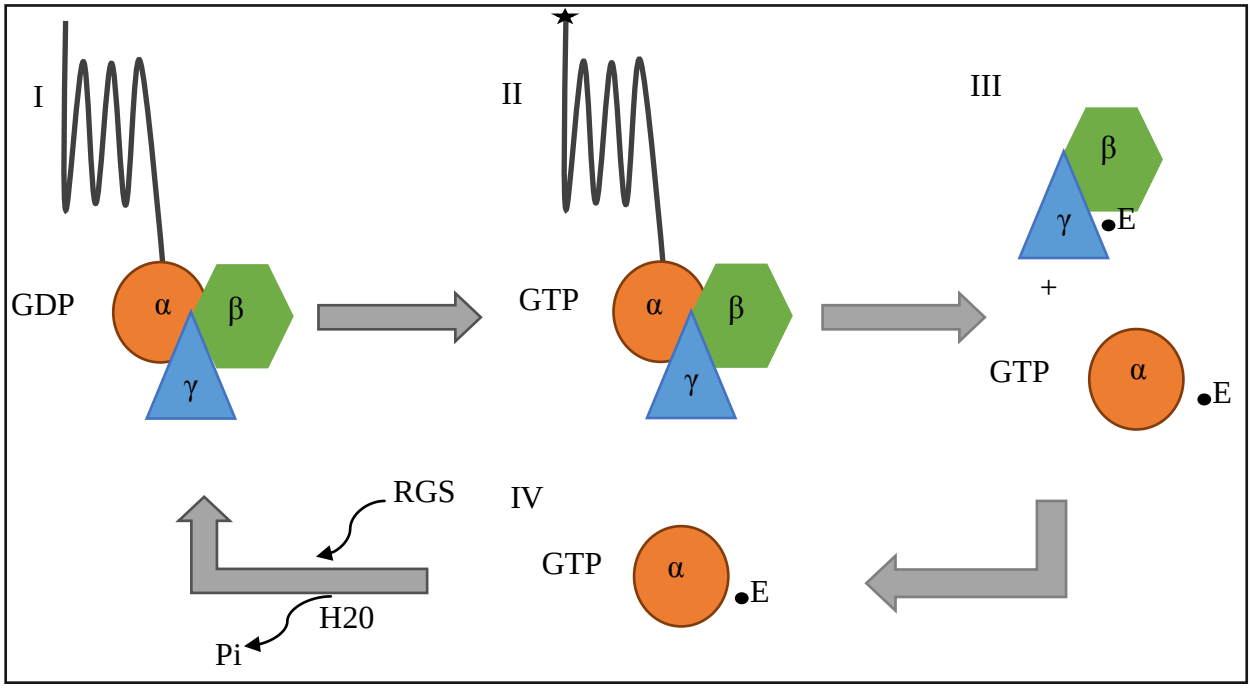

Figure 1.5 Illustration showing the activation of heterotrimeric G proteins by G-protein coupled receptor (GPCR).

In inactive form (I) the complex (G-αβγ) is attached to the membrane with the help of seven transmembrane receptor protein, here the Gα subunit is accompanying with the GDP. Once the receptor is activated by its ligand, which causes the conformational change and the receptor act as guanine nucleotide exchange factor (GEF), and the GDP is converted to GTP for α subunit (II). The GTP bound α subunit and βγ subunit separate from the receptor and activate downstream signaling by stimulating different effectors (E) molecules (III). The activated Gα protein (intrinsic activity) becomes hydrolyzes its GTP; GTPase-activating proteins (GAPs) further accelerate this activity. A regulator of G protein signaling (RGS) domain is present in most of the GAPs which show higher attraction for Gα-GTP transition state (IV) [Adapted from (Bastiani, 2006)]

1.3.5 Expression and Function of csGPCRs in *C. elegans*

The expression data of 375 csGPCRs given but only 320 transgene expression has been known at the single-cell resolution (Gun Taniguchi et al., 2014; Vidal et al., 2018). Most of these receptors show expression in chemosensory neurons, functional studies with a small number of these receptors show their role in recognition of environmental or pheromonal cues in the surroundings. Some csGPCRs are known to be expressed in non-sensory and non-neuronal cells, suggesting their role in sensing internal cues (Vidal et al., 2018). For example, the AIY interneuron involved in the process of associative learning and olfactory imprinting through the expression of *sra-11* csGPCRS. The food signal sensed by *sra-13* csGPCR, which is important for healthy vulva development (Battu et al., 2003; Remy and Hobert, 2005). Receptors from srr and srw family show expression in the pharyngeal organ and show sequence similarity with peptidergic receptors suggesting their role in governing internal signals (Krishnan et al., 2014; Robertson, 2006).

In *C. elegans*, most volatile and water-soluble chemicals sensed by 11 pairs of chemosensory neurons. The process through which volatile chemicals recognized is called olfaction, and recognition of soluble signals is called gustation. For different odorant, different sets of olfactory or gustatory receptors are present on the chemosensory neurons. The *C. elegans* genome is predicted to encode around 1300 functional csGPCRs; most of these receptors expressed in 11 pairs of chemosensory neurons (Bargmann, 2006; Vidal et al., 2018). As a consequence, a single or multiple neurons can express different sets of receptors and may be involved in detecting different cues and/or different concentration of cues (Bargmann, 2006; Gun Taniguchi et al.,

2014; Yoshida et al., 2012). The relationship between odorant (ligands) and the receptors is not yet completely known.

Pheromones are sensed by the neuron ASK along with, ASI and ASJ by the expression of different sets of csGPCRs e.g. SRBC-64, SRBC-66, (SRG)-36 and -37 and DAF-37 (Kim et al., 2009; McGrath et al., 2011; Park et al., 2012; Schackwitz et al., 1996). Volatile and water-soluble chemicals sensed by the AWA, AWB, AWC, along with ASH and ASI neurons (Bargmann, 2006). The ODR-10 GPCR is expressed in AWA neurons and is involved in sensing low concentrations of diacetyl (10^{-3}) (Sengupta et al., 1996). While the SRI-14 GPCR is expressed in ASH neurons and is involved in showing avoidance behaviors towards a high concentration of diacetyl (undiluted) (Gun Taniguchi et al., 2014; Yoshida et al., 2012). In addition, Dihydrocaffic acid and benzaldehyde detected by the ASH neurons (Aoki et al., 2011; Nuttley et al., 2001; Troemel et al., 1995). The ASH neuron is also involved in detecting noxious chemicals, osmotic solution, heavy metals, and shows response to mechanostimuli (Campbell et al., 2015; Hilliard et al., 2005, 2004, 2002). Thus, the ASH neurons are known to be polymodal neurons, sensing different cues. Likewise, the tail chemosensory neurons PHA and PHB are known to be involved in detecting various chemical cues and also act as polymodal neurons (Hilliard et al., 2002; Zou et al., 2017). A recent report (Vidal et al., 2018) suggests that that fifty percent of GPCRs that show expression in ASH also show expression in PHB neurons (**Table 3**). In this Thesis, we are looking at a newly identified GPCR, SRX-97, that shows strong expression in the ASH and PHB chemosensory neurons. Further, we characterize its role in sensing a high concentration of benzaldehyde (10^{-1}).

Table 3. List of csGPCRs which show expression in ASH and PHB chemosensory neurons

[Adapted from (worm book;(Vidal et al., 2018)]

Sr no.	ASH neuron	PHB neuron	Common GPCRs in ASH/PHB
1	*sra-6*	*sra-14*	srab-8
2	*sra-25*	*sra-39*	srab-11
3	*srab-7*	*srab-8*	srb-6
4	*srab-8*	*srab-11*	srab-17
5	*srab-9*	*srab-20*	srd-10

6	*srab-11*	*srb-6*	*srd-16*
7	*srab-24*	*srb-17*	*sre-27*
8	*srb-6*	*srd-10*	*srh-5*
9	*srb-17*	*srd-16*	*srh-18*
10	*srd-10*	*sre-27*	*srh-128*
11	*srd-15*	*sre-43*	*srh-210*
12	*srd-16*	*srh-5*	*srh-218*
13	*sre-4*	*srh-18*	*sri-5*
14	*sre-27*	*srh-128*	*sri-21*
15	*srg-25*	*srh-130*	*sri-26*
16	*srh-5*	*srh-142*	*srm-4*
17	*srh-7*	*srh-210*	*srsx-28*
18	*srh-10*	*srh-218*	*sru-8*
19	*srh-15*	*srh-240*	*sru-12*
20	*srh-18*	*srh-269*	*sru-38*
21	*srh-28*	*srh-270*	*srv-5*
22	*srh-79*	*sri-5*	*srx-105*
23	*srh-128*	*sri-21*	*srxa-6*
24	*srh-210*	*sri-26*	*srz-1*
25	*srh-218*	*srm-4*	*srz-45*
26	*sri-5*	*srr-3*	*str-84*
27	*sri-14*	*srr-4*	*str-90*
28	*sri-21*	*srr-7*	
29	*sri-26*	*srsx-28*	
30	*srm-1*	*srt-70*	
31	*srm-2*	*sru-1*	
32	*srm-4*	*sru-2*	
33	*srm-5*	*sru-8*	
34	*srsx-28*	*sru-12*	
35	*srsx-29*	*sru-30*	

36	*sru-8*	*sru-38*	
37	*sru-12*	*srv-5*	
38	*sru-38*	*srv-27*	
39	*srv-5*	*srw-145*	
40	*srv-11*	*srx-14*	
41	*srv-21*	*srx-105*	
42	*srx-47*	*srx-110*	
43	*srx-105*	*srxa-6*	
44	*srxa-6*	*srz-1*	
45	*srxa-7*	*srz-45*	
46	*srz-1*	*srz-56*	
47	*srz-27*	*str-52*	
48	*srz-45*	*str-84*	
49	*str-84*	*str-90*	
50	*str-90*		
51	*str-114*		

1.3.6 GPCRs and chemotaxis behavior

The behavior of *C. elegans* depicts its underlying neuronal activity. Various factors affect behaviors like internal conditions, past experiences, neuronal structures, and several different external factors. Genetic or functional changes in the neurons strongly affect the behavior of worms.

The different chemosensory neurons are known to be involved in sensing different environmental cues (**Table 1**). To determine the function of various csGPCRs different assays have designed according to their expression pattern in the neurons. I am interested in looking at the role of a novel csGPCR, SRX-97, in chemosensation by *C. elegans*. In this thesis, I have characterized this receptor using multiple chemotaxis assays that will be described in detail.

Chapter 2

Materials and Methods

2.1 SECTION A: Materials

2.1.1 Chemicals and reagents

All chemicals used in this study were either molecular biology or analytical grades and were obtained from commercial sources. The nematode growth media components, fine chemicals, and reagents were purchased from HiMedia India, Sigma Aldrich USA, Merck India, USA or Difco, USA. The oligonucleotides or primers were designed using Snapgene or ApE- A plasmid Editor Software and were purchased from Eurofins scientific and IDT (Integrated DNA technology). The Restriction enzymes, DNA polymerase (Phusion DNA polymerase), and other modifying enzymes, buffers, dNTPs, T4 DNA ligase, Calf Intestinal Phosphatase (CIP), and Antarctic phosphates, were purchased from New England Biolabs Inc, USA or Thermo Fischer scientific, USA. Prime STAR Phusion polymerases were purchased from the TaKaRa Bio. DNA ladder were obtained from the BR Biochem, India. Gel-extraction kits and plasmid miniprep columns were obtained from Qiagen, USA, or Bioneer, Korea. DNA extraction kits were purchased from Invitrogen, USA, and RNA isolation kit were procured from Qiagen, USA. Aldicarb PESTANAL, Pyrazine, Glycerol, Sodium dodecyl sulfate, Quinine, Copper sulfate were obtained from Sigma-Aldrich, USA. The benzaldehyde, Nonanone, Isoamyl alcohol, Diacetyl, and Octanol were purchased from the Sigma-Aldrich, USA or Hi media India.

2.1.2 Strains and Plasmids

The list of plasmids and strains used in this study are listed in Table 4-5 Most of the *C. elegans* strains used in this study were obtained from Caenorhabditis genetic centre (CGC) and plasmids were obtained from the Addgene. Strains and plasmids obtained from another lab are mentioned in the table 5.

Table 4 List of Plasmid constructs used in this study

S. no.	Plasmid used in this study	Plasmid numbers	Array numbers
1	P*rme-1*::mCherry	pBAB401	*indEx440*
2	P*rme-1::*RME-1(FL)	pBAB402	*indEx446*

3	P*vha-6*::RME-1(FL)	pBAB403	*indEx447*
4	RME-1genomic (FL)	pBAB467	*indEx467*
5	P*vha-6*::EHD1(WT)	pBAB405	*indEx405* and *indEx410*
6	P*vha-6*::mEGFP-EHD1	pBAB406	*indEx406* and *indEx411*
7	P*vha-6*::EHD1(T72A)	pBAB407	*indEx407* and *indEx412*
8	P*vha-6*::EHD1(F322A)	pBAB408	*indEx408* and *indEx413*
9	P*vha-6::*EHD1(Δ2-9)	pBAB409	*indEx409* and *indEx414*
10	P*vha-6*::EHD1(T94A)	pBAB410	*indEx410*
11	P*glr-1*::RME-1(FL)	pBAB442	*indEx421*
12	P*glr-1*::mCherry	pBAB443	*indEx443*
13	P*glr-1*::GFP::RAB-5	pBAB427	*indEx429*
14	P*glr-1*::GFP::RAB-7	pBAB428	*indEx428*
15	P*glr-1*::GFP::RAB-10	pBAB429	*indEx427*
16	P*glr-1*::GFP::RAB-11	pBAB430	*indEx469*
17	P*glr-1*::mCherry::RME-1_A	pBAB431	*indEx444*
18	P*glr-1*::mCherry::RME-1_D	pBAB432	*indEx458*
19	P*glr-1*::mCherry::RME-1_F	pBAB433	*indEx464*
20	P*glr-1*::mCherry::SEP::GLR-1	pBAB435	*indEx426*
21	P*glr-1*::mCherry::SEP::GLR-1(4KR)	pBAB434	*indEx459*
22	P*srx-97*::mCherry	pBAB460	*indEx466*
	P*srx-97*::GFP	pBAB459	*indEx476*
23	P*srx-97*::SRX-97::mCherry	pBAB461	*indEx462*
24	P*srx-97*::SRX-97_utr	pBAB462	*indEx477*
25	P*gcy-7::*GFP	pBAB463	*indEx481*
26	P*osm-10::*GFP	pBAB464	*indEx472*
27	P*srb-6::*GFP	pBAB465	*indEx470*
28	P*osm-10*::SRX-97_utr	pBAB466	*indEx479*
29	P*sra-6*::SRX-97_utr	pBAB467	*indEx480*

Table 5 List of mutant strains used in this study

Strain name	Genotype of the strain	Source and reference
DH1201	*rme-1(b1041)*	(6x outcrossed) CGC
CX2205	*odr-3*	CGC (3X outcrossed)
CX10	*osm-9*	CGC (3X outcrossed)
RB2464	*tax-2*	CGC (3X outcrossed)
NL792	*gpc-1*	CGC (3X outcrossed)
PR679	*che-1*	CGC (3X outcrossed)
BAB404	*srx-97*	This study (3X outcrossed)
BAB411	*rme-1(b1041); indEx405*	This study
BAB412	*rme-1(b1041); indEx410*	This study
BAB413	*rme-1(b1041); indEx406*	This study
BAB414	*rme-1(b1041); indEx411*	This study
BAB415	*rme-1(b1041); indEx407*	This study
BAB416	*rme-1(b1041); indEx412*	This study
BAB417	*rme-1(b1041); indEx408*	This study
BAB418	*rme-1(b1041); indEx413*	This study
BAB419	*rme-1(b1041); indEx409*	This study
BAB420	*rme-1(b1041); indEx414*	This study
BAB440	*indEx440*	This study
BAB442	*indEx442*	This study
BAB425	*rme-1(b1041); indEx442*	This study
BAB444	*indEx444*	This study
BAB458	*indEx458*	This study
BAB464	*indEx464*	This study
BAB461	*rme-1(b1041); indEx444*	This study
BAB460	*rme-1(b1041); indEx458*	This study
BAB465	*rme-1(b1041); indEx464*	This study
BAB443	*indEx443*	This study
BAB429	*indEx429*	This study
BAB428	*indEx428*	This study

BAB427	*indEx427*	This study
BAB469	*indEx469*	This study
BAB466	*indEx466*	This study
BAB467	*indEx476*	This study
BAB462	*indEx462*	This study
BAB477	*indEx477*	This study
BAB381	*indEx481*	This study
BAB472	*indEx472*	This study
BAB470	*indEx470*	This study
BAB479	*indEx479*	This study
BAB480	*indEx480*	This study
BAB467	*indEx467*	This study
BAB424	*rme-1(b1041); indEx467*	This study
BAB482	*srx-97; indEx477*	This study
BAB483	*srx-97; indEx479*	This study
BAB484	*srx-97; indEx480*	This study
BAB493	P*glr-1::*GLR-1::GFP(nuIs24)	Kaplan lab (Rongo et al., 1998)
BAB449	*rme-1(b1041);*P*glr-1*::GLR-1::GFP*(nuIs24)*	This study
VM484	***P****nmr-1::NMR-1::GFP*	This study
BAB452	*rme-1(b1041);*P*nmr-1*::NMR-1::GFP	This study
BAB448	*rme-1(b1041);*P*glr-1*::SNB-1::GFP(nuIs125)	This study
BAB491	(pDM1983)P*rig-3*::SEP::mCherry::GLR-1	Andrew Maricq lab (Hoerndli et al., 2013)
BAB492	(pDM2071)P*rig-3*::SEP::mCherry:GLR-1(4KR)	Andrew Maricq lab (Hoerndli et al., 2013)
BAB485	*rme-1(b1041);*P*rig-3*::SEP::mCherry::GLR-1	This study
BAB486	*rme-1(b1041);*P*rig-*	This study

	3::SEP::mCherry:GLR-1(4KR)	
BAB490	P*glr-1::*SNB-1::GFP*(nuIs125)*	Peter Juo lab (Juo et al., 2007)
BAB487	P*daf-7p::*GFP(*fk181*)	CGC
BAB489	P*str-2*::GFP (CX3695)	CGC

Table 6 List of Primers used for genotyping of the mutants in this study

Primer number	**Primer sequence for genotyping**	**Mutants genotype**	**Mutation type**
NK104	ggaagcattcctggaaatgctct	*rme-1*	deletion
NK105	ggagacttcccagatgtgaacaa	*rme-1*	deletion
NK113	cagctcatattccgagtgtgc	*rme-1*	deletion
NK207	ggatagaagattcacgtccggaag	*srx-97*	deletion
NK208	cagagcaaaccccacatgga	*srx-97*	deletion
NK209	tccatgtggggtttgctctg	*srx-97*	deletion
NK210	cttccaacatgaaaagcactatcttatcag	*srx-97*	deletion
NK263	ctacagtttagtgcttgccacag	*gpc-1*	deletion
NK264	tgtcgaaattaaagggtttcgagg	*gpc-1*	deletion
NK265	gctgtccaacgcaattttcg	*gpc-1*	deletion
NK266	agtaaaacactattatttattcttacctcagtcg	*unc-2*	substitution
NK267	agtaaaacactattatttattcttacctcagtta	*unc-2*	substitution
NK268	tgattgaatgcatgattgccag	*unc-2*	substitution
NK269	ggacccttcctctaataccttcg	*che-1*	substitution
NK270	ggacccttcctctaataccttaa	*che-1*	substitution
NK271	gcgagttaccgtatcacttgc	*che-1*	substitution
NK275	atgggctcatgccagagc	*odr-3*	substitution
NK276	gatttttcaagaaaaaaagtcacggaaaatga	*odr-3*	substitution
NK277	ccgagttgcgatatttcatttttttctat	*odr-3*	substitution
NK278	ttacatcattcctgctttttgtaaattcttctg	*odr-3*	substitution

Table 7 List of primers used for cloning of genes for this study

Primer number	Forward reverse	Primer sequence for gene	Gene name	Vector backbone
NK169 **NK194**	FP RP	ctctaagcatgccagctccatcttcgacatttgg ctctggatccgtgaatgtgtcagattgggtgcc	pGlr-1	pPD49.26 pPD95.75
NK239 **NK256**	FP RP	ctctctggatccatgtataatttttccgtactgttccacgag ctctctggtacctcattcatcgttgtcgttgagc	RME-1 gene	pPD49.26
NK237 **NK256**	FP RP	ctctatgctagcgagtctgtgaatagtgaagaacacaaaataaaacg ctctctggtacctcattcatcgttgtcgttgagc	mCherry RME-1A	pPD49.26
NK238 **NK256**	FP RP	ctctatgctagcagtaatctttttgaagaaggacaaaagaaaaagaagac ctctctggtacctcattcatcgttgtcgttgagc	mCherry RME-1D	pPD49.26
NK249 **NK256**	FP RP	ctctctgctagcttttcgtggcttggtggtgattc ctctctggtacctcattcatcgttgtcgttgagc	mCherry RME-1F	pPD49.26
NK128 **NK108**	FP RP	ctctaagcttgcatgtacctttataggtgcgctc atatctagatttatgggttttggtaggttttagtcgcc	P*vha-6*	pPD49.26
Nk199 **NK200**	FP RP	gtatactgcaggcatgtacctttataggtgcgctc ctctggatcctttatgggttttggtaggttttagtcgcc	P*vha-6*	pPD49.26
NK116 **NK118**	FP RP	ctctgcatgcccgtactgttccacgagctaatcg ctctccatggctcgatgtgtggggtgtgg	P*rme-1*	pPD49.26 -mCherry
NK129 **Nk130**	FP RP	ctcaagcttcaggagccaatggagttccaac gtatactgcaggcgggagaatattcaatttgaaaagagc	P*rme-1*	pPD49.26
NK181 **NK196**	FP RP	atcagcatgcatcttgaaaacctcaatcgaaccag ctctctcccgggggacatatcttgaaagtttggaatggag	P*srx-97*	pPD49.26 _mcherry
Nk214 **NK196**	FP RP	ctctctcgcatgcggtaagttttgcagtctaggcag ctctctcccgggggacatatcttgaaagtttggaatgga	P*srx-97*	pPD49.26 _mcherry
NK259 **NK260**	FP RP	ctctctgcatgcggaaccgtatttttgtgcaatagtcg ctctctcccggggcaagatgaaatttccaaaaaagtttattgatatgg	P*osm-10*	pPD95.75

NK262 **NK263**	FP RP	ctctctgcatgcgccaaaactgctgaacttttg ctctctcccgggcttctgtagaaatttcaagactgatcac	P*srb-6*	pPD95.75
NK264 **NK265**	FP RP	ctctctgcatgccagtagacaacgttcaaaattgtcg ctctctcccgggcgacataataaagtgggctgtaatttttag	P*srg-13*	pPD95.75
NK197 **NK279_**	FP RP	ctctctcccgggatgtccttatcgaattggacgc ctctctggtaccttcaacatgatcctattcaagtttggtatttttc	*srx-97_utr*	pPD49.26
NK197 **NK254**	FP RP	ctctctcccgggatgtccttatcgaattggacgc ctctctggtacctcaaaatgtgactgttaaaactgtgactt	*srx-97 gene*	pPD49.26 _mcherry
gRNA_1		atcaggtctcctcttccccacttatgactattacagttttag agctagaaatagcaag	*srx-97 gene*	pRB1017
gRNA_2		atcaggtctcctcttaaaattataaggcgtaggcagtttt agagctagaaatagcaag	*srx-97 gene*	pRB1017
Homology amr_1		atcatctagatcttccggacgtgaatcttctatc atcagcatgcatcttgaaaacctcaatcgaaccag	*srx-97 gene*	pPD95.75
Homology amr_1		atcagggccccattgcacaactgataagatagtgc atcacttaagttcaacatgatcctattcaagtttggt	*srx-97 gene*	pPD95.75

2.2 SECTION B: Methods

2.2.1 *C. elegans* strains maintenance

All worms or strains were maintained on nematode agar growth medium (NGM) plates seeded with OP50 *Escherichia coli* at 20OC under standard conditions (Brenner, 1974). The *C. elegans*, N2 (Bristol strain) was used as the wild-type (WT) control. Strains were synchronized by sodium hypochlorite treatment followed by allowing *C. elegans* to grow for about 72-80 hrs at 20^{O}C. All the assay or experiments were carried out with young adult hermaphrodites at 21- 23^{O}C. The occasional fungal or bacterial contamination which was observed on plates was removed by treatment with bleach. For long term storage in the lab, strains were maintained in liquid nitrogen and -80^{o}C using freezing media.

2.2.2 *C. elegans* genomic DNA isolation

Worms were grown on OP50 plates till the adult stage. First, worms were washed from the plates using 1 ml M9 buffer and transferred to 1.5 ml eppendorf tubes. Worms were washed using M9 buffer and allow to settle them using gravity for 2-3 min, removing the supernatant and again add fresh M9 buffer to the worm pellets, repeat this step for 3-4 times. Washing with M9 buffer facilitated the complete removal of bacteria. The worm pellet were finally suspended in 180 µl of Purelink genomic digestion buffer and 20 µl proteinase K. Worms suspended in lysis solution and were incubated at 55oC for 3-4 hrs for proper lysis. 20 µl RNaseA was then added, and the tube was incubated at room temperature for 3-5 minutes. Then 200µl lysis buffer and 200µl ethanol (96-100%) were added, followed by vertexing for the 5-10 second. The resulting lysate was added in the Purelink column and spun at 10,000X g for one minute. The collection tube was discarded, and the column placed in a new collection tube. Washing step performed with buffer one of the kit, prepared with ethanol. Again, the centrifugations were performed as before. Similar washing was done by placing the column in a new collection tube with buffer two, and centrifugation was done for 3 minutes. Then the column is transferred to the sterile microcentrifuge tube; 50µl of elution buffer was added for eluting the genomic DNA from the column. For this, centrifugation was done at maximum speed (12,000X g) for 1-2 minutes. Purified DNA was quantified and stored in -20^{o}C

2.2.3 *C. elegans* RNA isolation

Worms were grown on OP50 plates for the adult stage population. These worms were washed from the plates using M9 buffer in an RNase-free microcentrifuge tube. Worms were pelleted by centrifuging briefly at 4,000 rpm. The worms were washed 2-3 times to get rid of the bacterial food. The supernatant was removed, leaving 100µl of a solution on top of the worms. In the hood, 250 µL of Trizol reagent was added and vortexed for about 2 minutes. Samples were freeze-thawed thrice in liquid nitrogen to lyse the worms. Again, 200 µL of Trizol reagent was added, and samples were allowed to settle at room temperature for 5 minutes. To this, 140µl of chloroform was added, followed by vigorous shaking for 15 seconds. Samples were incubated at room temperature to settle for 2 minutes. Next, the samples were centrifuged at 12,000X g for 15 minutes at 4°C. The upper aqueous phase was transferred to a new 1.5 ml tube, and an equal volume of 70% EtOH was added. This mixture was transferred in a Qiagen RNeasy mini spin column. Samples were centrifuged at maximum speed (12,000 X g) for 30 seconds. To this

column, 700µl of buffer RW1 was added, followed by 500µl of buffer RPE, and this step repeated twice. After the final wash, an empty spin was given at maximum speed for two minutes, and the columns were transferred to a new 1.5 ml tube for elution. The RNA was eluted in 50µl of RNAse-free water and spinning at maximum speed.

2.2.4 Imaging experiments

All imaging was done with a 40x or 63x 1.4 NA Plan APOCHROMAT objective equipped with a Zeiss AxioCam MRm CCD camera using Zeiss AxioImager Z2 microscope. The worms were immobilized with 30mg/ml 2, 3-butanedione monoxamine (BDM) on 2% agarose pads. For quantitative analysis about 15-30 fluorescent worms (the actual number indicated in the graph) intensity was measured with wild type worms.

For the analysis of vacuoles in the intestine of worms, using a 40x objective z-stacks were taken with a 20 µm optical slice (20 slices at 0.5-micron distance). Image J software was used to obtain different images from z-stacks. The numbers of vacuoles were counted manually from these different images from the worm.

For quantitative imaging of GLR-1::GFP, NMR-1::GFP and synaptic vesicle (SV) marker was also done with the Zeiss 40x objective. To quantitate the number and size of puncta, worms were imaged in the ventral nerve cord in the posterior portion (distal region) of the *C. elegans* between the tail and the vulva. In the anterior region, we didn't see any significant change in *rme-1* mutants (n=15, size±1µm) compared to wild type (n=19, size±1.20). Image stacks were taken (approximately 10 µm) the GFP puncta were analyzed by taking the maximum intensity projections; with image, duplication threshold was set and further analyzed the puncta size and number using Image J software. For this analysis, the same exposure settings, and same fluorescence filters and equal camera gain were used for a specific wild type and transgenic lines. For graphs, an average value from the wild type, mutants and transgenic lines were taken, and in the data set ± S.E.M. is plotted. The Student's *t-test* ($p \leq 0.05$) in Graph Pad Prism 6 was used to calculate the Statistical difference between WT, mutants and transgenic lines. Firstly, the number and size of puncta was normalized to WT values, and then the graphs are plotted.

Translational reporter expression, superecliptic pHluorin, imaging was done using Leica HC PL APO 63x/ TCS SP8 confocal microscope. Laser lines from Multi-Ar (488) and He-Ne (594) with HyD detectors were used to measure the fluorescence. Worms were imaged in the posterior region for the AVA neuron distal neurites and head and tail region for ASH and PHB neurons.

For the co-localization study of P*srx-97*::mCherry with other known marker lines with GFP (like P*osm-10*, P*srb-6*), Z stacks were taken at 40x objective in Zeiss AxioImager microscope with a 30 μm optical slice (60 slices at 0.5micron distance). For each channel (mCherry/GFP) obtained maximum intensity projections separately. Further, the resulting images were merged to obtain co-localization (mCherry + GFP) images by using the Image J software to identify the neurons.

2.2.5 Rescue construct and transgenic

All construct was generated using the restriction digestion cloning method (Green and Sambrook, 2012; Sambrook et al., 1989). The pPD49.26 and pPD95.75 vectors were used to clone the entire construct. The transgenic lines were made using the standard microinjection technique as described previously (Mello and Fire, 1995; Mello et al., 1991). All the construct and primers used in this study already described.

EHD1 and its variants were digested from pET15B (Deo et al., 2018) using XbaI and KpnI and cloned under the *vha-6* promoter in the pPD49.26.

2.2.6 Pseudocoelom uptake assay

Basolateral uptake assays were performed as previously described (Grant et al., 2001; Ying et al., 2007). Briefly, Texas-Red BSA (1mg) was injected into the pseudocoelom of N2, *rme-1*, and transgenic adult animals and within few minutes of injection, the worms were imaged on a Zeiss Imager Z2 equipped with an AxioCam MRm using a 40x oil-immersion lens. The numbers of vacuoles were counted from two different transgenic lines.

2.2.7 Behavioral Assays:

2.2.7.1 Reversal Assay

The reversal assay was done using the young adult worms. The 90mm NGM plates were prepared 36-40 hrs before the assay timing. A healthy young adult worm was transferred from

the food plate to the plate without food. Allow the worms to crawl for 30-60 sec; this step is important to get rid of food attached to the worm. Then worm transferred to the new empty NGM plate and allow the worm to equilibrate with the plate for 1 min. After one-minute worms were scored for the number of reversal (frequency) for next 5 minute. If the reversal length is more than the worm's pharyngeal length, then only it was measured as reversal. The transfers of worms from plate to plate were carried out by using the eyelash pick or halocarbon oil, to avoid any injury.

2.2.7.2 Chemotaxis assay

The chemotaxis assay was done using the young adult worms.

All chemotaxis assays were performed with standard 90mm petri dish containing 10-12mL of chemotaxis medium (Agar, $MgSO_4$ (1M) $CaCl_2$ (1M) and KPO_4 (1M) pH6.6). Wherever required, odorants were diluted in ethanol and reported as ratio by volume. Modified, 90min quadrant plate chemotaxis assays were performed (Bargmann et al., 1993; Margie et al., 2013). Briefly, 5 min before to the assay, 1µL of 0.5 M Sodium azide was applied to four spots that were 6 cm apart from each other. Sodium azide acts as an anaesthetic agent to immobilize any worms that reach the vicinity of the spot during the assay. Fifty to one fifty worms were placed at the centre of the plate between the four spots, 2µL of ethanol was placed at the two-test spot and 2µL of the test odorant was placed at two test spots.

After 90min of chemotaxis, animals within each sector were counted, and a C.I. was calculated as the number of worms at the two test sector minus the number of worms at the two control sector, divided by the total number of animal from every sector of the plate excluding the non-moving worms from the centre. A positive Chemotaxis Index (C.I.) indicated an attraction to the chemical and a negative C.I. indicated an aversion

2.2.7.3 Kinetic of Chemotaxis assay

For kinetic analysis of chemotaxis approaches towards 10^{-1} source of benzaldehyde, a modified grid chemotaxis plate was used (Nuttley et al., 2001), and the sodium azide was avoided so that worms could leave a spot after a first visit. This grid consists of four parallel lines drawn 1cm

apart to divide the plate area into five sectors, distance between second and third line is 3cm. Two microliters of the benzaldehyde were placed on one small sheet of parafilm and ethanol on another as control, placed at opposite ends of the plate (6 cm away). After 60 min time interval, animals were immobilized by cooling the plates for 3 min at −30°C, and the plates were maintained at 4°C until counting. The number of animals in sectors A–E, with the test odorant being in A and B, were counted, and a kinetic C.I. was calculated as (no. of worms in A + no. of worms in B) − (no. of worms in D + no. of worms in E) / (total number of worms on the plate), yielding a W.C.I. range of +1.0 to −1.0. Those worms crawled up the side wall of the plate were considered lost. The score for each plate of 50–150 worms is one data point.

2.2.7.4 Dry drop avoidance Assay

A drop of a solution containing the test chemicals (0.1 SDS, quinine, CuSO4, glycerol, and pyrazine) dissolved in M13 (Tris, 30 mM; NaCl, 100mM; KCl, 10 mM) buffer, the drops are delivered on the agar 0.5-1 mm anterior of moving worms (Hilliard et al., 2002). Once the worm encounters the dry drop of chemicals, the head amphid neurons sense the chemicals and worms shows repulsion or avoidance behavior. Normally wild type worm's shows backward movement within 1 sec and some mutants like *odr-3* shows significant delay in response. The delays in response to these different chemicals were calculated in the assay. The drops of M13 buffer are used as control where worms didn't show any response. The glass capillaries (10mm) pulled on Bunsen burner to reduce the diameter of tip and used to deliver the drops.

2.2.8 Pharmacological Assay

2.2.8.1 Aldicarb Assay

Aldicarb assay was performed as described previously (Miller et al., 1996). The 1mM aldicarb was added to the molten agar of NGM and plates were prepared one day before the assay. The assay plates kept in dark and allowed to dry at room temperature. Young adult animals (20) were picked and placed on the aldicarb plates. Then the score of paralysis counted by gently prodding the head and tail region of the worms in every 10 min with the platinum wire pick. The worms which didn't show any movement after prodding scored as paralyzed worm. The assay was run

for about 2 hrs and done in triplicates, genotype of the worms being blind to the experimenter. The line graph was plotted with SEM.

At the neuromuscular junction, acetylcholine released from cholinergic motor neurons and binds to cholinergic receptors on muscles resulting in muscle contraction. The aldicarb drug competitively binds to acetylcholinesterase and inhibits the degradation of acetylcholine into acetate and choline; resulting in accumulation of acetylcholine at the NMJs. This causes persistent depolarization of muscle leads to hypercontraction and further complete paralysis of worms. This paralysis follows a typical graph, wild type worms get paralyzed in 120 min and the mutant's worm shows faster paralysis are called hypersensitive and those show slow paralysis rate are called resistant compared to WT. The increase or decrease in cholinergic signaling shows such phenotype.

2.2.9 CRISPR/Cas9 mediated deletion of *srx-97* gene

The clustered regularly interspaced short palindromic Repeats (FF)/Cas9 system was used to create *srx-97* deletion mutation as described previously (Dickinson and Goldstein, 2016). The Cas9 enzyme which is present in archea and some bacteria shows adaptive immunity against the pathogens like phages and phasmids. The binding sequence of two small RNAs determines the cleavage specificity of the Cas9 enzyme. One is called CRISPR RNA (crRNA) which determines the specificity and the second is trans-activating crispr RNA (trcrRNA) which base pair with the crRNA and activates the Cas9 enzyme. The chimeric single guide RNA (sgRNA) can be made containing this two small RNA with the Cas9 protein which shows the sequence dependent cleavage activity on DNA. The 20 bp guide sequence at the 5'end of sgRNA involve in binding to the target DNA which gives specificity to Cas9 cleavage activity. Moreover this 20 bp sgRNAs sequence could be modified as per the desired target genes. Besides, Cas9 firstly interact with a protospacer-adjacent motif (PAM) on the target DNA molecule. This is a very crucial step for determining the specificity or nicking activity of Cas9 enzyme. Generally used Cas9 enzyme is from the *streptococcus pyogenes* (Sp) which recognize the NGG as a PAM sequence. The SpCas9 can be engineered to cleave any target or desired DNA sequence having the GG dinucleotide and changing the desired 20 bp guide sequence at the 5' end of sgRNA. The Cas9 generated double strand break in the target DNA can be used to make small indel mutations through non-homologous end joining (NHEJ), and the addition or deletion of the larger sequence

by providing the exogenous DNA molecule which act as repair template and having the desired modifications called homology directed repair (HDR). We use CRISPR/Cas9 HDR method to make the deletion mutation in *srx-97* gene.

To analyse the desired guide sequences present in *srx-97* gene we used CRISPR design tool developed by Feng Zhang's laboratory (Hsu et al., 2013) and available at http://crispr.mit.edu. We then selected the guide sequence having the perfect specificity in the first exon and towards the 3' UTR region of the *srx-97* gene. Further to check the activity or efficiency of selected guide sequence, we used the guide RNA prediction algorithm design by the http://crispr.dfci.harvard.edu/SSC/. The selected guide sequence is rich in GC contain, has the 3'GG ending which is known to be most active in *C. elegans* system and one or no pyrimidine sequence in last four bases before the PAM sequence. The selected two guide RNAs cloned separately into the pRB1017 which have CeU6 promoter (Arribere et al., 2014). The *C. elegans* U6 (CeU6) snRNA is transcribed by the RNA polymerase III and is known to be an essential component of splicing machinery thus shows ubiquitous expression. The Cas9 enzyme is expressed from the pJW1259 vector under *erf-3* promoter, specifically design for the deletion in *C. elegans* (Ward, 2015). The Selection Excision Cassette (SEC) containing plasmid were used which has three parts. 1) The hygromycin resistance gene, allowing modifications in wild type or any genetic background. 2) The sqt-1(e1350) gene mutation which gives a dominant roller phenotype once it inserted into the genome. Thus, helps in analysing the homozygous insertion and excision based on the phenotype and 3) the heat shock promoter driven Cre recombinase, once it got activated the entire selection cassette excise from the genome. The SEC from the plasmid pDD287 was cloned along-with flanking loxP sites into pPD95.75 vector. The resulting plasmid was used to clone homology arms (500-600bp) besides the loxp sites using restriction enzyme based cloning methods.

The plasmid mixture containing repair template (40ng/µl), sgRNA_1 (10ng/µl), sgRNA_2 (10ng/µl), pJW1259 (50ng/µl), pCFJ90 (2.5ng/µl) and p*vha-6*::mCherry (15ng/µl) was injected into 20-30 adult hermaphrodite animals (containing 4-5 eggs).

Molecular mechanism of CRISPR/Cas9 and selection of *srx-97* mutant worms

The CRISPR/Cas9 mechanism is widely studied and used for genome editing (Dickinson and Goldstein, 2016; Jiang and Doudna, 2017). Here, a source for the Cas9 enzyme, we used the plasmids (pJW1259) having a Cas9 gene (Ward, 2015). The two different targeted 20 bp gRNA designed and sequenced from *the srx-97* gene and was cloned in the two separate plasmids (pRB1017) having the gRNA scaffold (Arribere et al., 2014). The homology arms were cloned in a separate plasmid having SEC cassette. After injection, the Cas9 enzymes with gRNA (Cas9-gRNA) firstly recognize the PAM sequence, which is present immediately downstream of the target sequence in the *srx-97* gene. Once the PAM sequence identified, the gRNA forms watson crick base pairing with the target sequence of *srx-97* gene. The binding of CRISPR/Cas9 on the target sequence activates the helicase and endonuclease activity, leading to a double-stranded break in the genomic DNA. In the case of *srx-97* gene, the break occurs in the first exon and near the 3' UTR region of the gene. The gene gets deleted from two sides, and the fragment gets degraded.

The SEC cassette having the homology arm of about 500-600 bp with the *srx-97* gene was used for homologous recombination. After homologous recombination, the cassette is integrated into the genome of *C. elegans* genome. The first confirmation of cassette integration is the worms become resistant to antibiotic hygromycin and shows fluorescence. We can select these worms and check the dominant roller phenotype. Once the cassette is integrated into the genome of worms, the progeny laid by transgenic worms shows the 100 percent penetrance of the roller phenotype. The selection cassette can be removed from the genome of these transgenic worms by simply giving heat shock (34^oC). The normal non-fluorescent worms selected for analyzing the deleted genomic sequence of *srx-97* gene through the PCR or sequencing.

In brief, the worms were kept at 20C. Hygromycin was added after the 60 hrs of injection, directly on the worms containing plate. The hygromycin treated plates were left for 10 days at 20C. Next 20-30 non fluorescent rollers were single out on normal seeded NGM plates after 10 days. Once the 100% roller progeny were observed on the plates, to remove the SEC from such worms, kept these plates at 34^0C for 3-4 hrs. The normal moving worms then picked and allow to

be grown for their progeny. The genomic DNA was isolated from these worms, confirms the desired deletion using PCR and sent it for sequencing.

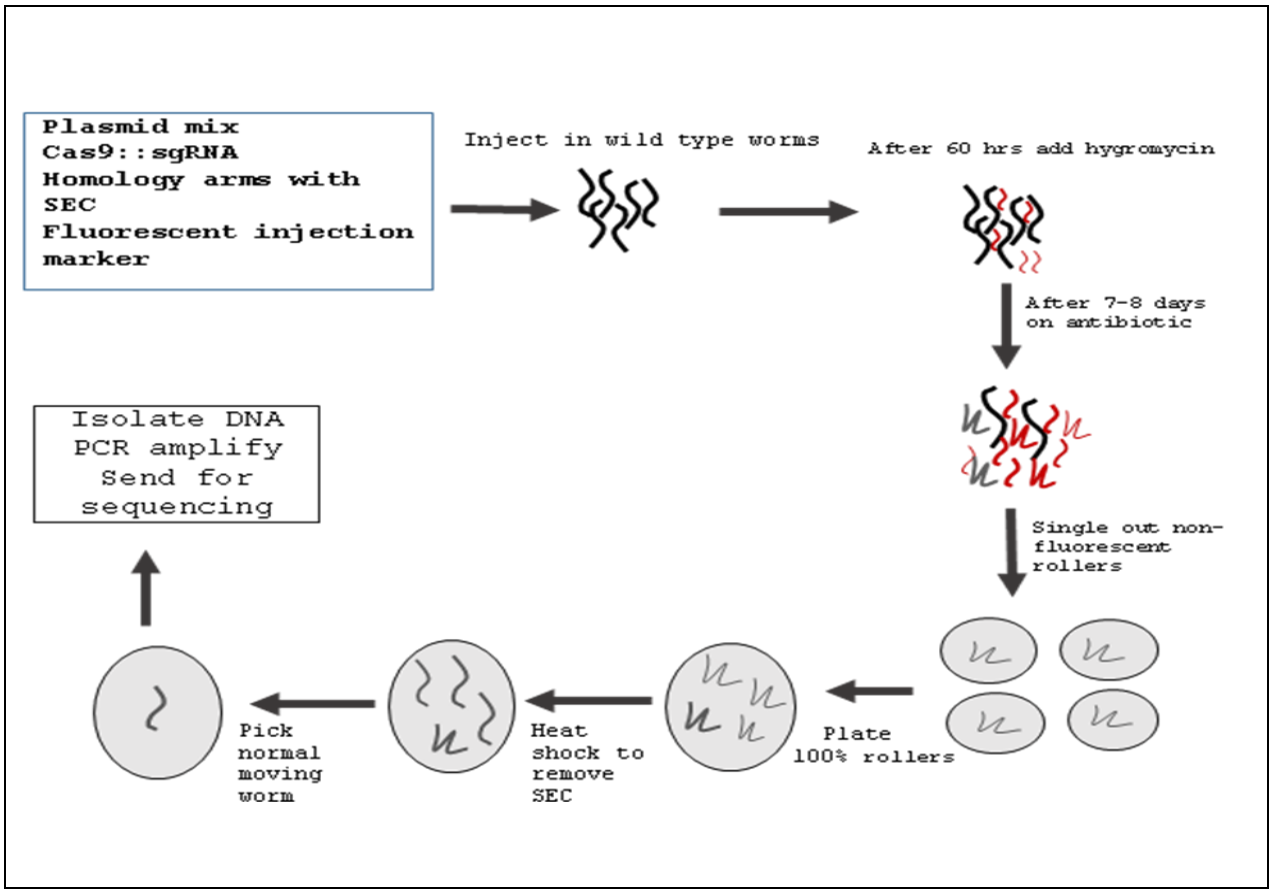

Figure 2.1 CRISPR/Cas9 mediated *srx-97* gene.

The flow chart of CRISPR/Cas9 mediated deletion of *srx-97* gene. The plasmid mix was injected in 25-30 wild type worms. Post 60 hrs of injection added the hygromycin (250µgml) on the plates containing the progeny of worms. Only the hygromycin resistance worm grows on the antibiotic plates. From such plates single out 30-40 non-fluorescent worm, showing expression of dominant roller phenotype. Check the plates for the 100% roller progeny, which confirms that CRISPR/Cas9 works and SEC cassette integrated into the genome of the worm. To remove the SEC, heats shock 40-50 L1-L2 worms at 34^0C for 3-4hrs from plate having 100% roller progeny. Next pick the normal moving worms and PCR or sequenced the modification in gene of interest.

Chapter 3

To explore the endocytic role of EHD1, an EH domain containing protein in the intestine of *C. elegans*

3.1 Introduction

Endocytosis and recycling pathways are important for cells to maintain healthy cellular physiology like nutrient uptake and presentation of various molecules or receptors on the plasma membrane. The endocytic recycling compartment (ERC), which is a dynamic organelle having a network of membrane tubules and vesicles in the perinuclear region, manages the recycling process (Grant and Donaldson, 2009; Maxfield and McGraw, 2004). After endocytosis, various membrane-bound and soluble cargoes delivered in the ERC; these are further sorted and recycled back to the plasma membrane through transport carriers. The mechanism of how the transport carriers released from the ERC is still largely undefined. Recent studies attribute recycling functions to an ATP-binding Eps15-homology domain-containing protein (EHD1), having a C-terminal EH domain (Caplan et al., 2002; Grant and Caplan, 2008; Lin et al., 2001b). Mammals have 4 EHD paralogs, EHD1-4, which shows a ~70% amino acid identity to each other. Despite such high sequence similarity, EHD proteins localized to different cellular compartments. EHD1 and 3 localized to the ERC, EHD2 is present at the plasma membrane while EHD4 localized to a Rab5-positive early endosome (Blume et al., 2007; Daumke et al., 2007; Sharma et al., 2008).

A previous report showed that the depletion of EHD1 leads to enlargement of ERC while the addition of purified EHD1 restores its normal tubular morphology (Cai et al., 2013, 2012; Lee et al., 2015). Thus, EHD1 was proposed to be involved in membrane remodeling and fission at the ERC (Lee et al., 2015). The structure of EHD proteins contains a dynamin-like, ATP-binding G-domain, which self-assembles on tabulated liposomes having electron-dense coats, and in turn, stimulates ATP hydrolysis (Daumke et al., 2007; Pant et al., 2009). These structural similarities would suggest that EHDs function in the same way as classical dynamins for remodeling and fission of the membrane (Daumke et al., 2007). Regardless of these insights, the exact mechanisms of ATP hydrolysis in EHD1's membrane remodeling functions remain uncharacterized.

Studies in model organisms with a single ortholog of EHD, most similar to EHD1 in mammals, have revealed functions associated with endocytosis and recycling. The Past1 ortholog in *D. melanogaster* is known to be involved in endocytosis (Koles et al., 2015). The *C. elegans* single ortholog, RME-1, promotes the recycling of internalized receptors from the ERC to the plasma

membrane (Grant et al., 2001). To understand the role of EHD1 in recycling, we used the cross-complementation assay in *C. elegans* and found that the ATP hydrolysis and membrane binding activities of EHD1s are necessary for endocytic recycling (in collaboration with Pucadyil's laboratory). The behavior of EHD1 was further analyzed using purified EHD1 that was reconstituted in an *in vitro* reconstitution assay having the template mimicking the tubular morphology of ERC (Pucadyil's laboratory performed this work). Our results specify that for the functional activity, the ATP bound EHD1 favors the high-positive membrane curvature to bind and form the active membrane scaffold, which bulges the underlying tube. Further, the ATP hydrolysis causes the bulge to expand, and the intermediate thin region undergoes fission. The N terminal region of EHD1 is important for forming the stable scaffold on the membrane, as deletion of these residues causes a defect in recycling activity.

3.2 Results

3.2.1 EHD1 rescues the vacuolated intestinal phenotype in *rme-1* mutants

A Supported membrane tube assay system (SMrTs) was used to screen and analyze molecules involved in membrane fission reaction in real-time (Dar et al., 2017). The EHD1 protein was found to have membrane fission ability in SMrTs from goat brain extract in Pucadyil's lab (www.pucadyillab.com). The role of EHD1 in the recycling process and its structural similarity with the dynamin indicate that EHD1 could be involved in the fission process at the membrane.

EHD1 depletion or Knocked out in mammalian cells shows a slightly delayed recycling process from the ERC due to compensatory mechanisms from the other paralogs of EHDs (George et al., 2007; Lee et al., 2015; Rapaport et al., 2006). The *C. elegans* single ortholog RME-1 shows 67% identity over its entire length with the human EHD1 (Grant and Caplan, 2008a). RME-1 (Receptor-mediated endocytosis) is known to be involved in a similar process on recycling endosomes (Grant et al., 2001). In the case of the intestinal epithelial cells of *C. elegans*, a null mutation in *rme-1* shows large vacuoles due to a defect in the recycling of basolateral transport vesicles (**Figure 3.1C**) (George et al., 2007; Grant et al., 2001). The endocytosed vesicles continuously fuse to the ERC with no way out, causing the ERC to expand. This can be visualized as vacuoles in the intestine of worms (**Figure 3.1A**). The increased number of vacuoles can be visualized in *rme-1* mutants by injecting Texas Red-labeled bovine serum

albumin (TR-BSA) in the pseudocoelom (body cavity) of worms (George et al., 2007; Grant et al., 2001), these vacuoles are not seen in the intestine of wild type worms (**Figure 3.1B**). Previous reported have indicated that the vacuoles in the intestine of the *rme-1* mutants could be rescued by the expression of EHD1 under intestine-specific promoter (P*vha-6*) (George et al., 2007). In order to reconfirm these results, we expressed WT EHD1 in *rme-1* mutant background and found that this construct could rescue the *rme-1* phenotype significantly (**Figure 3.1D and E**). These experiments show the evolutionarily conserved function of EHD1 across species.

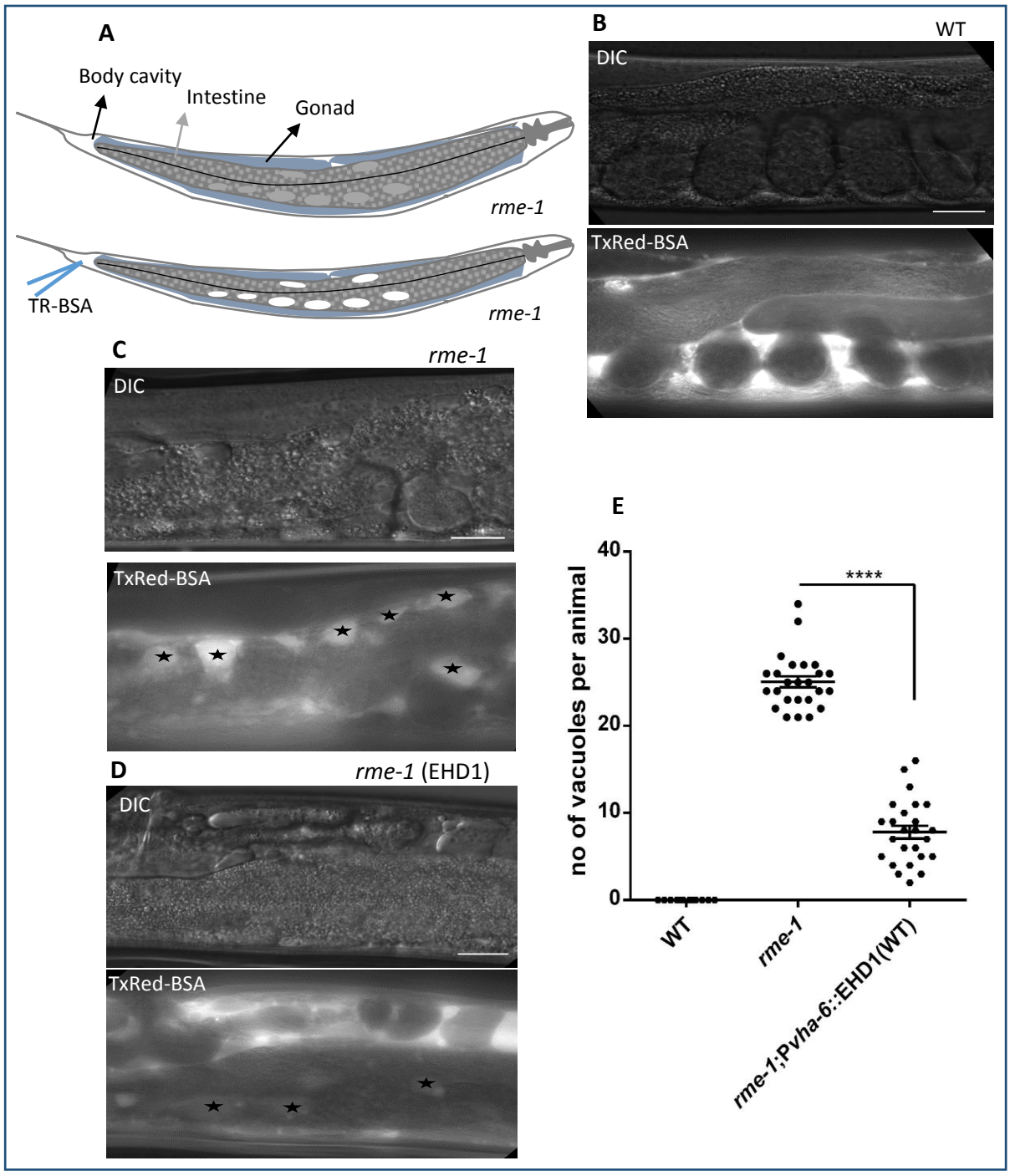

Figure 3.1 EHD1 rescues the vacuolated intestinal phenotype of *rme-1* mutants

A) Cartoon showing the *rme-1* mutant worms, vacuoles in the intestine becomes visible upon uptake of TxRed-BSA which is injected in the pseudocoelom of the worms B) The vacuoles are not seen in the wild type (WT) worms. C) The vacuoles become visible in *rme-1* mutant worms. D) Significantly rescue of the *rme-1* phenotype was seen by expressing the EHD1 (WT) ortholog under an intestine-specific promoter. Asterisks mark vacuoles. The vacuoles are counted per worms and dot is plotted. Scale bars = 20 μm (E). Statistical significance was calculated with student unpaired two-tailed *t*-test and ****$P < 0.0001$

We used this cross-complementation assay in *C. elegans* to study the function of different domains of EHD1 in endocytic recycling. This work was in collaboration with Pucadyils laboratory, where they developed an *in vitro* assay using purified EHD1 protein and liposomal membranes. Mainly phosphatidylserine (PS) is used to make the liposomal tubes as reported; it recruits the EHD1 on ERC (Lee et al., 2015).

3.2.2 The ATPase domain of EHD1 is necessary for the endocytic recycling

The molecular structure and domains involved in membrane modeling are widely studied for the EHD2 protein. EHD2 shows a 70% amino acid identity with the EHD1, suggesting that most of the domains conserved between these two molecules. The EHD2 ATPase domain is known to be essential for membrane remodeling, as mutations in the ATP binding region and ATP hydrolysis domain show aberrant phenotypes (Daumke et al., 2007). A mutation in the phosphate-binding (p-) loop, T72A, which similarly prevent ATP binding like other GTPases, shows the distribution of EHD2 (T72A) in the cell cytoplasm while wild type EHD2 localize on the endomembrane (Daumke et al., 2007). We propose that these mutations in EHD1 could show the same phenotype. The WT EHD1 rescues the vacuolated phenotype significantly. However, a mutation in the phosphate-binding domain of EHD1 (T72A) in the *rme-1* mutant background showed no rescue of the phenotype (**Figure 3.2A, B, and D**), suggesting that the ATP binding domain is important for oligomerization of EHD1 in the recycling endosomes.

Likewise, the mutation in the ATP hydrolysis domain (T94A) of EHD2 shows the normal membrane localization but defective membrane hydrolysis, causing increased tubular structure to compare to the WT EHD2 (Daumke et al., 2007). Similarly, the EHD1 (T94A) rescue line shows the significant number of vacuoles compared to the WT EHD1 rescue line (**Figure 3.2A, C, and D**). Further, suggesting the importance of the hydrolysis domain in EHD1 membrane fission reactions.

Thus, these results strongly suggest that ATP binding and ATP hydrolysis activity are also necessary for EHD1 functions in recycling endosomes. Similar results were also seen by using the liposome co-sedimentation assays and different analogs of ATP like non-hydrolysable analog (AMP-PNP), the slowly hydrolyzing analog (ATP-γ-S) and ADP (Pucadyil's laboratory).

Together these data suggest that that ATP binding and hydrolysis activity is necessary for the EHD1 functions, and EHD1 favors curved membrane surface like tubules (Deo et al., 2018).

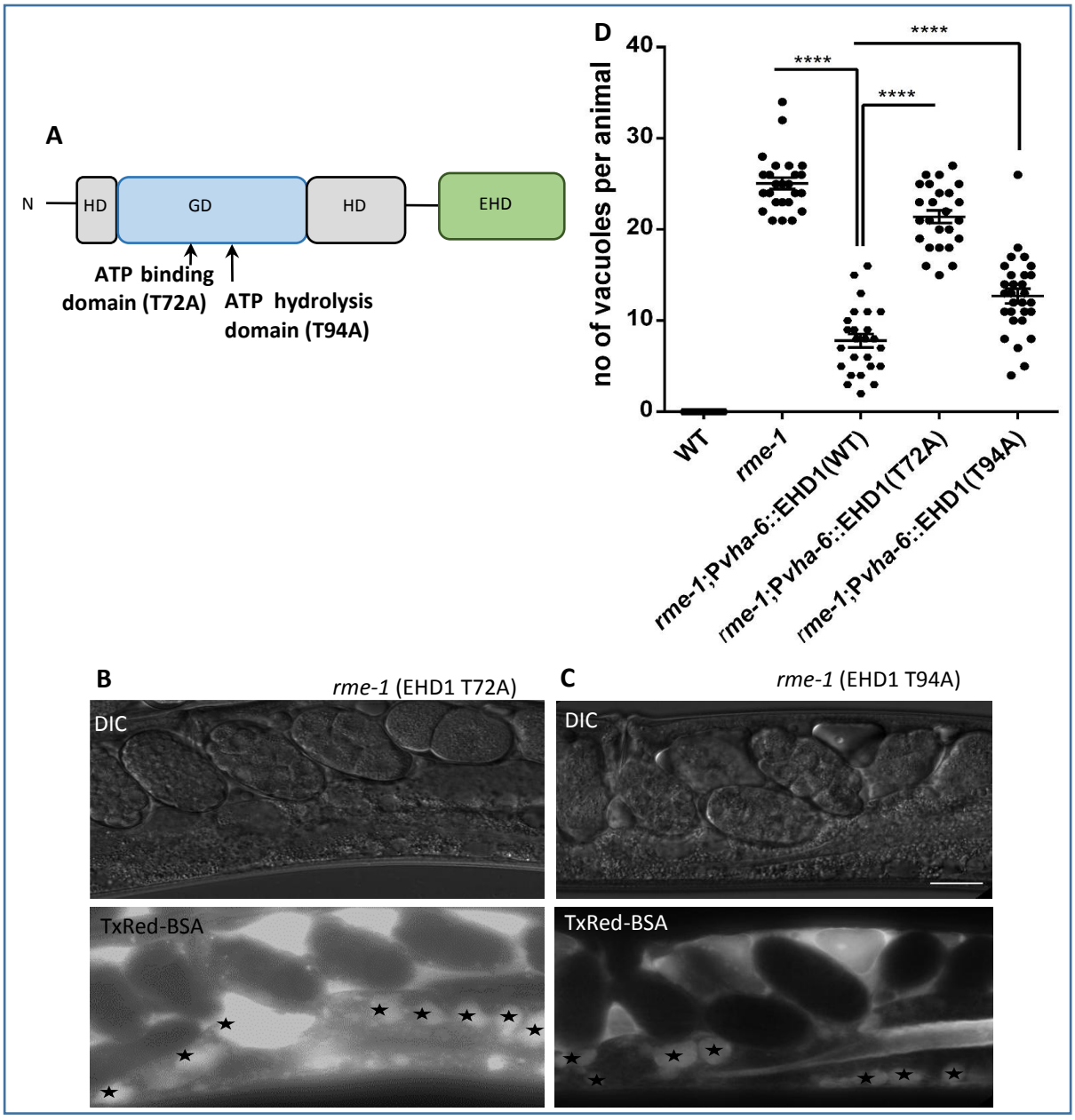

Figure 3.2 EHD1 rescues the vacuolated intestinal phenotype of *rme-1* mutants

A) Cartoon image showing the EHD1 protein, with the point mutations in ATP binding and hydrolysis domains. B) The vacuoles are seen in (DIC) and become visible after TxRed-BSA injection in the EHD1 (T72A) rescue line and C) EHD1 (T94A) rescue line under intestine-specific promoter. Asterisks mark vacuoles. D) The dot plot is showing the number of vacuoles counted per worms. Scale bars = 20 µm. Statistical significance was calculated with student unpaired two-tailed *t*-test and ****$P < 0.0001$

3.2.3 The N-terminal domain and the second helical domain cause defects in stable scaffolding of EHD1 on the recycling endosomes

The N-terminal residues are partially conserved among EHD family members (**Figure 3.3A**). Various studies propose that the N-terminal region of EHDs helps in allosteric conversion from closed auto-inhibited states in solution to an open, active state on the membrane. In addition, the N-terminal region of EHD2 is involved in binding and segregating with the membrane of liposomes (Shah et al., 2014). To look at the role of EHD1 N-terminal, we made small deletions in the N-terminal domain of EHD1 (Mutations made in Pucadyil's lab). We next used these constructs for cross complementation in *rme-1* mutant worms. We found that the deletion in the N-terminal domain of EHD1 could not rescue the *rme-1* phenotype (**Figure 3.3A, C, and D**). Additionally, in vitro assay of EHD1 (Δ2–9) with liposomal tubes further proved that there is less bulging and no fission of the membrane with this N-terminal deletion (Deo et al., 2018a). These results indicate that the deletion of the N-terminal region of EHD1 causes instability in scaffold formation, which then leads to a defect in membrane fission.

The polybasic stretch of amino acids near the second helical domain is involved in membrane binding in the EHD2 protein. An F322A mutant in EHD2, converting lysine to alanine, causes the distribution of this protein in the cytoplasm instead of endomembrane. In the case of EHD1, the mutation in the second helical region does not rescue the *rme-1* mutant phenotype (**Figure 3.3A, B, and D**), suggesting that the second helical domain is important for binding and localization of this protein to the membrane. These results confirm what was seen with the co-sedimentation assay of purified EHD1 with the membrane containing anionic phosphatidylserine (PS) (Deo et al., 2018),suggesting that the EHD1 activity gets stimulated after the helical domain binding to the membrane-, similar to dynamin (Ramachandran and Schmid, 2008).

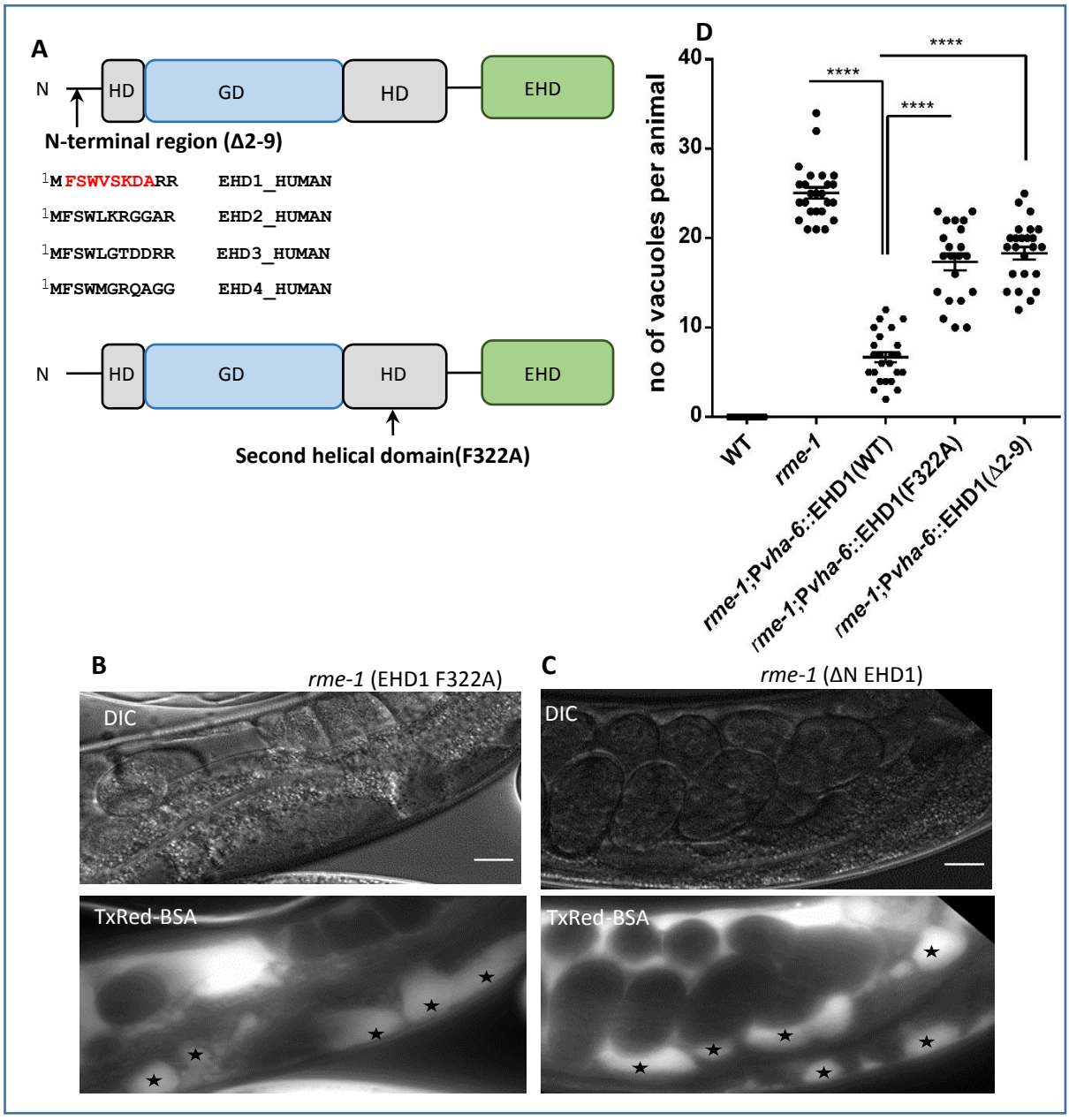

Figure 3.3 EHD1 variants rescue the vacuolated intestinal phenotype of *rme-1* mutants

A) Cartoon showing the variants of EHD1 protein, the mutation in the second helical domain and N-terminal region along with the alignment with other EHDs. B) The vacuoles are seen in (DIC) and become visible after TxRed-BSA injection in pseudocoelom EHD1 (F322A) rescue line and C) EHD1 (Δ2-9) rescue line under intestine-specific promoter. Asterisks mark the vacuoles. D) The dot plot showing the number of vacuoles counted per worms. Scale bars = 20 µm. Statistical significance was calculated with student unpaired two-tailed *t*-test and ****$P < 0.0001$

3.2.4 In vitro study of EHD1

In Pucadyil's lab, using purified EHD1 in SMrT based test, they found that EHD1 functional domains (ATP binding and ATP hydrolysis) play an important role in binding of EHD1 to the reconstituted lipid membranes. The ATP binding facilitates the recruitment of EHD1 on the membrane, and the hydrolysis of ATP causes its dissociation from the membrane.

Further studies using different non-hydrolysable analogs of ATP such as AMP-PNP, the slow hydrolyzing analog ATP-γ-S, and ADP were used to study the ATPase cycle of EHD1 controlling membrane remodeling and scission at different stages. They found that the EHD1 scaffold on the membrane tubes forms a brighter bulge with varying tube range (10-25 nm), whereas the dynamin scaffold labelled region shows dim membrane fluorescence with constant radius of the tube (11 nm) (Deo et al., 2018). These results suggest that EHD1 scaffold causes remodeling of the membrane and scission differently than the classical dynamin. Further STED (Stimulated emission depletion) microscopy and coarse-grained molecular dynamics simulations demonstrate that EHD1 mediated membrane remodeling and scission involves a mechanism that is different from that of classical dynamin (Deo et al., 2018).

3.3 Discussion

Our collaborative results on EHD1 suggest a new, unusual mechanism in the EHD1 function. The foundation of protein scaffolds governs membrane remodeling, and previously reports suggest that the BAR family of proteins tabulates the membrane, and dynamin is involved in the constriction of the underlying membrane (Daumke et al., 2007; Jarsch et al., 2016; McMahon and Gallop, 2005). This study, along with results from Pucadyil's laboratory shows that EHD1 causes bulging of the membrane. The exact molecular mechanism is not yet completely known; we speculate that the scissor shaped EHD dimer forms a convex-shaped membrane-binding surface, to which lipid binds and forms a bulge like structure. The GTPase activity causes constriction in dynamin, while ATP hydrolysis assists the formation of self-assembly of EHD1 in the membrane (**Figure 3.4**) (Carr and Hinshaw, 1997; Chappie et al., 2010). However, for a more extended period, ATP hydrolysis caused the dissociation of EHD1 from the membrane. The N- terminal region, due to their interaction with the membrane, confers stability to the

EHD1 scaffold in the presence of ATP induced disassembly. Although mutations in N –terminal region of EHD1 forms a scaffold and causes membrane bulging, the protein complex disappears once it comes in contact with ATP (Deo et al., 2018).

The in vitro reconstitution and molecular dynamic simulation results (www.pucadyillab.com) explain an inherent activity of EHD1 to remodel and cause membrane scission (Deo et al., 2018). The self-assembled scaffold of EHD1 causes bulges on the limited tube, which further causes thinning of the adjacent area resulting in the fission on the tube, suggesting the unique way of EHD1 catalyzing membrane remodeling which further leads to fission on the same tube. We propose that EHD1 works in the same way on ERC tubes. It has been reported that mutation in EHD1 causes expansion of the ERC tubules supporting our hypothesis that membrane modeling causes scission in the tubes (Cai et al., 2012; Lee et al., 2015).

Membrane cargo sorting and vesicle fission are essential steps in endocytosis and are regulated by different proteins in a spatiotemporal manner. In clathrin-dependent endocytosis, the adaptor bound cargos manage the early sorting. Further, the complex of protein binding partners causes an increase in membrane curvature, which leads to transient recruitment of dynamin on the neck, causing fission. At steady-state, ERC contains ample amounts of lipid and proteins binding partners of EHD1. Moreover, at the early endosome, the kinesin motor protein KIF3A generates tubules and sorts the soluble and membrane-bound cargos based on geometry sorting (Delevoye et al., 2014; Maxfield and McGraw, 2004). Since curvature is an important determinant of the EHD1 function, it could be working in the same way as bulging and fission of the ERC tube in vivo for membrane-bound cargos. However, for soluble cargoes, the intermediate hemi fusion steps should be non-leaky to protect the cargos inside the vesicles. Unlike dynamin (Antonny et al., 2016; Dar et al., 2017), EHD1 mediated fission appears to be an indirect mechanism and could become active with the help of BAR proteins which may reduce the membrane flow or recruitment of an unidentified protein to catalyze the fission on bulge induced thin tubes.

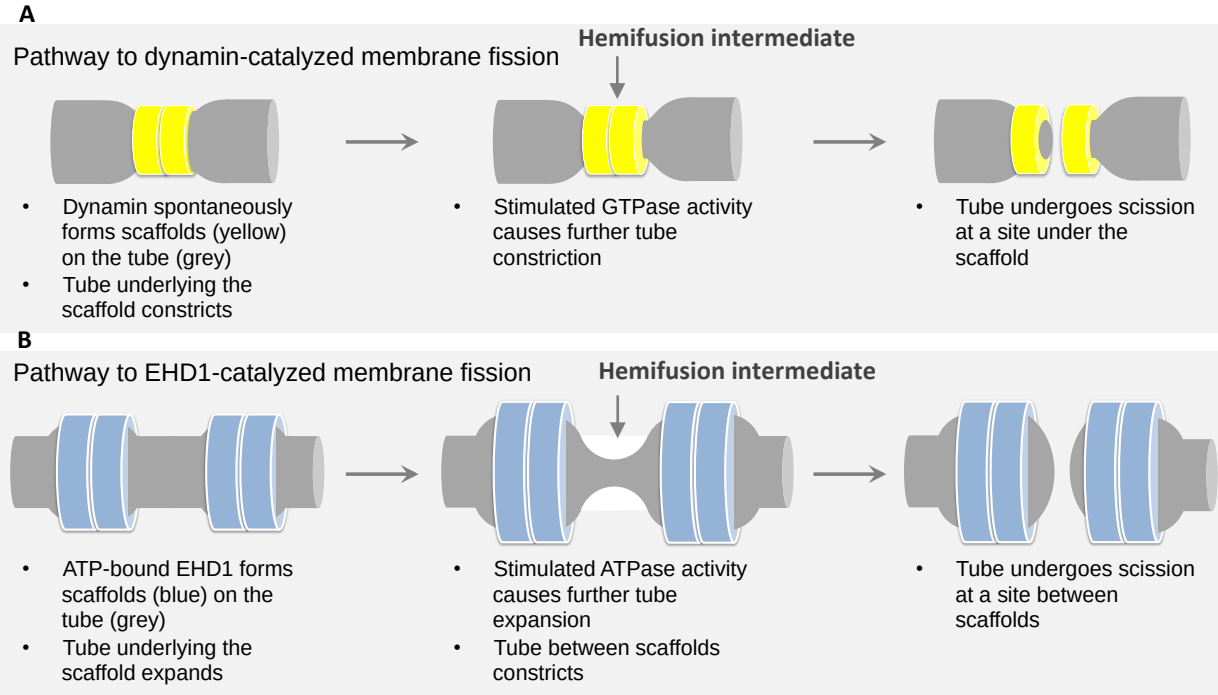

Figure 3.4 Proposed model for dynamin and EHD1-catalyzed membrane fission

(A) Addition of dynamin (yellow) to a membrane tube (grey) leads to spontaneous self-assembly of a scaffold, which constricts the underlying tube. Stimulated GTP hydrolysis by the scaffold induces further tube constriction and subsequent scission at a site under the scaffold. B) ATP-bound EHD1 forms a scaffold that leads to a bulging-out of the underlying tube. Stimulated ATP hydrolysis leads to further tube expansion and in parallel constriction at regions between scaffolds. Tube scission occurs at a site adjacent to the scaffold. Image courtesy Pucadyil lab.

Both models predict that EHD1 is necessary but not sufficient to catalyze membrane fission. It will be interesting to find the new molecule which synergizes with EHD1 activity through which they control the release of transport carriers from ERC; this hunt will open new opportunities for future research.

Chapter 4

To explore the endocytic role of RME-1, an EH domain containing protein in the interneurons of *C. elegans*

4.1 Introduction

The constant recycling of α-amino-3-hydroxy-5-methyl-4-isoxazole propionic acid (AMPA)-type glutamate receptors (AMPARs) in and out of synaptic membranes is a crucial mechanism involved in the maintenance of excitatory synaptic strength. Research has shown that the addition of functional AMPARs into the plasma membrane strengthens synapse and signaling (Kennedy, 2016). Thus the addition and removal of functional receptors in an experience-dependent manner underlie fundamental network properties like learning and memory (Jackson and Nicoll, 2011). Since the neurons are complex polar cells, most of the synapses are far away from the cell body, hence maintaining synaptic strength is the major challenge for the synaptic machinery. Various mammalian studies have provided an insight into the long-range supply of AMPA receptors at synapses through local synthesis, lateral diffusion, and motor-dependent transport (Adesnik et al., 2005; Greger and Esteban, 2007; Ho et al., 2011). Once the receptors reach the synapse, multiple proteins in the endosomal trafficking machinery are involved in regulating the strength of the synapse (Lasiecka and Winckler, 2011). Thus, the molecular machinery required for transport, endocytosis, as well as intracellular membrane trafficking processes, eventually maintain the quality of the signal transmitted at each synapse.

Different endocytic pathways have been reported to be involved in regulating synaptic strength (Glebov et al., 2015; Jung and Haucke, 2007). One pathway is the clathrin-dependent pathway, where the transmembrane regions of the receptors, along with the different adaptor proteins, recruit clathrin molecules on the budding vesicles. Once the vesicle is released from the membrane, the clathrin lattice is removed, and the vesicle fuses to early endosome. These trafficking events are regulated by the small RAB family of GTPases, Rab-5 (Brown et al., 2005). Likewise, Clathrin independent pathways are known to be involved in the regulation of AMPARs numbers at the synapse (Glebov et al., 2015). Clathrin-independent endocytosis also occurs in cholesterol and lipid raft rich microdomains of the plasma membrane; RAB-10 GTPase is known to be involved in regulating the endocytosis of GLR-1, an AMPA receptors subunit in *C. elegans* (Glodowski et al., 2007). Once the endocytic vesicles reach the early endosome, due to its acidic pH, the receptor gets separated from its ligand and is recycled back to the plasma membrane or stored in recycling endosomes. Thus, recycling occurs through direct or a fast pathway through early endosomes and indirect or slow pathways through the recycling

endosomes. The recycling endosomes are reported to regulate receptor recycling through the clathrin-dependent/independent pathways.

The recycling endosomes (REs) are known to have a multi-tubular and dense vesicular morphology suggesting intense dynamic activity in the endosomal compartments (Goldenring, 2015; IJzendoorn, 2006; Marsh et al., 1995). Moreover, it is reported that different endocytosed receptors follow different routes for recycling (Goldenring, 2015). In highly polar cells like neurons, recycling endosome morphology and distribution is very different than in non-neuronal cells. At the region of the active synapse, local endocytic vesicles or recycling endosomes are present to regulate synaptic strength. The small GTPase Rab11 is associated with the recycling endosome and involve in membrane trafficking in a region of dynamic membrane reorganization. Recently the EH domain-containing molecule EHD1/RME-1 was identified on the recycling endosome, and mutations in *rme-1* were shown to cause delayed recycling of several important receptors in cell lines (Grant and Donaldson, 2009a). In the case of neuronal cells, it is reported to regulate the AMPA receptor trafficking at the synapse (Koles et al., 2015; Park, 2004).

AMPA type subunits, GLR-1 and GLR-2, are encoded by the *C. elegans* genome. Previously it was reported that GFP labeled GLR-1 receptors localize to post-synaptic sites and act as functional receptors (Rongo et al., 1998). The functional GLR-1 receptors in interneurons are required to maintain sensory circuits, which control the backward movement or reversal and nose touch response in worms (Glodowski et al., 2007). An increase or decrease in synaptic GLR-1 levels is associated with defects in reversal frequencies and nose touch behavior in *C. elegans* (Hart et al., 1999; Zheng et al., 2015). Hence, by comparing the GLR-1 mediated behavior in the different genetic backgrounds, one could get insight into the abundance of functional GLR-1 receptors at the post-synaptic plasma membrane.

GLR-1 receptor abundance is maintained by clathrin-dependent and independent pathways in *C. elegans*. Mutation in *unc-11* (a clathrin adaptor protein) and *rab-10* (a small GTPase), shows increased accumulation of GLR-1 at synaptic sites (Burbea et al., 2002; Glodowski et al., 2007). Here we look at the role of RME-1 protein in recycling endosomes. We found that mutations

in *rme-1* show increased the accumulation of GLR-1 at distal synaptic sites and reduce the level of reversal frequency. This phenotype could be rescued by expressing *rme-1* under a glutamatergic neuron-specific promoter, suggesting the role of RME-1 in recycling endosome of neurons and in the regulation of glutamate receptor trafficking in worms.

4.2 Results

4.2.1 Mutation in *rme-1* shows decreased GLR-1 signaling

In the epithelial cells of the intestine, RME-1 is known to be involved in regulating the recycling or trafficking of molecules (Grant et al., 2001b; Grant and Caplan, 2008b). Further, the mechanism and binding of RME-1/EHD1 has been recently shown to be involved in the scission like activity at the Endosomal recycling compartment (ERC) in the epithelial cells of the intestine (Deo et al., 2018) and the previous chapter). It is known that RFP::RME-1 shows punctate localization in the ventral nerve cord of the worms (Glodowski et al., 2007). However, the role of RME-1 in the *C. elegans* nervous system is largely unknown.

Previously it was reported that in *Drosophila melanogaster* and hippocampal cell lines, AMPA receptor trafficking is regulated by EHD1 ortholog (Koles et al., 2015; Park, 2004). The command interneurons of *C. elegans* are shown to express AMPA type glutamate receptors GLR-1 in the post-synaptic region (Rongo et al., 1998). The GLR-1 receptors in the command interneurons maintain the reversal behavior of the worm during spontaneous locomotion (Brockie et al., 2001; Zheng et al., 2015). Based on these reports, we hypothesized that *rme-1* mutation could cause defects in GLR-1 receptor trafficking in the *C. elegans* nervous system and affect reversals. To understand the role of RME-1 in reversal, we performed spontaneous reversal assay and found that *rme-1* mutant worms showed reduced reversal frequencies (**Figure 4.1 and Movie1 and 2**). We further reconfirmed this phenotype by using a rescue construct containing the full-length genomic *rme-1* under its own promoter (P*rme-1*) and the intestine-specific promoter (P*vha-6*) in *the rme-1* mutant background. The endogenous promoter showed rescue of the reversal phenotype, but the expression of RME-1 under the intestine-specific promoter showed no rescue (**Figure 4.1 and Movie7**). The genomic RME-1 without the promoter was used to check any internal promoter but showed no rescue (**Figure 4.1**). Further, to check the role of RME-1 in GLR-1 receptor recycling, we cloned the *rme-1* gene (genomic)

under the *glr-1* promoter (glutamatergic neurons specific promoter), which shows expression in the command interneurons (Rongo et al., 1998). We found that this construct rescued the reversal phenotype, and the rescued animals showed reversal frequencies indistinguishable from wild type (WT) (**Figure 4.1 and Movie3**). Thus, suggesting the role of RME-1 in GLR-1 receptors recycling in the interneurons of *C. elegans.*

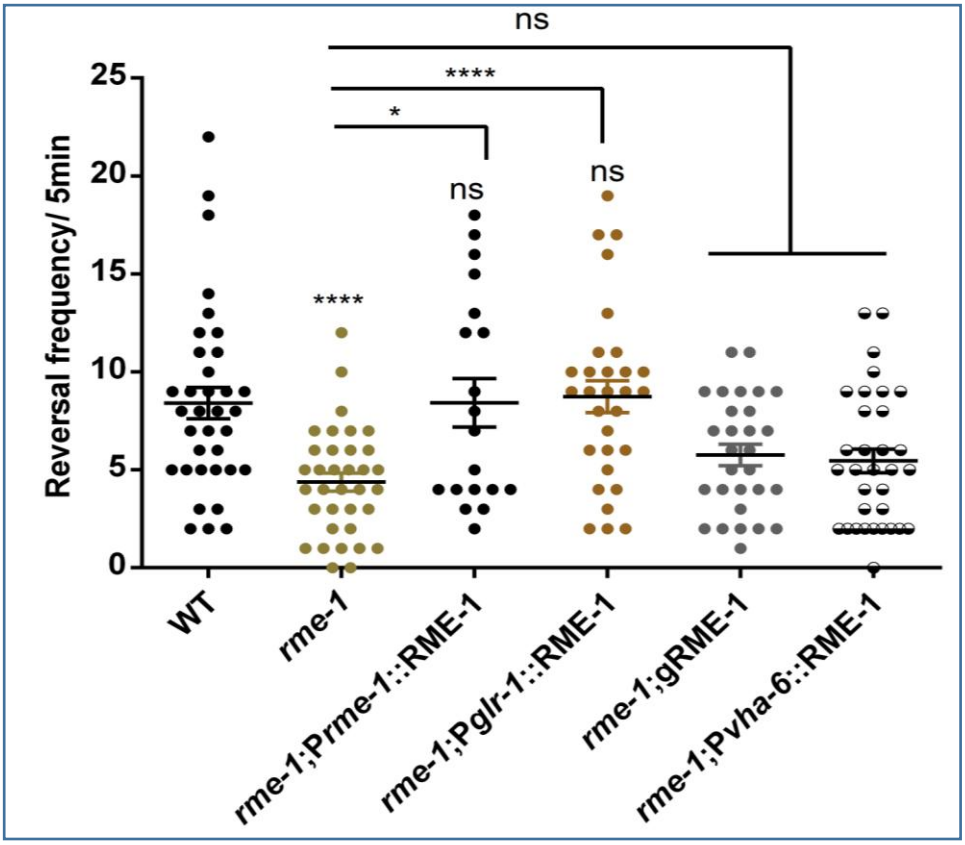

Figure 4.1 *rme-1* mutants show a reduced level of spontaneous reversal frequency

Reversal assay results of *rme-1* mutants and their rescue lines. First two dot plots show the reversal frequency in WT and *rme-1* mutant worms. The reduced number of reversal frequency is rescued by expressing *rme-1* gene under endogenous promoter (P*rme-1*), glutamate neurons specific promoter (P*glr-1*), intestine specific promoter (P*vha-6*) and control genomic *rme-1* without any promoter. In this dot plot, numbers of worms scored for reversal assay are defined by the dots. Each dot represents the number of spontaneous reversals per five minutes from one worm. The error bars represent the SEM and statistical significance (one-way ANOVA) is represented as "ns" for not significant, "*" $p<0.05$, and "****" $p<0.0001$

Based on these studies and decreased reversal frequency of *rme-1* mutants, we postulated that RME-1 could be affecting glutamatergic signaling through GLR-1 receptors in command

interneurons. If RME-1 were involved in the recycling of GLR-1 receptors, then the reversal frequency of *rme-1;glr-1* double mutants would be comparable to the *glr-1* single mutants. Mutations in *glr-1* have already been shown to have a reduced level of reversal frequency (Zheng et al., 1999), the double mutant of *rme-1*; *glr-1* shows a reduction in reversal frequency similar to the *glr-1* single mutants (**Figure 4.2 Movie 3 and 8**). Further, suggesting that along with other endocytic molecules, *rme-1* plays an important role in regulating the transport of GLR-1 containing vesicles from the endosome.

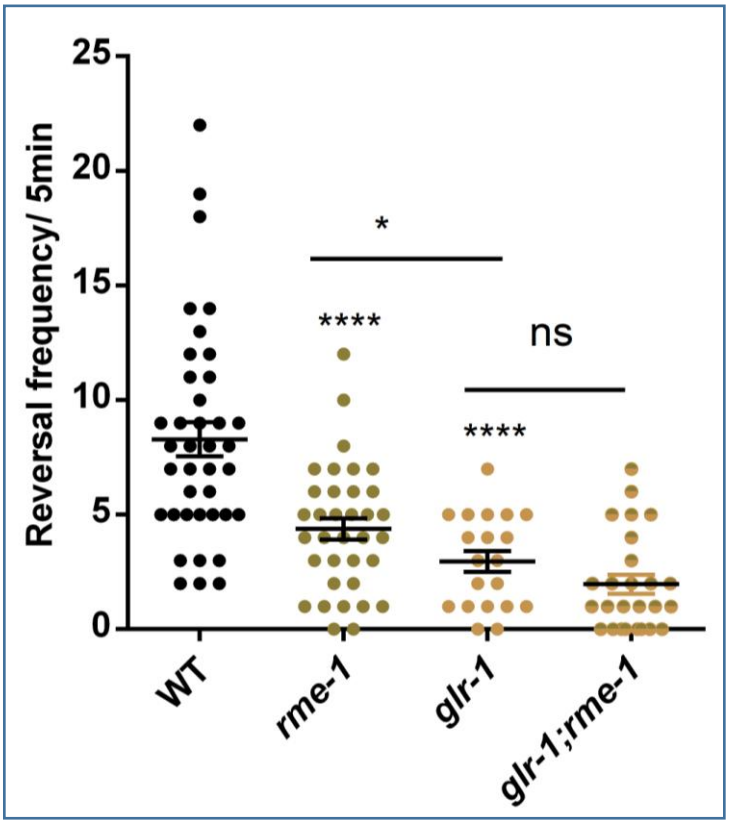

Figure 4.2 RME-1 based regulation of reversal behavior could occur through GLR-1

Reversal assay results of *rme-1* mutants, *glr-1* mutants, and *rme-1;glr-1* double mutants with WT controls. The double mutant (*rme-1;glr-1*) shows the similar phenotype like the single *glr-1* mutant. Signifying both molecules are in the same pathway. In this dot plot, the numbers of animals scored for reversal assay are defined by a dot. Each dot represents the number of spontaneous reversals per five minutes from one worm. The error bars represent the SEM and statistical significance (one-way ANOVA) is represented as "ns" for not significant, "*" $p<0.05$, and "****"$p<0.0001$

4.2.2 RME-1 is required for recycling AMPA GLR-1 receptors at the distal synapse

Previously it was shown that the genomic region of *glr-1* tagged to GFP (GLR-1::GFP) could be used to visualize synaptic structures in transgenic worms (Rongo et al., 1998; Rongo and Kaplan, 1999). In transgenic worms GLR-1::GFP receptors were expressed and found in a punctate pattern in the ventral nerve cord interneurons. These ventral cord puncta form synaptic connections with the several presynaptic neurons (Burbea et al., 2002; Rongo et al., 1998). The size and numbers of this GLR-1::GFP puncta in the ventral cord can be calculated by quantitative fluorescence microscopy. To estimate the total abundance of GLR-1::GFP in the ventral nerve cord, we calculated the density of puncta and the width of each puncta. Considering that the GFP added in the C-terminal domain of GLR-1, then the total fluorescence density and size of each puncta should be contributed by the GLR-1::GFP molecules present in the plasma membrane as well as in sub-synaptic endosomal compartments (Burbea et al., 2002). Therefore, the *GLR-1::GFP* fluorescence measurements reported here by using the quantitative fluorescence microscopy indicates the sum of the plasma membrane and endosomal receptor pools.

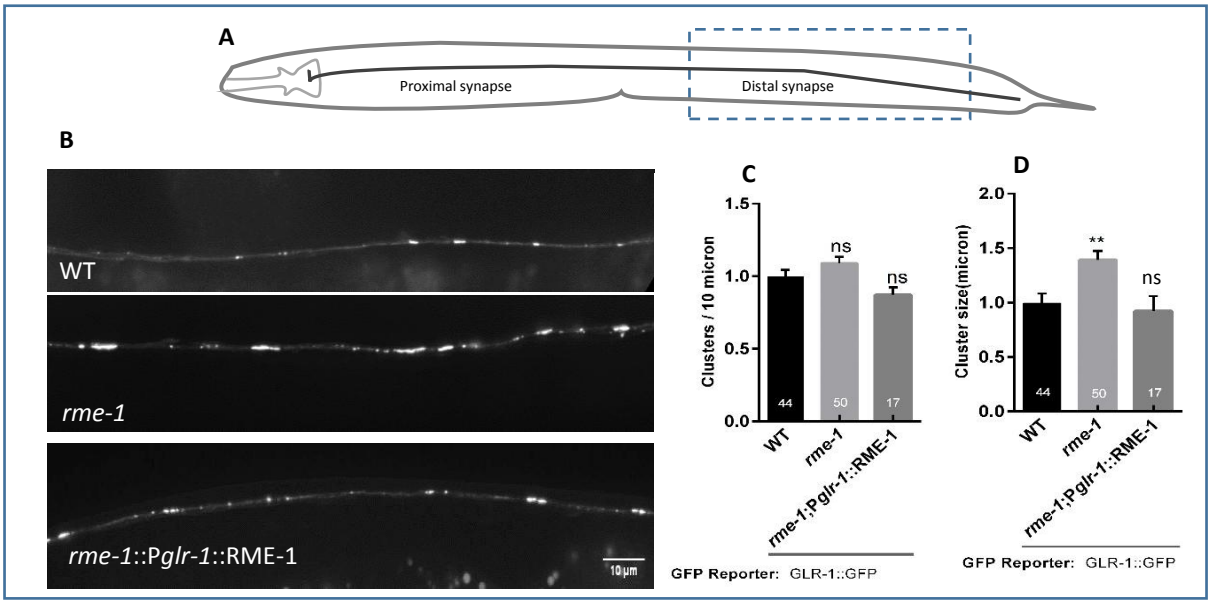

Figure 4.3 Increased GLR-1::GFP puncta size in *rme-1* mutant worms

GLR-1::GFP punctal density and size measured in the posterior region of the glutamatergic command interneurons. A) Cartoon of *C. elegans* with the mid-black line showing the glutamatergic interneurons and the proximal and distal regions (dotted box), where the punctal density and size was measured. B)

GLR-1::GFP puncta distribution in wild type (WT), *rme-1* mutants and the glutamate neuron specific rescue line (P*glr-1*::RME-1) C) Bar graph showing the number of clusters of GLR-1::GFP puncta and D) size of these puncta in WT, *rme-1* mutants, and the glutamate neuron specific rescue line. The error bar represents the SEM and statistical significance (Students *t*-test) is represented as "ns" for not significant, and "**" $p<0.01$.

The pool of *glr-1* receptors is regulated by different endocytosed molecules. Clathrin-dependent and -independent endocytosis (CIE) pathways regulate the activity of synaptic signaling through molecules like RAB-5 (Park et al., 2009), UNC-11 (an ortholog of the AP180 clathrin adaptor protein) and RAB-10 (a small GTPase in CIE) by regulating the trafficking of GLR-1::GFP in the synapse. Any defect in these molecules leads to an increase in the size of puncta (Burbea et al., 2002; Glodowski et al., 2007). As indicated in the previous section, we observed no significant change in the number of synaptic puncta, but the average size of the GLR-1::GFP puncta in the *rme-1* mutant background showed an increase in the distal postsynaptic regions (**Figure 4.3**). The increased level of GLR-1::GFP puncta size suggests that there is a defect in the recycling of GLR-1 receptors from the recycling endosomes. Further, this defect were rescued by expressing *the rme-1* gene under the glutamatergic promoter (P*glr-1*) **(Figure 4.3 B and C)**, suggesting that RME-1 could be involved in trafficking or recycling of GLR-1 receptors in the distal postsynaptic region of the nerve cord in *C. elegans*.

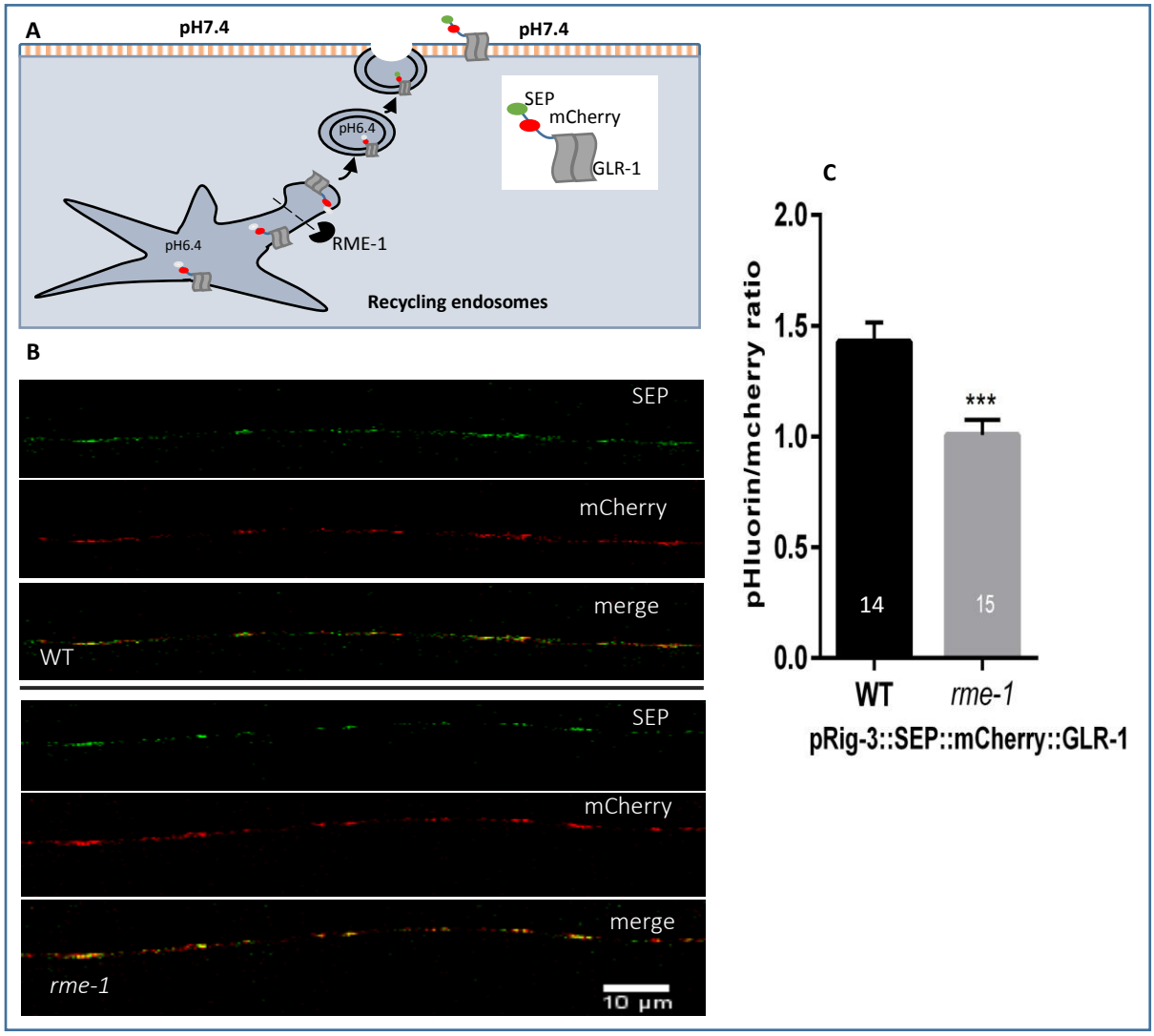

Figure 4.4 Number of Functional GLR-1 receptors are reduced in *rme-1* mutants.

SEP::mCherry::GLR-1 puncta intensity is measured in the distal region of the AVA glutamatergic command interneuron. A) Cartoon image showing the functional SEP::mCherry::GLR-1 receptor, localization in recycling endosome (bleached GFP due to acidic pH) and on plasma membrane (active GFP and mCherry) B) These fluorescence puncta distribution in wild type (WT) and *rme-1* mutant worms. B) The bar graph shows the (ratio of pHluorin to mCherry) fluorescence intensity in WT and reduced in *rme-1* mutants. The error bar represents the SEM and statistical significance (Students *t*-test) is represented as "ns" for not significant, and "***" p<0.001

To check the activity of the increased puncta in the *rme-1* mutant background, whether these are active GLR-1 receptors on the plasma membrane or trapped receptors within the endomembrane, we used the pHluorin line. The promoter *rig-3* shows expression in the AVA glutamatergic

command interneuron; AVA neuron is involved in the initiation of reversals (Piggott et al., 2011). The functional GLR-1 receptor is tagged with the pH-sensitive GFP i.e., pHluorin and mCherry (Hoerndli et al., 2013) (**Figure 4.4 A**). The pH-sensitive pHluorin doesn't show the fluorescence when it is in the acidic condition as in recycling endosomes (pH~6.4) (IJzendoorn, 2006) but once in the neutral condition or on the plasma membrane, it shows GFP fluorescence. By calculating the ratio of GFP/mCherry, we can find the localization of the protein in the endomembrane or on the plasma membrane. Our results confirm that the number of active GLR-1 receptors in the distal neurite region is reduced in *rme-1* mutants (**Figure 4.4 B and C**), suggesting that there is a defect in the recycling of GLR-1 receptors in the *rme-1* mutant background.

4.2.3 RME-1D Isoform localizes to the ventral nerve cord

We found that the P*rme-1* tagged to mCherry shows ubiquitous expression (**Figure 4.4**) as reported previously (Grant and Caplan, 2008)

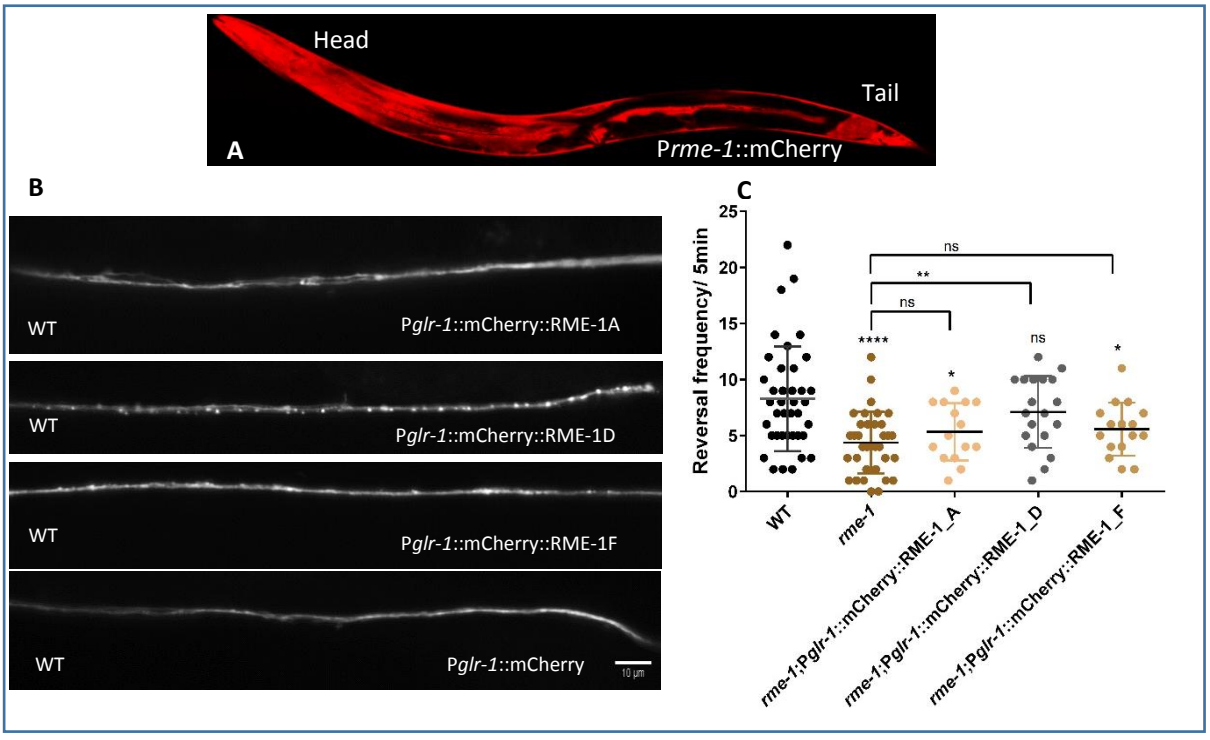

Figure 4.5 RME-1D Isoform localizes to nerve cord and regulates the reversal phenotype

A) Expression of the promoter *rme-1* (P*rme-1*::mCherry), shows ubiquitous expression B) Expression of different isoform under the P*glr-1* in the nerve cord, RME-1D isoform shows localization in the ventral

nerve cord. C) Rescue of the reversal phenotype by using these different *rme-1* gene isoforms in *rme-1* mutant background. Each dot represents the number of spontaneous reversals per five minutes from one worm. The error bars represent the SEM and statistical significance (one-way ANOVA) is represented as "ns" for not significant, "*" p<0.05, "**" p<0.01 and "****" p<0.0001

The *rme-1* gene encodes for nine alternatively spliced isoforms (www.wormbase.org). To study the role of these different isoforms, we isolated the cDNA from adult worms and were able to amplify three different isoforms (*rme-1* A, D, and F). Further, to check the role of these different isoforms in glutamatergic neurons, we cloned these isoforms under the glutamatergic promoter (P*glr-1*) with an N-terminal mCherry fluorescence tag. All three isoforms showed expression in the interneurons cell bodies, but the RME-1D isoform shows visible punctate localization in the ventral nerve cord (**Figure 4.5 A**). While the localization of RME-1A and RME-1F Isoforms are not visible as a puncta in the nerve cord or visibility may be beyond our microscope resolution limit (**Figure 4.5 B**).

Further, we checked the rescue of reversal behavior in all three isoforms in the *rme-1* mutant background; we found that the RME-1D isoform completely rescued the reversal behavior defect (**Figure 4.5 C Movie 4, 5, and 6**). Additionally, we also looked at the increased puncta size in the *rme-1* mutants, by using the RME-1D Isoform rescue line, and the size of the puncta reduces significantly (**Figure 4.6**). We are further confirming that the RME-1D isoform is involved in regulating the GLR-1 receptor trafficking.

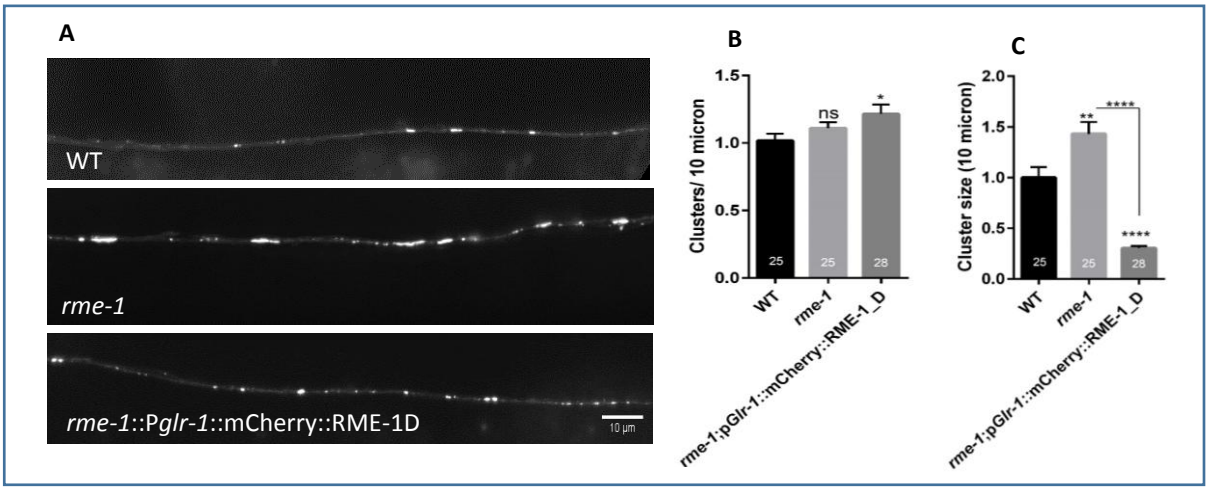

Figure 4.6 RME-1D isoform regulates GLR-1 receptor trafficking in ventral nerve cord

A) Shows GLR-1::GFP puncta distribution in wild type (WT), *rme-1* mutants and the RME-1D rescue line B) The bar graph shows the number of clusters of GLR-1::GFP puncta, increased in case of *rme-1d* rescue line C) Graph shows the size of these puncta in WT, *rme-1* mutants, and the reduced size in *rme-1d* rescue lines. The error bar represents the SEM and statistical significance is represented as ns and statistical significance (Students *t*-test) is represented as "ns" for not significant, "*" $p<0.05$, and "**" $p<0.01$

4.2.4 Synapse formation and trafficking of NMDA receptor is normal in *rme-1* mutants

The trafficking defect of GLR-1 in *rme-1* mutants could also be due to a defect in proper synapse formation. To investigate this, we looked for a general defect in synapse formation with the help of the synaptic vesicle protein Synaptobrevin-1 (SNB-1) (Nonet et al., 1998). The SNB-1::GFP when expressed under the *glr-1* promoter, mark the presynaptic regions and shows punctate localization along the ventral nerve cord of wild type worms (Burbea et al., 2002; Rongo et al., 1998). We found a similar localization of SNB-1::GFP in the *rme-1* mutant background. When we quantified the size and number of puncta, no significant differences were found between the *rme-1* mutant worms and wild type (**Figure 4.7**). Thus, these results reveal that the effect of the *rme-1* mutation on GLR-1 trafficking is not due to gross synaptic disorganization

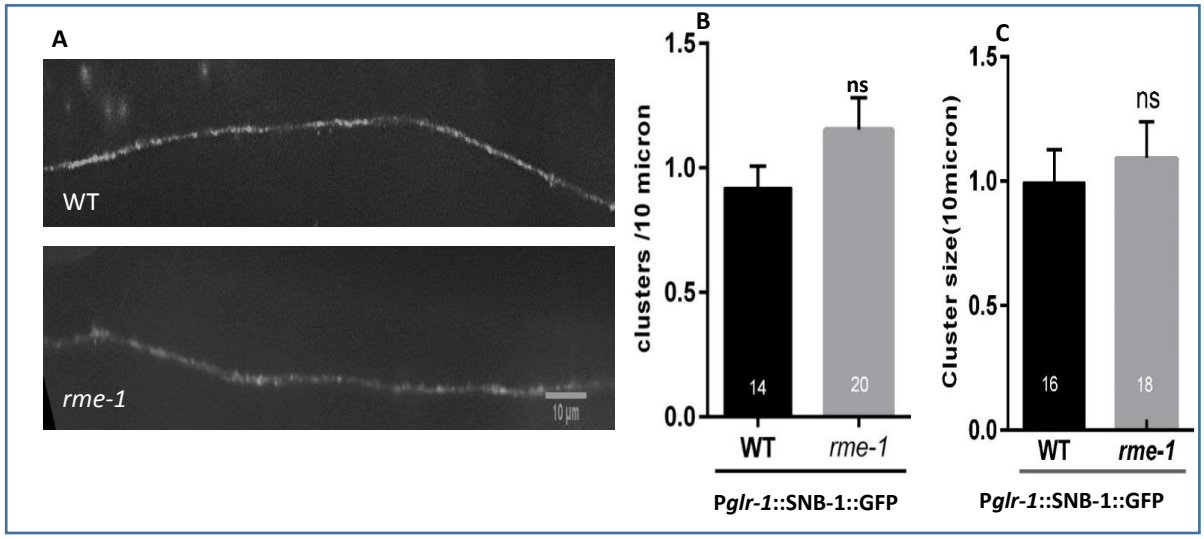

Figure 4.7 Synaptobrevin localization is normal in *rme-1* mutants

SNB-1::GFP puncta density and size in the distal region of the glutamatergic command interneurons. A) SNB-1::GFP puncta distribution in wild type (WT) and *rme-1* mutants. B) The bar graph shows the number of clusters of SNB-1::GFP puncta C) The bar graph shows the size of these puncta in WT and *rme-1* mutants. The error bar represents the SEM and statistical significance (Students *t*-test) is represented as "ns" for not significant, "*" $p<0.05$, and "**" $p<0.01$

Previous work has shown that the NMDA (NMR-1 and NMR-2 in the case of *C. elegans*) type of glutamate receptors (Brockie et al., 2001), NMR-1, is known to regulate reversal behavior in *C. elegans* (Brockie et al., 2001). To explore the possibility of *rme-1* mutants affecting NMR-1 localization, we analyzed the localization of NMR-1 receptors using the NMR-1::GFP line with a glutamatergic neuron-specific promoter (NMR-1).

The density and size of NMR-1::GFP puncta were not significantly different in *rme-1* mutants when compared to the wild type worms (**Figure 4.8**), suggesting that RME-1 is involved in recycling of only GLR-1 receptors and does have any effect on NMR-1 localization in the ventral nerve cord.

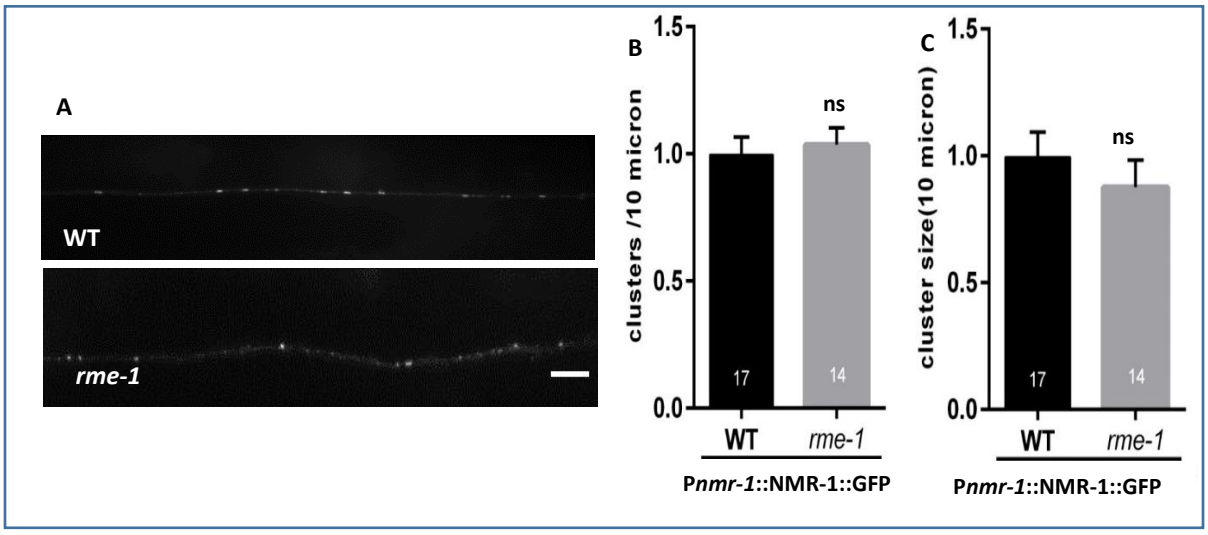

Figure 4.8 NMR-1 receptor localization is normal in *rme-1* mutants.

NMR-1::GFP puncta density and size measured in the distal region of the glutamatergic command interneurons. A) NMR-1::GFP puncta distribution in wild type (WT) and *rme-1* mutants B) The bar graph shows the number of clusters of NMR-1::GFP puncta. C) The bar graph indicating the size of these puncta in WT and *rme-1* mutant are same. The error bar represents the SEM and statistical significance (Students t-test) is represented as "ns" for not significant, "*" $p<0.05$, and "**" $p<0.01$

4.3 Discussion

In this study, we have identified the role of RME-1 in regulating AMPA type GLR-1 receptors in the *C. elegans* nervous system. The previous report in hippocampal cell lines suggests that during long term potentiation (LTP), *Rme-1* in recycling endosomes supplies the AMPA

receptors, and a mutation in *Rme-1* hampers the recycling of AMPA receptors (Park, 2004). In the case of glutamatergic neurons in *C. elegans,* different endocytic molecules like UNC-11 in endocytosis and LIN-10, RAB-10 are known to regulate GLR-1 receptor trafficking (Burbea et al., 2002; Glodowski et al., 2007; Rongo et al., 1998). Here we also found that the mutation in *rme-1* leads to decreased reversal frequency in worms. Further the GLR-1::GFP level in the distal postsynaptic region is increased, These defects could be rescued by expressing *rme-1* genomic or RME-1D isoform in glutamatergic neurons, suggesting that RME-1 is involved in trafficking of GLR-1 AMPA receptors in the interneurons of *C. elegans.*

RME-1 is reported to be involved in the trafficking of different cargos in cells (Grant and Caplan, 2008; Grant and Donaldson, 2009). In the case of intestinal epithelial cells, RME-1 localized to the recycling endosome. Any defect in RME-1 results in unusually large size of recycling endosomes in the epithelial cells of the intestine due to the continuous influx of the incoming vesicles. Most of the receptors which are going through recycling endosomes get trapped, or their recycling gets hampered. We found that the size of GLR-1::GFP puncta increases in the *rme-1* mutant background, but it is very difficult to see the large vacuolar structure in the neurons due to its small size in comparison with the intestine.

The human genome encodes for the four orthologs (EHD1-EHD4) of RME-1 that have different functions in the endocytic process (George et al., 2007). The EHDs are reported to play important roles in neuronal development, axon outgrowth, and pathfinding (Bhattacharyya et al., 2016; Dhekne et al., 2018; Ioannou and Marat, 2012; Wu et al., 2019). Like EHD4 involved in endocytosis of Nogo-A, a repulsive cue for axonal growth cones (Joset et al., 2010; Sharma et al., 2008). In case of mature neurons, EHDs plays different roles, like EHD1 along with EHD4 shows localization on early endosome (Lasiecka et al., 2010) and involve in endocytosis(Shao et al., 2002). EHD1/EHD4 form the hetero-oligomeric complexes that mediate transcytosis (Somatodendrite to axonal transport) of L1/NgCAM in hippocampal neuronal cells (Yap et al., 2010). Likewise, EHD1/3 is involved in transcytosis of β-secretase (Buggia-Prévot et al., 2013). Past1, an EHD ortholog in drosophila, is involved in controlling postsynaptic membrane elaboration and AMPA receptor levels (Koles et al., 2015). We were able to amplify three different isoforms from adult worms. The RME-1D isoform, having truncated N-terminal

domain, showed a robust punctate localization in the distal neurite region (**Figure 4.4 B**). Further, we used the pHluorin line and confirmed that the increased puncta are underneath the plasma membrane. Suggesting, the functional number of receptors on the plasma membrane gets reduced in *rme-1* mutant background.

The early endosome recycles back the vesicles in the same place while recycling from the REs is slower and returns internalized cargos to several locations on the plasma membrane (Yap and Winckler, 2012). Further, the recycling endosomes in highly polar cell-like neurons are distributed randomly, with the different synaptic regions of dendrites and axons having a local endosomal system, where it regulates the synaptic strength (Itofusa and Kamiguchi, 2011). The in vivo analysis of EHD1 shows localization in the axonal terminal in mice brain (Buggia-Prévot et al., 2013). Recently, it was reported that the functional level of GLR-1 receptors is more in the distal region when compared to the proximal region of the neurons, this process is called distance-dependent scaling through which cell maintain synaptic signaling (Hoerndli et al., 2013; Shipman et al., 2013). As well, it was proposed that the newly synthesized GLR-1 receptors travel to the nearest plasma membrane using the KLP-4 kinesin molecule (Monteiro et al., 2012) and for the distal synapse transport, the cell uses a different kinesin machinery like UNC-116 (Hoerndli et al., 2013; Juo et al., 2007; Rongo, 2013). Also, the more proximal synapse is maintained through Clathrin independent endocytosis (Kramer et al., 2010), and the distal synapse maintained by Clathrin dependent endocytosis. In the case of the *rme-1* mutant worms, the increased synaptic level of AMPA receptors was found near the distal nerve cord of the worms, no change was found in the anterior or proximal synapse. On the basis of these results, we propose that the RME-1 which is present in the recycling endosomes could be involved in maintaining the recycling of GLR-1 receptors in the distal region (**Figure 4.9**) OR RME-1 could be involved in the endocytosis and transport of GLR-1 receptors in the distal region of interneurons in *C. elegans.*

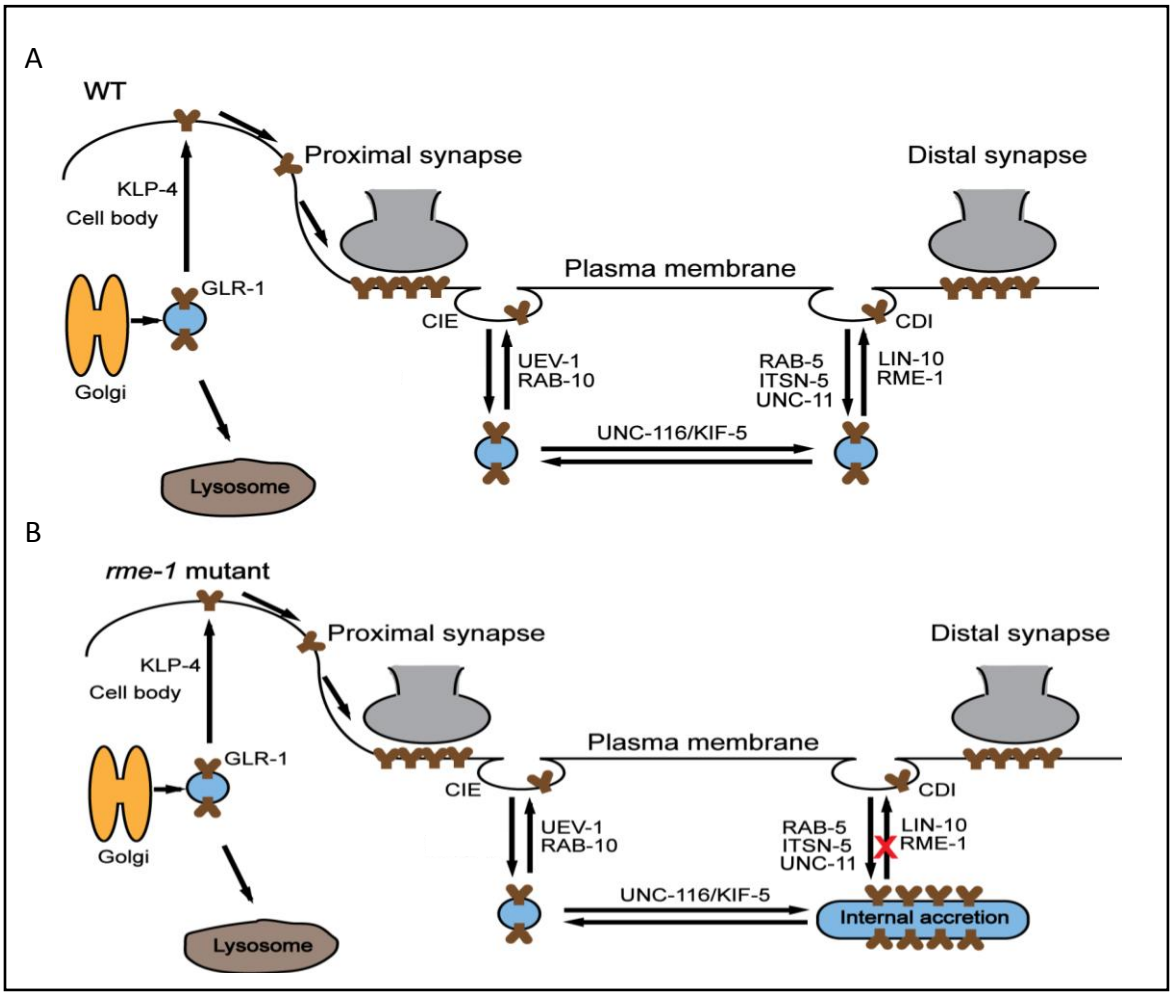

Figure 4.9 Possible Model for RME-1 function

The previous finding suggests that the GLR-1 receptor is maintained through two different pathways clathrin-independent pathway and Clathrin dependent pathway. A) Cartoon showing both pathways at the proximal and distal region along the ventral cord of WT worms. The clathrin-independent pathway which requires RAB-10 and UEV-1 for recycling is mostly present in the proximal synapse, and the Clathrin dependent pathway, which requires RAB-5 and ITSN-1 and UNC-11 for endocytosis and LIN-10 for the recycling is present in the distal synapse. KLP-4 is involved in the transport of newly synthesized GLR-1 receptors from the cell body to the overlying membrane, and through diffusion, these receptors travel to the proximal synapse. UNC-116 kinesin protein is involved in the transport of vesicles between the proximal synapse to the distal synapse of the nerve cord. B) Cartoon showing that recycling in the distal region is hampered in *rme-1* mutants. The mutants show large accretions due to their failure to exits from the endosomal compartment

Chapter 5

To explore the role of SRX-97, a G-protein coupled receptor in chemosensory neurons of *C. elegans*

5.1 Introduction

Animals sense a wide range of volatile and water-soluble chemicals through their olfactory system. The olfactory system is made up of several neurons that express different sets of seven-transmembrane G protein-coupled receptors (GPCRs). The odorant binds to the GPCRs, which further activates intracellular signaling pathways and changes the animal's response to external cues.

C. elegans is a soil-dwelling animal that possesses a well-developed sensory system for its survival. Worms generally perceive their environment through various sensory neurons in order to find food sources, mate & escape from dangerous conditions. The majority of the chemosensation is carried out by 11 pairs of chemosensory neurons that express around 1300 functional chemosensory (cs) G-protein coupled receptors (GPCR) (Robertson, 2006; Vidal et al., 2018). This diversity of chemosensory (cs) GPCR allows the animal to discriminate between different odors. Thus, the specific expression of any GPCR or combined expression of different GPCRs on specific neurons or different neurons can modulate the animal's perception of the same odorant.

The olfactory neurons that are involved in sensing a large number of attractive cues are AWA and AWC. These two pairs of neurons are involved in showing chemotaxis to various chemicals like diacetyl, pyrazine, benzaldehyde, and butanone. The avoidance behavior towards the repellent nonanone and 1-octanol is mediate through the sensory neurons AWB, ASH, and ADL. Also, many of the volatile chemicals detected by olfactory neurons could act as attractants at low concentrations and repellents at higher concentrations (Yoshida et al., 2012). For example, diacetyl which is sensed by ODR-10, a GPCR in the AWA neuron at lower concentration acts as an attractant (Sengupta et al., 1996) and at higher concentration, it is sensed by the SRI-14 GPCR in the ASH neuron and acts as a repellent (Gun Taniguchi et al., 2014). Thus, the ASH neurons are known to be involved in sensing higher concentrations of volatile chemicals (Gun Taniguchi et al., 2014; Yoshida et al., 2012). Additionally, the ASH neuron is a polymodal neuron involved in showing avoidance behavior towards different nociceptive signals like noxious chemicals, nose touch, hyperosmolarity, and volatile repellents (Bargmann, 2006; Hilliard et al., 2005, 2004, 2002). The ASH neuron carries out these various functions through

different receptor activation; for example, touch is detected by mechanically gated ion channels MEC-4 and MEC-10, while hyperosmolarity is detected by OSM-10 (Hart et al., 1999). The ASH neuron forms strong synaptic connections with the AVA command interneuron, which regulates the backward locomotion of worms (Bastiani, 2006). So, the activation of the ASH neuron also provokes backward locomotion or reversals in worms.

ASH neuron is also reported to be involved in sensing pure benzaldehyde (Aoki et al., 2011; Troemel et al., 1995). Here, we show that SRX-97, a newly found csGPCR, shows expression in the ASH neuron. The CRISPR/Cas9 mediated *srx-97* null mutant shows defects in chemotactic behavior, specifically towards higher concentrations of benzaldehyde. Further, the mutant phenotype is rescued by the endogenous and neuron-specific expression of the *srx-97* gene, suggesting concentration-dependent behavioral plasticity in *C. elegans.*

5.2 Results

5.2.1 SRX-97 encodes for a seven-transmembrane GPCR

C. elegans have fourteen chemosensory neurons in the anterior amphid and posterior phasmid regions; however, it can detect several different chemical cues ranging from volatile to water-soluble odorants. Each pair of chemosensory neuron expresses a subset of GPCRs which detects characteristic chemical cues and allows the worms to navigate its surrounding, like to move towards an attractant or repel from the danger. Seven percent of the *C. elegans* genome is dedicated to encoding for the chemoreceptors of which about 1300 genes encodes for the G protein-coupled receptors (Robertson, 2006; Vidal et al., 2018). The functions of most of the receptors are still unknown.

Here, we analyzed one such uncharacterized GPCR, SRX-97 of the SRX family belonging to SRG superfamily that encodes around 320 genes (Robertson, 2006; Vidal et al., 2018). The *srx-97* gene encodes a predicted protein of 317 amino acids (**Figure 4.1A and B**). Hydrophobicity analysis shows that the SRX-97 protein could encode for a seven-transmembrane domain protein, showing the characteristic topology of GPCRs (**Figure 5.1B**). Previously in aldicarb based RNAi screen *srx-97* showed hypersensitivity towards the aldicarb drug (Kavita Babu unpublished data). To performed detailed studies of *srx-97* loss of function mutants, we took the

help of gene editing CRISPR technique and made a complete deletion of the *srx-97* gene (from 61bp of the first exon to the 3' UTR region, deleting 1797 bp sequence) (Dahiya et al., 2019; Dickinson et al., 2015; Dickinson and Goldstein, 2016) (**Figure 5.1C**). We next outcrossed the *srx-97* line with the wild type strain three times. Upon performing the aldicarb assay, we found that the *srx-97* mutants did not show any significant defects in comparison to the wild type animals, where *rig-3* mutants show hypersensitivity (Babu et al., 2011) (**Figure 5.1D**). We next went on to analyze the expression of the *srx-97* gene.

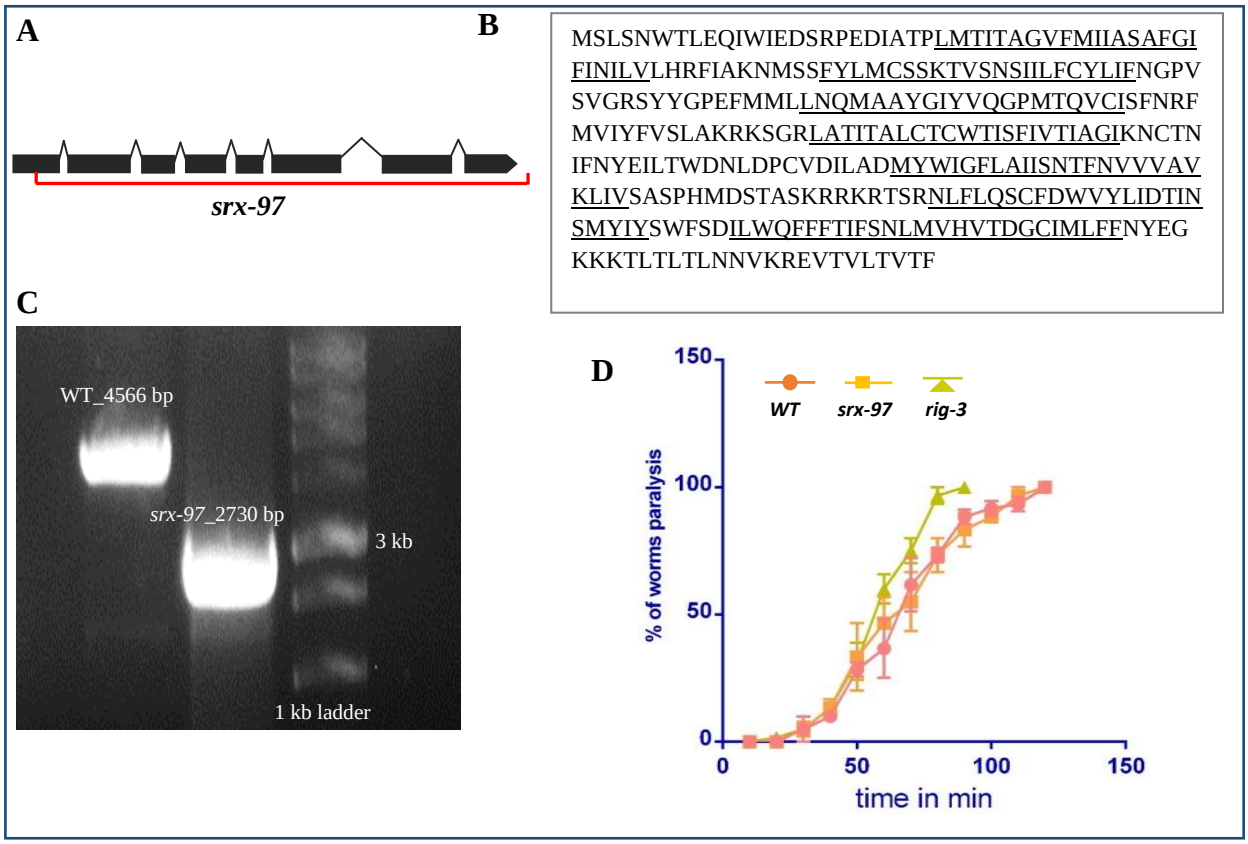

Figure 5.1 The *srx-97* gene structure and CRISPR/Cas9 generated mutation
A) Exonic structure of the *srx-97* gene and the red line showing the deletion. B) The amino acid sequence showing the predicted seven-transmembrane domain of SRX-97. C) Amplification size of *srx-97* gene deleted using the CRISPR/Cas9 compared to the wild type. D) Aldicarb assay for the *srx-97* mutants, wild type, and the hypersensitive *rig-3* mutants. *srx-97* mutant worms behaved like WT worms. Error bars show the SEM and statistical significance (Students *t*-test).

5.2.2 P*srx-97*::mCherry transgene shows unique expression in the ASH and PHB chemosensory neurons

Chemosensory GPCRs are classified into nine different classes based on their sequence homology with Rhodopsin class (Fredriksson et al., 2003). *C. elegans* encode 1341 genes encoding GPCRs of which the expression pattern of only 320 genes is known to a single-cell resolution (Robertson, 2006; Gun Taniguchi et al., 2014; Vidal et al., 2018). It is reported that GPCRs are also expressed in non-neuronal tissue and are involved in sensing the internal cues. Some GPCRs change their expression pattern after starvation or dauer (Vidal et al., 2018). Still, the expression of the majority of csGPCRs is not known.

To determine the expression pattern of SRX-97, a 2kb region upstream of the predicted translational start codon with six bp of the first exonic region was used as a promoter to generate the P*srx-97::*mCherry reporter line. In transgenic animals, mCherry shows expression specifically in a single head amphid neuron and tail phasmid neuron (**Figure 5.2**). No expressions were seen in any other parts of the body, signifying that SRX-97 may be involved in chemosensory signaling.

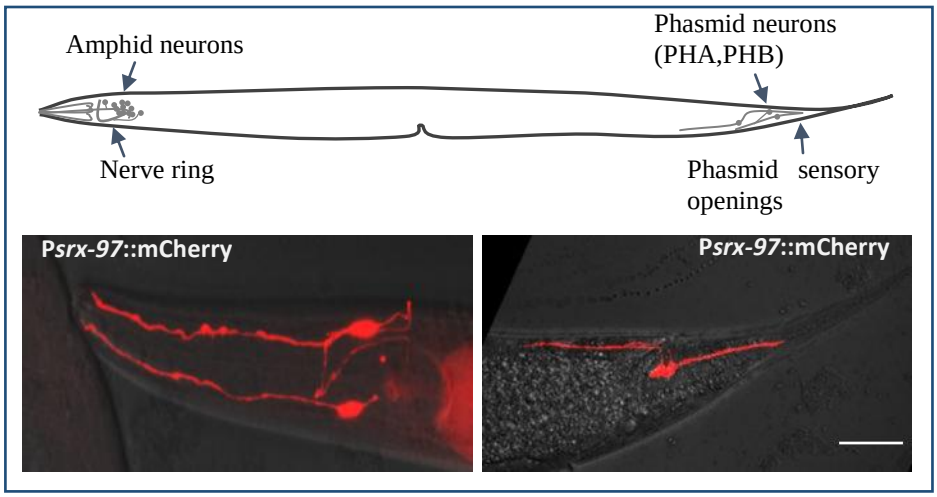

Figure 5.2 Expression of P*srx-97*::mCherry in the amphid and phasmid region of the worm

A) The cartoon image showing the location of the amphid and phasmid neurons in *C. elegans.* B) Expression of the P*srx-97*::mCherry transgenic construct in the amphid region and the phasmid region of the worm. Scale bar 20µm

To confirm the neurons on the basis of cilium morphology and the cell body position in the head region we crossed the line with the P*str-2*::GFP which shows expression in the AWC neuron

(Troemel et al., 1999) (**Figure 5.3A**) and with the P*daf-7*::GFP line expressed in the ASI neuron (Schackwitz et al., 1996) (**Figure 5.3B**). Neither of these neurons showed colocalization with the P*srx-97*::mCherry expression. Further, we made the P*srb-6*::GFP transgenic line, which shows expression in ASH and ADF neurons in the amphid region (Troemel et al., 1995). While P*srx-97::*mCherry line shows colocalization with one neuron (**Figure 5.3C**). This result suggests that P*srx-97*::mCherry could be expressed in either the ASH or the ADF neuron. To further understand P*srx-97*::mCherry expression, we made a second transgenic line with P*osm-10*::GFP, which expresses in the amphid ASH and ASI neurons and the PHA/PHB neurons in phasmid region (**Figure 5.3D, E**) (Hart et al., 1999). The colocalization in common single neurons in both marker lines confirms that the P*srx-97* is expressed the ASH neuron. In the tail region, P*srx-97*::mCherry shows colocalization with the second phasmid neuron, i.e., PHB neuron (**Figure 5.3E**). Additionally, a recent report suggests that 50% of GPCRs which expressed in ASH neurons also show expression in the PHB neuron (Vidal et al., 2018).

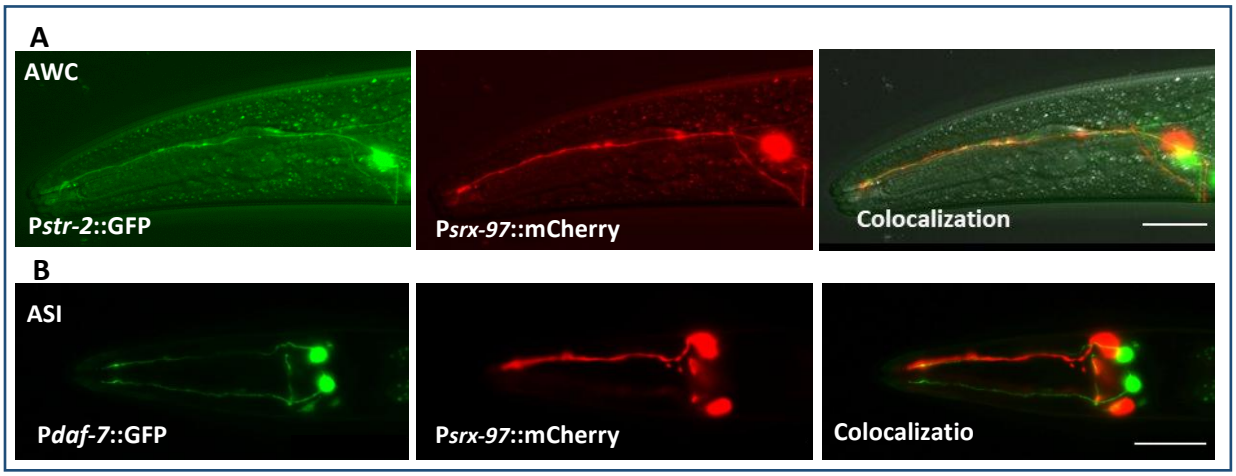

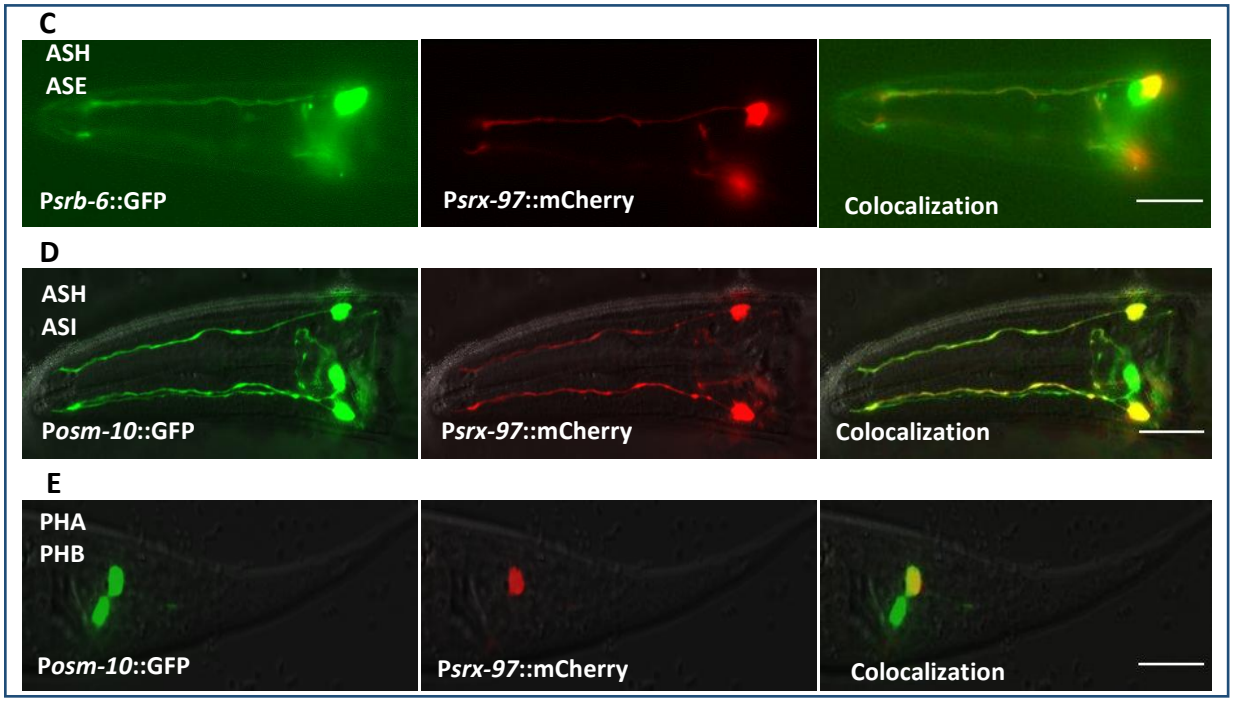

Figure 5.3 P*srx-97*::mCherry shows expression in ASH and PHB neuron

A) Expression of P*str-2*::GFP in the AWC neuron B) Expression of P*daf-7*::GFP in the ASI neuron C) Expression of P*srb-6*::GFP in the ASH and ADL neuron and showing colocalization with the P*srx-97*::mCherry D) Expression of P*osm*-10::GFP in the ASH and ASI neuron and colocalization with the P*srx-97*::mCherry and E) Expression of P*osm*-10::GFP in the tail PHA and PHB neuron and showing colocalization with the P*srx-97*::mCherry. Scale bar 20µm.

We next analyzed the SRX-97 translation reporter and found that SRX-97::mCherry transgenic lines show localization of SRX-97 proteins towards the cilium tip of the ASH neurons (**Figure 5.4**), yet again indicating that this protein could be involved in sensing environmental cues from the surrounding expressed in ASH neurons also show expression in the PHB neuron.

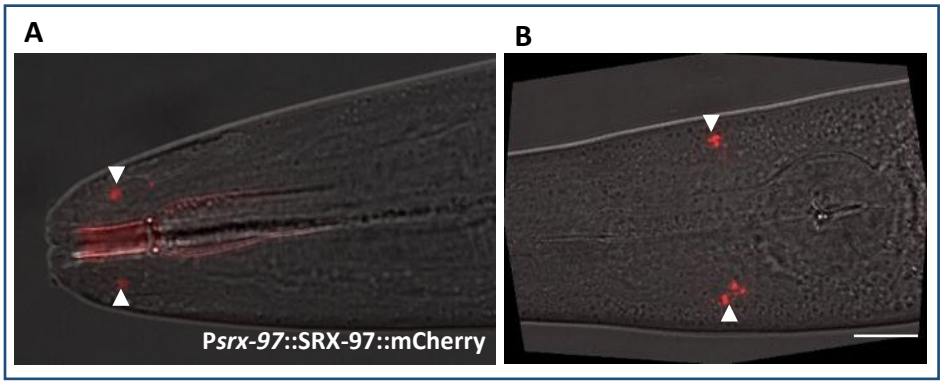

Figure 5.4 P*srx-97*::SRX-97::mCherry shows expression in ASH neuron.

The SRX-97 protein (shown in arrowhead) is synthesized in the cell body (B) and localized toward the cilium tip (A) of the ASH neurons.

5.2.3 *srx-97* mutants shows defect in response to high concentrations of volatile Benzaldehyde

ASH is a polymodal neuron, it can respond to noxious, mechanical or osmotic stimuli. To characterize the role of the SRX-97 GPCR, we have checked the response of the *srx-97* mutant line to several compounds like SDS, Cu2+, quinine, glycerol, pyrazine and acetic acid(Hilliard et al., 2005, 2004, 2002; Kaplan and Horvitz, 1993). The *srx-97* mutant worms did not show any significant defects in avoidance assay towards these compounds as compared to the wild type animals. For control, we used *odr-3* mutants, showed the significant defect (Hilliard et al., 2005) (**Figure 5.5 and Table 8**).

The ASH neurons are also known to be involved in detecting volatile chemicals (Troemel et al., 1995). To check this, we used a modified chemotaxis plate, having four quadrants, two opposite quadrants for test solution, and two for control (**Figure 5.6A**). The control or test spot was 3 cm away from the worms loading center. But, before the addition of control or test solution, we have added the sodium azide, which paralyzes the worms once they reach the respective spots. Further, we calculate the chemotaxis index by measuring the number of worms in each quadrant with the formula shown in (**Figure 5.6A**). It is well known that in chemotaxis assays, the ASH neuron is involved in showing aversive behaviors towards the repellant 1-Octanol and Nona none (Chao et al., 2004). However, we found no significant change in the chemotaxis index towards these chemicals in *the srx-97* mutants when compared to the control of wild type worms (**Figure 5.6 B**). Recent findings suggest that the ASH neuron is involved in sensing higher concentrations of chemicals such as Isoamyl alcohol (Yoshida et al., 2012), and Diacetyl (Gun Taniguchi et al., 2014). In chemotaxis assays, we checked through a range of concentration for these chemicals and found that the *srx-97* mutant worms didn't show any significant defect in chemotaxis assay towards the Isoamyl alcohol and diacetyl when compared to wild type worms (**Table 9**).

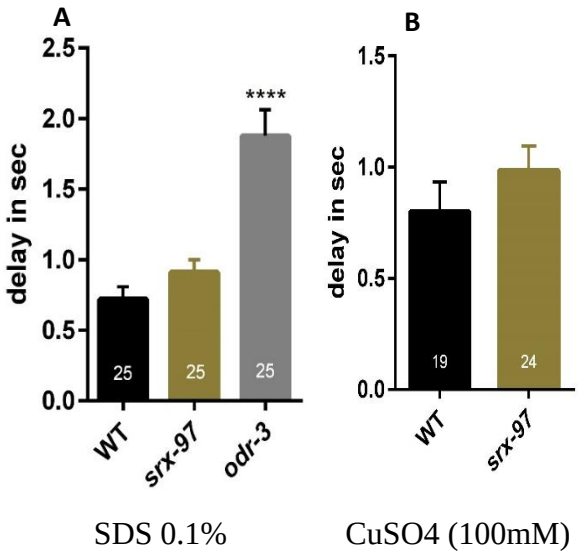

Table 8 avoidance assay toward water soluble chemicals

Chemicals	Genotype	Avoidance in second
Acetic acid (0.1 M)	Wild type srx-97	1.70±0.15 (n=21) 1.57±0.10 (n=20)
Glycerol (2M)	Wild type srx-97	1.30±0.08 (n=21) 1.20±0.06 (n=21)
Dihydrocaffeic acid (1mM)	Wild type srx-97	0.60±0.04 (n=20) 0.80±0.10 (n=21)
Pyrazine (10mM)	Wild type srx-97	1.00±0.40 (n=18) 1.20±0.30 (n=20)
Quinine (10mM)	Wild type srx-97	0.70±0.20 (n=15) 1.00±0.06 (n=21)

Figure 5.5 Avoidance assay of *srx-97* mutants towards water-soluble chemicals

A) Graph shows the delay in avoidance towards the dry spot of 0.1% SDS by wild type, *srx-97* mutants and *odr-3* mutants. B) Graph shows the response towards the 100mM $CuSO_4$ C) Table shows the delay in avoidance of *srx-97* mutants and wild type towards different water-soluble chemicals. The error bars represent the SEM and statistical significance is represented as "ns" for not significant and ***p<0.001

ASH neurons are also known to be involved in detecting benzaldehyde (Gun Taniguchi et al., 2014; Troemel et al., 1995) as one such GPCR, DCAR-1 having homology with SRX family shows defect towards benzaldehyde (Aoki et al., 2011). In the chemotaxis assay, the *srx-97* mutant worms showed significantly more attraction towards the higher concentration of benzaldehyde (10^{-1}) when compared to wild type (**Figure 5.6D**). At lower concentrations (10^{-2} and 10^{-3}), there is no significant difference in comparison to the wild type animal. As reported the ASH neuron previously is involved in responding to the higher concentration of benzaldehyde (0.1%v/v), and the medium or lower concentration (0.005-0.0001%) of benzaldehyde is sensed by the AWC and AWA neurons (Leinwand et al., 2015) Suggesting a concentration-dependent behavioral change. The phenotype could be rescued by expressing the *srx-97* under its native promoter and partially rescued with the promoter *osm-10*, which shows expression in the ASH and ASI neurons (**Figure 5.7A**) (Hart et al., 1999). These data

suggest that the csGPCR SRX-97 is responsible for sensing the higher concentration of benzaldehyde.

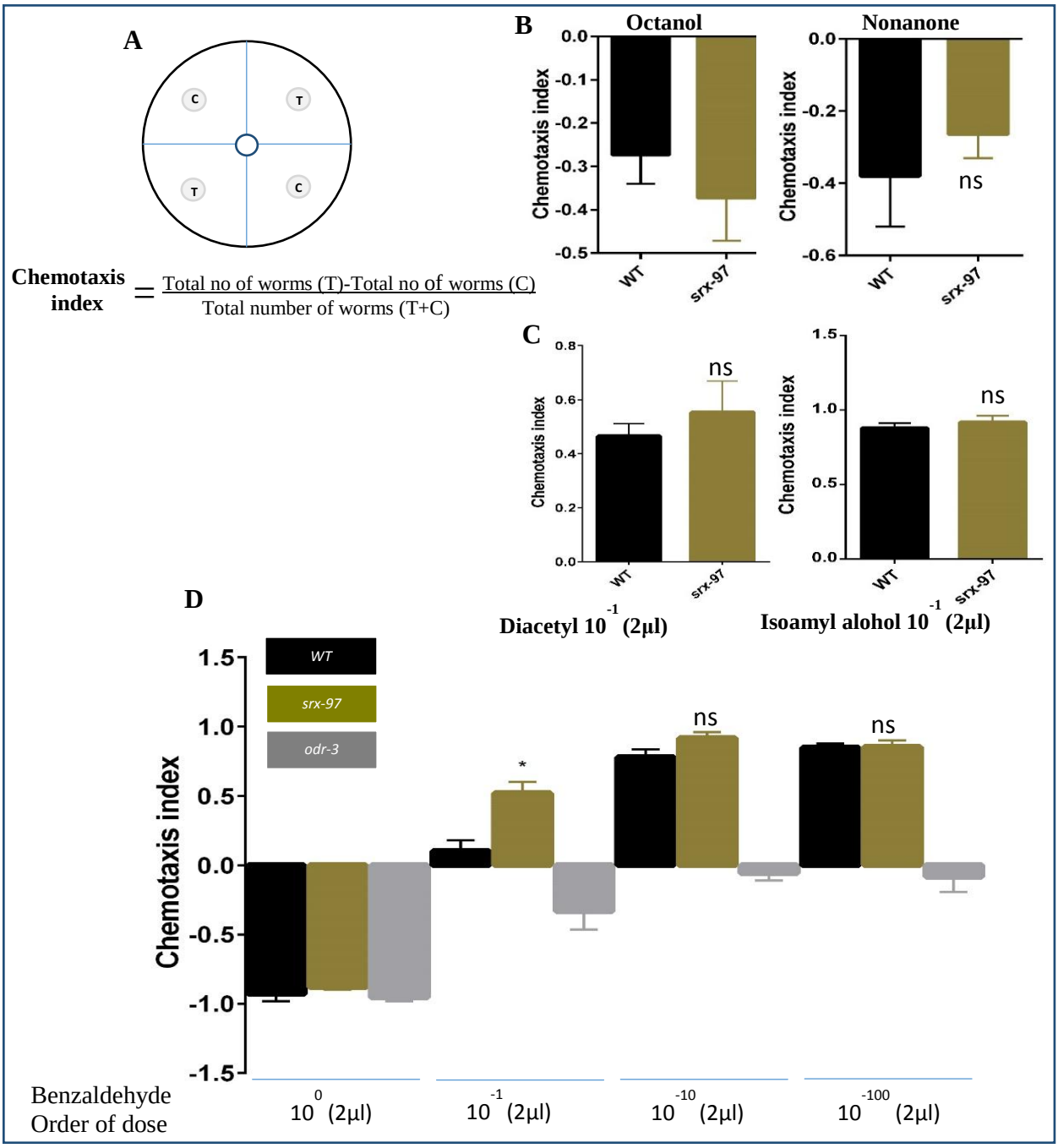

Figure 5.6 *srx-97* mutant worms chemotaxis index towards the different volatile chemicals

A) The plate showing the four quadrants, two opposite quadrants shows the control spot and the test spot, 50-150 worms are added in the central spot and the chemotaxis index calculate by using the given formula (T/C) represents both test/control quadrants B) The chemotaxis showing the negative index toward the repellents octanol and nonanone C) The chemotaxis index towards the higher concentration

(10^{-1}) of diacetyl and isoamyl alcohol D) The chemotaxis index towards the different concentration of benzaldehyde. The assay was done in triplicate and the graph is plotted by taking the data from 3-5 days. The error bars represent the SEM and statistical significance (one-way ANOVA) is represented as "ns" for not significant and "*" $p<0.05$

Further, we analyzed the frequency of *srx-97* mutant worms attraction towards the higher concentration of benzaldehyde (Nuttley et al., 2001). Here, we have added a higher concentration of benzaldehyde on the small sheet (0.5-1cm diameter) of parafilm so it would not be soaked in the media. We also excluded the addition of sodium azide on the control and test spot, which acts as a paralyzing agent so the worms can move freely towards the control or test spot (**Figure 5.7 B**). After a 60 min incubation period, we kept the assay plate in 4 degrees by giving them the cold shock at -30 degrees for two minutes to immobilize the worms. The numbers of worms were counted sector-wise and calculated the chemotaxis frequency by the given formula (**Figure 5.7 B**). Again, the *srx-97* mutants showed a significant increase in the attraction towards benzaldehyde (**Figure 5.7 C**). This defect was rescued by expressing the *srx-97* under its endogenous promoter. Suggesting the SRX-97 is responsible for sensing the higher concentration of benzaldehyde

Table 9 Chemotaxis index toward volatile chemicals

Volatile Chemicals	srx-97 (CI)	WT (CI)	P value
Diacetyl (10^{-10})	0.82	0.80	0.33
Diacetyl (10^{-100})	0.84	0.85	0.99
Isoamyl alcohol (10^{-10})	0.83	0.84	0.33
Isoamyl alcohol (10^{-100})	0.952	0.946	0.33

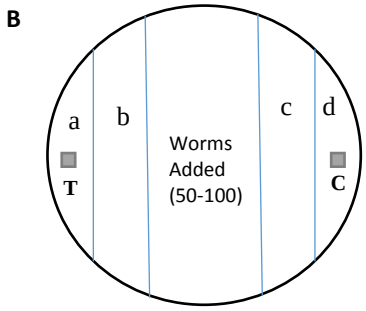

$$\text{Chemotaxis Frequency} = \frac{\text{Number of worms in (a+b)-Number of worms in (c+d)}}{\text{Total number of worms}}$$

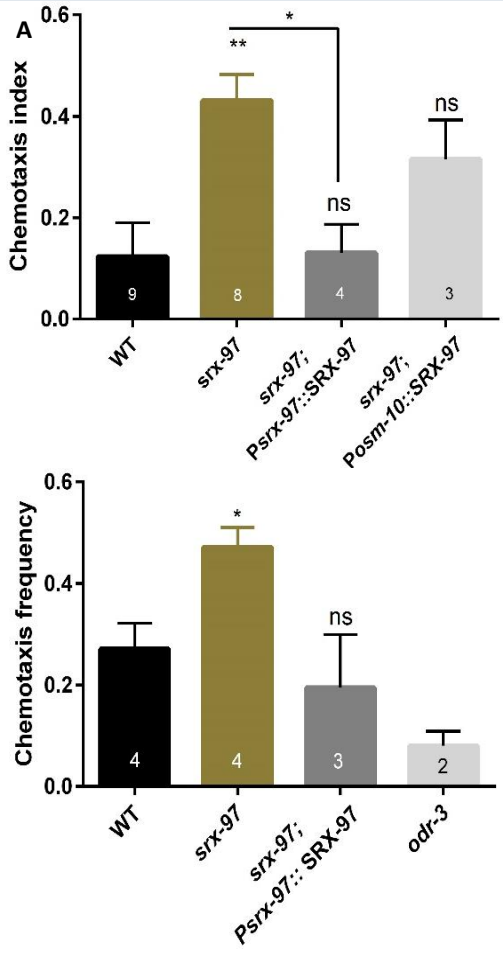

Figure 5.7 The *srx-97* mutant worms show attraction towards the higher concentration of volatile benzaldehyde

A) The chemotaxis index towards the higher concentration of benzaldehyde and rescue using the endogenous promoter and the *osm-10* promoter. B) The design of plates for analyzing the chemotaxis frequency and the formula. Each sector (a,b,c and d) having 1cm in width. C) The chemotaxis frequency towards the higher concentration of benzaldehyde and rescue using the endogenous promoter and control *odr-3* mutants. The assay was done in triplicate and the graph is plotted by taking the data from different days (N=days). The error bars represent the SEM and statistical significance (one-way ANOVA) is represented as "ns" for not significant, "*" $p<0.05$ and ** $p<0.01$

5.2.4 The defect in sensory signaling could affect the chemotaxis towards higher concentrations of benzaldehyde

In ASH neurons, various GPCRs associated sensory molecules are reported to be required for signal transduction. Among these G i/o like protein ODR-3 is a Gα protein which is primarily required for sensory signal transduction and involved in response towards osmotic strength, high salt concentration, nose touch and volatile chemicals (Hilliard et al., 2004; Roayaie et al., 1998a; Zhang et al., 2016). OSM-9 is a member of the vanilloid subfamily of transient receptor potential channel TRPV proteins, which regulates the avoidance of osmotic strength and nose touch (Colbert et al., 1997; Murayama and Maruyama, 2013; Zou et al., 2017). The GPC-1 encodes the γ subunit of GPCRs and is expressed in the chemosensory neurons (Hilliard et al., 2005; Jansen et al., 2002). The cyclic nucleotide-gated channel (CNG) consisting of TAX-2 and TAX-4 subunits are responsible for detecting the volatile chemicals in AWC neuron (Coburn and Bargmann, 1996; Komatsu et al., 1996; Zagotta and Siegelbaum, 1996) but the source of activating cGMP is still unknown. All these pathway mutants were used for the chemotaxis assay and showed a negative chemotaxis index toward the higher concentration of benzaldehyde except the *osm-9* mutants, which shows a slightly positive response to benzaldehyde (**Figure 5.8**). Further, the double mutant with the *srx-97* showed the phenotype like the single mutant of the signal transduction molecules. Suppression of the *srx-97* mutant phenotype by these downstream molecules, suggest that either *srx-97* redundantly function to sense the higher concentration of benzaldehyde or there is possibility that these downstream molecules are also expressed in the other sensory neurons like AWA and AWC which are involved in sensing the lower concentration of benzaldehyde and shows aversions at higher concentrations (Leinwand et al., 2015; Nuttley et al., 2001; Roayaie et al., 1998b). As per the report, not a single downstream molecule has been identified that is involved in showing attraction to the pure or higher concentration of benzaldehyde.

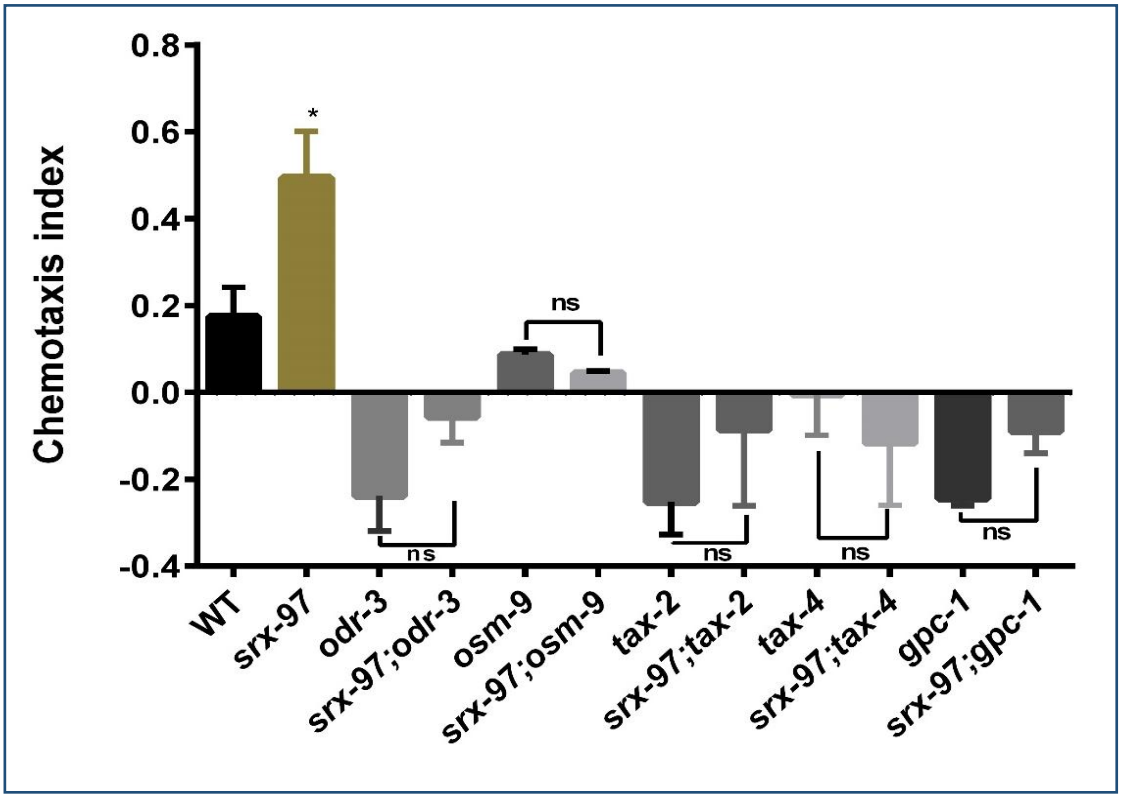

Figure 5.8 The *srx-97* mutants and other signaling mutants show chemotaxis towards the higher concentration of benzaldehyde.

The chemotaxis index towards the higher concentration of benzaldehyde by WT, *srx-97* mutants shows positive and other single and double mutant with the *srx-97* showing the negative chemotaxis index. Assay was done in triplicate and the graph is plotted by taking the data from 2-3 days. The error bars represent the SEM and statistical significance is represented as "ns" for not significant and "*" $p<0.05$

5.3 Discussion

In this study, we have characterized the expression and function of the GPCR, SRX-97. From our expression studies, it is clear that SRX-97 shows expression in the ASH and PHB neurons. Further, the chemotaxis experiments reveal that the GPCR SRX-97 senses high concentrations of benzaldehyde. Our data indicate that in comparison with wild-type (WT) animals, *srx-97* null mutant *C. elegans* show increased attraction towards higher concentrations of benzaldehyde (10-1). We also show that SRX-97::mCherry driven by its native promoter (P*srx-97*) shows localization towards the cilium tip of the ASH neuron. Since the cilia are the compartment where signal sensation and transduction occur, the localization of SRX-97 at the cilium tips suggests its

role in sensory perception or transduction of sensory signal/s. These results further suggest that SRX-97 expressed in the ASH neuron is responsible for detecting benzaldehyde from its surroundings.

Other than SRX-97, ASH neurons also express different sets of GPCRs, which sense benzaldehyde (Robertson, 2006; Gun Taniguchi et al., 2014; Vidal et al., 2018). For example, DCAR-1 is expressed in ASH neurons and is involved in sensing undiluted benzaldehyde(Aoki et al., 2011). Since the *srx-97* mutant animals show reduced and not completely abolished response towards high concentrations (10^{-1}) of benzaldehyde. It is possible that SRX-97 may act as a constituent of a receptor complex on the ASH neuron that may specifically detect benzaldehyde at high or undiluted concentrations but not at low concentrations. Low concentration of benzaldehyde, on the other hand, is sensed by the AWC neuron (Bargmann et al., 1993; Leinwand et al., 2015). The normal chemotaxis response of *srx-97* mutants towards undiluted and low concentration of benzaldehyde may suggest that animals sense their surroundings by activating different receptors and the corresponding neurons in a concentration-dependent manner and shows appropriate behavioral response.

The GPCRs signal through the heteromeric G proteins signaling cascades and transduce the signals from the environment through intracellular mediators, which play an essential role in triggering behavior. The cyclic nucleotide-gated channels (TAX-2 and TAX-4) detect volatile chemicals in AWC neurons and other amphid neurons (Coburn and Bargmann, 1996; Komatsu et al., 1996; Zagotta and Siegelbaum, 1996; Zhang et al., 2016), We found that the SRX-97 GPCR expression in ASH neuron is not responsible for activating these channels (**Figure 5.8**). The ASH and AWC neuron express the Gα protein ODR-3 which is involved in signal transduction through the sensation of osmotic strength, nose touch, and olfaction (Bargmann et al., 1993; Hilliard et al., 2004; Roayaie et al., 1998a; Troemel et al., 1997). The AWC neuron acts as a primary olfactory neuron involved in sensing the lower concentration of benzaldehyde (Leinwand et al., 2015), and mutation in *odr-3* showed defects in chemotaxis (Roayaie et al., 1998a). Likewise, OSM-9 is a TRPV protein expressed in ASH neurons, and mutation showed defect towards undiluted benzaldehyde (Colbert et al., 1997; Tobin et al., 2002; Troemel et al., 1995). In our 90 minutes quadrant plate chemotaxis assay, we found that both *odr-3, osm-*

9 mutants, and their double mutants with *srx-97* showed defect towards the higher concentration of benzaldehyde like their single mutants (**Figure 5.8**). In the assay, animals have placed 3cm away from the source, and previously *osm-9* mutant showed a defect in aversion when the animals are in short-range (few mm) towards the undiluted benzaldehyde (Troemel et al., 1995). We hypothesize that the distance between the sources or diffusion gradient of a test chemical may activate primary sensory neurons like AWC and AWB and mutation in the downstream signaling molecules allows worms to move away from the source

Our results suggest that there could be alternative pathways for signal transduction in ASH neurons through GPCRs like SRX-97. To our knowledge, not a single downstream signaling molecule has been identified, the loss of which shows attraction to the undiluted or high concentration of benzaldehyde through the ASH neuron in the chemotaxis assay. The *C. elegans* genome encodes for the 21 Gα, 2 Gβ, and 2 Gγ genes (Cuppen et al., 2003; Jansen et al., 1999). Out of these, 11 Gα proteins are known to express in ASH neurons (Bastiani, 2006). Our results hypothesize that the ASH neuron is involved in aversion to the undiluted or high concentration of benzaldehyde through multiple or redundant chemosensory pathways involved in the signaling through GPCRs like SRX-97.

In conclusion, our results suggest that SRX-97 is a key mediator in chemotaxis towards high concentrations of benzaldehyde in the chemosensory system of *C. elegans*. However, the downstream signaling components still need to be deciphered, which can help in providing a better overview of SRX-97 dependent pathways. Further, these investigations may offer insights into the nature of signal transduction in ASH neurons and their physiological role in concentration-dependent avoidance responses.

Summary and Future directions

In a collaborative project, we investigated the mechanistic understanding of the dynamin-like EHD1 in the scission of the REs membrane. Multiple reports have proposed that the molecule having the structural similarity with the dynamin are involved in pinching of the transport vesicles from REs (Naslavsky and Caplan, 2005). Various studies show that EHD1 localizes to the REs and its knockdown of EHD1 or RME-1 (EHD1 ortholog in *C. elegans*) causes delayed recycling of several important molecules on the plasma membrane (Grant and Caplan, 2008). Further, *in vitro* SMrTs data from our collaborators suggested the role of EHD1 in pinching of lipid membranes. In *C. elegans*, mutation in the *rme-1* gene causes an increased number of transport vesicles to the REs in the intestine of *C. elegans*, which manifests as large vacuoles in the intestinal cells (Grant et al., 2001). Similar to previous reports, we found that the expression of EHD1 rescues the increased number of vacuoles developed in *rme-1* mutants (George et al., 2007), (Section 3.2.2, Fig. 3.2) Further, using EHD1 variants lacking individual domains, we showed that the N-terminal domain, second helical domain as well as ATPase domain are important for endocytic recycling (Section 3.2.3, Fig. 3.3). In conjunction with SMrTs data from our collaborators, we propose that the N-terminal and second helical domain is important for stable scaffolding on the REs, while the ATPase domain is crucial for binding to the REs. Further, SMrTs data from our collaborators suggests that that EHD1 is necessary but not sufficient to carry out the scission on the REs membrane. Mainly it is involved in remodeling of membrane, and some other unknown protein, assists in the scission of transport vesicles from the endosomal recycling compartment (Deo et al., 2018). Thus data from study opens a new avenue to look at the different interacting partners of EHD1 for scission on the REs membrane (Grant and Caplan, 2008).

Various reports have proposed that the mutation in *ehd1/rme-1* causes delayed recycling of receptors in neurons (Jovic et al., 2010; Lasiecka et al., 2010; Park, 2004; Rongo, 2013). Further, multiple studies proposed that the neurons have a various endosomal systems to regulate the number of receptors available on the membrane (Yap and Winckler, 2012). In one such study, it was found that the RME-1 controls the GluR1/AMPA receptors recycling in hippocampal neurons (Park, 2004). To this end, we checked whether the RME-1 also regulates the GLR-1 receptor recycling in *C. elegans* interneurons, known to be involved in regulating the reversal behavior of the worms (Burbea et al., 2002; Juo and Kaplan, 2004; Piggott et al., 2011; Zheng et

al., 1999). We found the expression of *rme-1* from glutamate neuron-specific promoter rescues defective reversal behavior of *rme-1* mutant worms (Section 4.2.1, Fig. 4.1). Further, by using the GLR-1::GFP line, we found that the defective recycling was more profound in the distal region of the interneurons (Section 4.2.2, Fig. 4.2). Additionally, we found that there was no significant effect in the trafficking of the NMR-1 receptors, previously known to be involved in regulating reversal behavior in worms (Section 4.2.4, Fig. 4.8). Based on these data combined we show that RME-1 is involved in regulating recycling of GLR-1 receptors. Previously it was proposed that the proximal synapse is maintained by the other trafficking molecules (Kramer et al., 2010); based on our results, we proposed that the RME-1 plays an important role in maintaining the synapse at the distal-end of the neurons. However, the molecular details underlying these neuronal endosomal system is ill-defined (Goldenring, 2015; Yap and Winckler, 2012). By looking at live trafficking of RME-1 like molecules, as well as their localization in a spatiotemporal manner may help in assorting their functioning to proximal or distal endosomes. Further, pHluorin based study for various receptors in the glutamatergic neurons, will allow us to better understand the role of these molecules in trafficking of receptors in neurons.

The third chapter deals with finding expression and function of yet another uncharacterized GPCR, SRX-97. Further, we found that the SRX-97 is expressed in the chemosensory neurons (ASH and PHB). Subsequently, we explored its role in *C. elegans* chemosensory activity mediated by ASH polymodal neurons. We constructed *srx-97* deletion using the CRISPR/Cas9 system. We found that the *srx-97* mutants shows defect in the concentration-dependent chemosensation towards the higher concentration of benzaldehyde and this defect could be rescued by using the endogenous promoter, neuron-specific promoter ((P*osm-10*), further defect was also shown by doing ASH neuron ablation (Section 5.2.3, Fig. 5.7 and 5.8). These results confirm that the SRX-97 GPCR is involved in sensing the higher concentration of benzaldehyde. We tried to uncover the downstream signaling by looking at the previously reported G proteins and activated ion channels (Jansen et al., 2002; Leinwand et al., 2015; Nuttley et al., 2001; Roayaie et al., 1998b; Taniguchi et al., 2014; Yamada et al., 2009) but unable to find molecules works through this GPCR. Further studies are needed to identify the molecules involved in downstream signaling as well as the receptors which get activated in a benzaldehyde

concentration-dependent manner in various sets of neurons to convey their signaling to the downstream neural network and modulate the behavior of animals.

Appendix

Appendix Table 1. 1 List of movies used in this thesis

Sr No	Movie No.	Details
1	Movie 1	Showing reversal behavior of wild type worm
2	Movie 2	Showing reversal behavior of *rme-1*mutant worm
3	Movie 3	Showing reversal behavior of P*glr-1*:: RME-1 rescue worm
4	Movie 4	Showing reversal behavior of P*glr-1*:: RME-1D rescue worm
5	Movie 5	Showing reversal behavior of P*glr-1*:: RME-1A rescue worm
6	Movie 6	Showing reversal behavior of P*glr-1*:: RME-1F rescue worm
7	Movie 7	Showing reversal behavior of P*vha-6*:: RME-1 rescue worm
8	Movie 7	Showing reversal behavior of *glr-1* mutant worm
9	Movie9	Showing reversal behavior of *glr-1;rme-1* double mutant

Appendix Table 1. 2 Reagents used in this thesis

Lab	Reagent Strain / Plasmid	Citation
Thomas Pucadyil Lab	All EHD1 Variants plasmid	Deo et al., 2018
Andrew Maricq lab	pDM1983, pDM2071	Hoerndli et al., 2013
Peter Juo lab	*nuIs25*	Juo et al., 2007
Kaplan lab	*nuIs24*	Rongo et al., 1998

Bibliography

Adesnik H, Nicoll RA, England PM (2005) Photoinactivation of native AMPA receptors reveals their real-time trafficking. Neuron 48:977–985.

Antonny B et al. (2016) Membrane fission by dynamin: what we know and what we need to know. The EMBO Journal 35:2270–2284.

Aoki R, Yagami T, Sasakura H, Ogura K -i., Kajihara Y, Ibi M, Miyamae T, Nakamura F, Asakura T, Kanai Y, Misu Y, Iino Y, Ezcurra M, Schafer WR, Mori I, Goshima Y (2011) A Seven-Transmembrane Receptor That Mediates Avoidance Response to Dihydrocaffeic Acid, a Water-Soluble Repellent in *Caenorhabditis elegans*. Journal of Neuroscience 31:16603–16610.

Arribere JA, Bell RT, Fu BXH, Artiles KL, Hartman PS, Fire AZ (2014) Efficient Marker-Free Recovery of Custom Genetic Modifications with CRISPR/Cas9 in *Caenorhabditis elegans*. Genetics 198:837–846.

Ascaño M, Richmond A, Borden P, Kuruvilla R (2009) Axonal Targeting of Trk Receptors via Transcytosis Regulates Sensitivity to Neurotrophin Responses. J Neurosci 29:11674–11685.

Attwood TK, Findlay JB (1994) Fingerprinting G-protein-coupled receptors. Protein Eng 7:195–203.

Babu K, Hu Z, Chien S-C, Garriga G, Kaplan JM (2011) The Immunoglobulin super family protein RIG-3 prevents synaptic potentiation and regulates Wnt signaling. Neuron 71:103–116.

Bargmann C (2006) Chemosensation in *C. elegans*. WormBook.

Bargmann CI (1998) Neurobiology of the *Caenorhabditis elegans* Genome. Science 282:2028–2033.

Bargmann CI, Hartwieg E, Horvitz HR (1993) Odorant-selective genes and neurons mediate olfaction in *C. elegans*. Cell 74:515–527.

Bastiani C (2006) Heterotrimeric G proteins in *C. elegans*. WormBook.

Battu G, Hoier EF, Hajnal A (2003) The *C. elegans* G-protein-coupled receptor SRA-13 inhibits RAS/MAPK signalling during olfaction and vulval development. Development 130:2567–2577.

Bhattacharyya S, Rainey MA, Arya P, Dutta S, George M, Storck MD, McComb RD, Muirhead D, Todd GL, Gould K, Datta K, Waes JG, Band V, Band H (2016) Endocytic recycling protein EHD1 regulates primary cilia morphogenesis and SHH signaling during neural tube development. Scientific Reports 6.

Blume JJ, Halbach A, Behrendt D, Paulsson M, Plomann Markus (2007) EHD proteins are associated with tubular and vesicular compartments and interact with specific phospholipids. Experimental Cell Research 313:219–231.

Bredt DS, Nicoll RA (2003) AMPA receptor trafficking at excitatory synapses. Neuron 40:361–379.

Brenner S (1974) The genetics of *Caenorhabditis elegans*. Genetics 77:71–94.

Brockie PJ, Mellem JE, Hills T, Madsen DM, Maricq AV (2001) The *C. elegans* Glutamate Receptor Subunit NMR-1 Is Required for Slow NMDA-Activated Currents that Regulate Reversal Frequency during Locomotion. Neuron 31:617–630.

Brown TC, Tran IC, Backos DS, Esteban JA (2005) NMDA Receptor-Dependent Activation of the Small GTPase Rab5 Drives the Removal of Synaptic AMPA Receptors during Hippocampal LTD. Neuron 45:81–94.

Buggia-Prévot V, Fernandez CG, Udayar V, Vetrivel KS, Elie A, Roseman J, Sasse VA, Lefkow M, Meckler X, Bhattacharyya S, George M, Kar S, Bindokas VP, Parent AT, Rajendran L, Band H, Vassar R, Thinakaran G (2013) A Function for EHD Family Proteins in Unidirectional Retrograde Dendritic Transport of BACE1 and Alzheimer's Disease Aβ Production. Cell Reports 5:1552–1563.

Burbea M, Dreier L, Dittman JS, Grunwald ME, Kaplan JM (2002) Ubiquitin and AP180 Regulate the Abundance of GLR-1 Glutamate Receptors at Postsynaptic Elements in *C. elegans*. Neuron 35:107–120.

Cai B, Caplan S, Naslavsky N (2012) cPLA2α and EHD1 interact and regulate the vesiculation of cholesterol-rich, GPI-anchored, protein-containing endosomes. MBoC 23:1874–1888.

Cai B, Giridharan SSP, Zhang J, Saxena S, Bahl K, Schmidt JA, Sorgen PL, Guo W, Naslavsky N, Caplan S (2013) Differential Roles of C-terminal Eps15 Homology Domain Proteins as Vesiculators and Tubulators of Recycling Endosomes. J Biol Chem 288:30172–30180.

Campbell JC, Chin-Sang ID, Bendena WG (2015) Mechanosensation circuitry in *Caenorhabditis elegans*: A focus on gentle touch. Peptides 68:164–174.

Caplan S, Naslavsky N, Hartnell LM, Lodge R, Polishchuk RS, Donaldson JG, Bonifacino JS (2002) A tubular EHD1-containing compartment involved in the recycling of major histocompatibility complex class I molecules to the plasma membrane. The EMBO Journal 21:2557–2567.

Carr JF, Hinshaw JE (1997) Dynamin Assembles into Spirals under Physiological Salt Conditions upon the Addition of GDP and γ-Phosphate Analogues. J Biol Chem 272:28030–28035.

Chalfie M, Sulston JE, White JG, Southgate E, Thomson JN, Brenner S (1985) The neural circuit for touch sensitivity in *Caenorhabditis elegans*. J Neurosci 5:956–964.

Chao MY, Komatsu H, Fukuto HS, Dionne HM, Hart AC (2004) Feeding status and serotonin rapidly and reversibly modulate a *Caenorhabditis elegans* chemosensory circuit. Proc Natl Acad Sci USA 101:15512–15517.

Chappie JS, Acharya S, Leonard M, Schmid SL, Dyda F (2010) G domain dimerization controls dynamin's assembly-stimulated GTPase activity. Nature 465:435–440.

Coburn CM, Bargmann CI (1996) A putative cyclic nucleotide-gated channel is required for sensory development and function in *C. elegans*. Neuron 17:695–706.

Colbert HA, Smith TL, Bargmann CI (1997) OSM-9, A Novel Protein with Structural Similarity to Channels, Is Required for Olfaction, Mechanosensation, and Olfactory Adaptation in *Caenorhabditis elegans*. J Neurosci 17:8259–8269.

Croll NA (1975) Behavioural analysis of nematode movement. Adv Parasitol 13:71–122.

Cuppen E, van der Linden AM, Jansen G, Plasterk RHA (2003) Proteins Interacting With *Caenorhabditis elegans* Gα Subunits. Comp Funct Genomics 4:479–491.

Dahiya Y, Rose S, Thapliyal S, Bhardwaj S, Prasad M, Babu K (2019) Differential regulation of innate and learned behavior by creb1/crh-1 in *Caenorhabditis elegans*. J Neurosci 0006–0019.

Dar S, Kamerkar SC, Pucadyil TJ (2017) Use of the supported membrane tube assay system for real-time analysis of membrane fission reactions. Nature Protocols 12:390–400.

Daumke O, Lundmark R, Vallis Y, Martens S, Butler PJG, McMahon HT (2007) Architectural and mechanistic insights into an EHD ATPase involved in membrane remodelling. Nature 449:923–927.

Davis ES, Wille L, Chestnut BA, Sadler PL, Shakes DC, Golden A (2002) Multiple subunits of the *Caenorhabditis elegans* anaphase-promoting complex are required for chromosome segregation during meiosis I. Genetics 160:805–813.

Delevoye C, Miserey-Lenkei S, Montagnac G, Gilles-Marsens F, Paul-Gilloteaux P, Giordano F, Waharte F, Marks MS, Goud B, Raposo G (2014) Recycling endosome tubule morphogenesis from sorting endosomes requires the kinesin motor KIF13A. Cell Rep 6:445–454.

Deo R, Kushwah MS, Kamerkar SC, Kadam NY, Dar S, Babu K, Srivastava A, Pucadyil TJ (2018) ATP-dependent membrane remodeling links EHD1 functions to endocytic recycling. Nat Commun 9:5187.

Dhekne HS, Yanatori I, Gomez RC, Tonelli F, Diez F, Schüle B, Steger M, Alessi DR, Pfeffer SR (2018) A pathway for Parkinson's Disease LRRK2 kinase to block primary cilia and Sonic hedgehog signaling in the brain. eLife 7:e40202.

Dickinson DJ, Goldstein B (2016) CRISPR-Based Methods for *Caenorhabditis elegans* Genome Engineering. Genetics 202:885–901.

Dickinson DJ, Pani AM, Heppert JK, Higgins CD, Goldstein B (2015) Streamlined Genome Engineering with a Self-Excising Drug Selection Cassette. Genetics 200:1035–1049.

Doherty GJ, McMahon HT (2009) Mechanisms of endocytosis. Annu Rev Biochem 78:857–902.

Emmons SW (2015) The beginning of connectomics: a commentary on White et al. (1986) 'The structure of the nervous system of the nematode *Caenorhabditis elegans*.' Philosophical Transactions of the Royal Society B: Biological Sciences 370:20140309.

Fares H, Grant B (2002) Deciphering endocytosis in *Caenorhabditis elegans*. Traffic 3:11–19.

Fredriksson R, Lagerström MC, Lundin L-G, Schiöth HB (2003) The G-Protein-Coupled Receptors in the Human Genome Form Five Main Families. Phylogenetic Analysis, Paralogon Groups, and Fingerprints. Mol Pharmacol 63:1256–1272.

Furuta T, Tuck S, Kirchner J, Koch B, Auty R, Kitagawa R, Rose AM, Greenstein D (2000) EMB-30: An APC4 Homologue Required for Metaphase-to-Anaphase Transitions during Meiosis and Mitosis in *Caenorhabditis elegans*. Mol Biol Cell 11:1401–1419.

George M, Ying G, Rainey MA, Solomon A, Parikh PT, Gao Q, Band V, Band H (2007) Shared as well as distinct roles of EHD proteins revealed by biochemical and functional comparisons in mammalian cells and *C. elegans*. BMC Cell Biol 8:3.

Giridharan SSP, Cai B, Vitale N, Naslavsky N, Caplan S (2013) Cooperation of MICAL-L1, syndapin2, and phosphatidic acid in tubular recycling endosome biogenesis. Mol Biol Cell 24:1776–1790.

Glebov OO, Tigaret CM, Mellor JR, Henley JM (2015) Clathrin-Independent Trafficking of AMPA Receptors. J Neurosci 35:4830–4836.

Glodowski DR, Chen CC-H, Schaefer H, Grant BD, Rongo C (2007) RAB-10 regulates glutamate receptor recycling in a cholesterol-dependent endocytosis pathway. Molecular biology of the cell 18:4387–4396.

Goldenring JR (2015) Recycling endosomes. Curr Opin Cell Biol 35:117–122.

Grabbe C, Dikic I (2009) Functional Roles of Ubiquitin-Like Domain (ULD) and Ubiquitin-Binding Domain (UBD) Containing Proteins. Chem Rev 109:1481–1494.

Grant B, Zhang Y, Paupard M-C, Lin SX, Hall DH, Hirsh D (2001) Evidence that RME-1, a conserved *C. elegans* EH-domain protein, functions in endocytic recycling. Nature cell biology 3:573–579.

Grant BD, Caplan S (2008) Mechanisms of EHD/RME-1 protein function in endocytic transport. Traffic 9:2043–2052.

Grant BD, Donaldson JG (2009) Pathways and mechanisms of endocytic recycling. Nature Reviews Molecular Cell Biology 10:597–608.

Gray JM, Hill JJ, Bargmann CI (2005) A circuit for navigation in *Caenorhabditis elegans*. Proceedings of the National Academy of Sciences of the United States of America 102:3184–3191.

Green MR, Sambrook J (Eds.) (2012) Molecular cloning: a laboratory manual, 4. ed. Cold Spring Harbor, N.Y: Cold Spring Harbor Laboratory Press.

Greger IH, Esteban JA (2007) AMPA receptor biogenesis and trafficking. Curr Opin Neurobiol 17:289–297.

Hall DH, Russell RL (1991) The posterior nervous system of the nematode *Caenorhabditis elegans*: serial reconstruction of identified neurons and complete pattern of synaptic interactions. J Neurosci 11:1–22.

Hart AC, Kass J, Shapiro JE, Kaplan JM (1999) Distinct signaling pathways mediate touch and osmosensory responses in a polymodal sensory neuron. Journal of Neuroscience 19:1952–1958.

Hilliard MA, Apicella AJ, Kerr R, Suzuki H, Bazzicalupo P, Schafer WR (2005) In vivo imaging of *C. elegans* ASH neurons: cellular response and adaptation to chemical repellents. The EMBO Journal 24:63.

Hilliard MA, Bargmann CI, Bazzicalupo P (2002) *C. elegans* responds to chemical repellents by integrating sensory inputs from the head and the tail. Current Biology 12:730–734.

Hilliard MA, Bergamasco C, Arbucci S, Plasterk RH, Bazzicalupo P (2004) Worms taste bitter: ASH neurons, QUI-1, GPA-3 and ODR-3 mediate quinine avoidance in *Caenorhabditis elegans*. The EMBO journal 23:1101–1111.

Ho VM, Lee J-A, Martin KC (2011) The Cell Biology of Synaptic Plasticity. Science 334:623–628.

Hoerndli FJ, Maxfield DA, Brockie PJ, Mellem JE, Jensen E, Wang R, Madsen DM, Maricq AV (2013) Kinesin-1 regulates synaptic strength by mediating the delivery, removal, and redistribution of ampa receptors. Neuron 80:1421–1437.

Hsu PD, Scott DA, Weinstein JA, Ran FA, Konermann S, Agarwala V, Li Y, Fine EJ, Wu X, Shalem O, Cradick TJ, Marraffini LA, Bao G, Zhang F (2013) DNA targeting specificity of RNA-guided Cas9 nucleases. Nat Biotechnol 31:827–832.

Hu G-M, Mai T-L, Chen C-M (2017) Visualizing the GPCR Network: Classification and Evolution. Sci Rep 7.

Huotari J, Helenius A (2011) Endosome maturation. EMBO J 30:3481–3500.

IJzendoorn SCD van (2006) Recycling endosomes. Journal of Cell Science 119:1679–1681.

Ioannou MS, Marat AL (2012) The Role of EHD Proteins at the Neuronal Synapse. Sci Signal 5:jc1–jc1.

Itofusa R, Kamiguchi H (2011) Polarizing membrane dynamics and adhesion for growth cone navigation. Mol Cell Neurosci 48:332–338.

Jackson AC, Nicoll RA (2011) The expanding social network of ionotropic glutamate receptors: TARPs and other transmembrane auxiliary subunits. Neuron 70:178–199.

Jansen G, Thijssen KL, Werner P, Hazendonk E, Plasterk RH (1999) The complete family of genes encoding G proteins of *Caenorhabditis elegans*. Nature genetics 21:414.

Jansen G, Weinkove D, Plasterk RHA (2002) The G-protein γ subunit gpc-1 of the nematode *C.elegans* is involved in taste adaptation. EMBO J 21:986–994.

Jarsch IK, Daste F, Gallop JL (2016) Membrane curvature in cell biology: An integration of molecular mechanisms. J Cell Biol 214:375–387.

Jiang F, Doudna JA (2017) CRISPR–Cas9 Structures and Mechanisms. Annual Review of Biophysics 46:505–529.

Joset A, Dodd DA, Halegoua S, Schwab ME (2010) Pincher-generated Nogo-A endosomes mediate growth cone collapse and retrograde signaling. J Cell Biol 188:271–285.

Jovic M, Sharma M, Rahajeng J, Caplan S (2010) The early endosome: a busy sorting station for proteins at the crossroads. Histology and histopathology 25:99.

Jung N, Haucke V (2007) Clathrin-Mediated Endocytosis at Synapses. Traffic 8:1129–1136.

Juo P, Harbaugh T, Garriga G, Kaplan JM (2007) CDK-5 regulates the abundance of GLR-1 glutamate receptors in the ventral cord of *Caenorhabditis elegans*. Molecular biology of the cell 18:3883–3893.

Juo P, Kaplan JM (2004) The Anaphase-Promoting Complex Regulates the Abundance of GLR-1 Glutamate Receptors in the Ventral Nerve Cord of *C. elegans*. Current Biology 14:2057–2062.

Kaksonen M, Roux A (2018) Mechanisms of clathrin-mediated endocytosis. Nat Rev Mol Cell Biol 19:313–326.

Kaplan JM, Horvitz HR (1993) A Dual Mechanosensory and Chemosensory Neuron in *Caenorhabditis elegans*. Proceedings of the National Academy of Sciences of the United States of America 90:2227–2231.

Katritch V, Cherezov V, Stevens RC (2013) Structure-function of the G protein-coupled receptor superfamily. Annu Rev Pharmacol Toxicol 53:531–556.

Kennedy MB (2016) Synaptic Signaling in Learning and Memory. Cold Spring Harb Perspect Biol 8.

Kim K, Sato K, Shibuya M, Zeiger DM, Butcher RA, Ragains JR, Clardy J, Touhara K, Sengupta P (2009) Two Chemoreceptors Mediate Developmental Effects of Dauer Pheromone in *C. elegans*. Science 326:994–998.

Koles K, Messelaar EM, Feiger Z, Crystal JY, Frank CA, Rodal AA (2015) The EHD protein Past1 controls postsynaptic membrane elaboration and synaptic function. Molecular biology of the cell 26:3275–3288.

Komatsu H, Mori I, Rhee JS, Akaike N, Ohshima Y (1996) Mutations in a cyclic nucleotide-gated channel lead to abnormal thermosensation and chemosensation in *C. elegans*. Neuron 17:707–718.

Kramer LB, Shim J, Previtera ML, Isack NR, Lee M-C, Firestein BL, Rongo C (2010) UEV-1 Is an Ubiquitin-Conjugating Enzyme Variant That Regulates Glutamate Receptor Trafficking in *C. elegans* Neurons. PLOS ONE 5:e14291.

Krishnan A, Almén MS, Fredriksson R, Schiöth HB (2014) Insights into the Origin of Nematode Chemosensory GPCRs: Putative Orthologs of the Srw Family Are Found across Several Phyla of Protostomes. PLoS ONE 9:e93048.

Lasiecka ZM, Winckler B (2011) Mechanisms of polarized membrane trafficking in neurons — Focusing in on endosomes. Molecular and Cellular Neuroscience 48:278–287.

Lasiecka ZM, Yap CC, Caplan S, Winckler B (2010) Neuronal Early Endosomes Require EHD1 for L1/NgCAM Trafficking. Journal of Neuroscience 30:16485–16497.

Latek D, Modzelewska A, Trzaskowski B, Palczewski K, Filipek S (2012) G protein-coupled receptors — recent advances. Acta Biochim Pol 59:515–529.

Lee S, Uchida Y, Wang J, Matsudaira T, Nakagawa T, Kishimoto T, Mukai K, Inaba T, Kobayashi T, Molday RS, Taguchi T, Arai H (2015) Transport through recycling endosomes requires EHD1 recruitment by a phosphatidylserine translocase. The EMBO Journal 34:669–688.

Leinwand SG, Yang CJ, Bazopoulou D, Chronis N, Srinivasan J, Chalasani SH (2015) Circuit mechanisms encoding odors and driving aging-associated behavioral declines in *Caenorhabditis elegans.* eLife 4:e10181.

Lin SX, Grant B, Hirsh D, Maxfield FR (2001a) Rme-1 regulates the distribution and function of the endocytic recycling compartment in mammalian cells. Nature cell biology 3:567.

Lin SX, Grant B, Hirsh D, Maxfield FR (2001b) Rme-1 regulates the distribution and function of the endocytic recycling compartment in mammalian cells. Nat Cell Biol 3:567–572.

Maricq AV, Peckol E, Driscoll M, Bargmann CI (1995) Mechanosensory signalling in *C. elegans* mediated by the GLR-1 glutamate receptor. Nature 378:78–81.

Marsh EW, Leopold PL, Jones NL, Maxfield FR (1995) Oligomerized transferrin receptors are selectively retained by a lumenal sorting signal in a long-lived endocytic recycling compartment. J Cell Biol 129:1509–1522.

Maxfield FR, McGraw TE (2004) Endocytic recycling. Nat Rev Mol Cell Biol 5:121–132.

McGrath PT, Xu Y, Ailion M, Garrison JL, Butcher RA, Bargmann CI (2011) Parallel evolution of domesticated *Caenorhabditis* species targets pheromone receptor genes. Nature 477:321–325.

McMahon HT, Gallop JL (2005) Membrane curvature and mechanisms of dynamic cell membrane remodelling. Nature 438:590–596.

Mellem JE, Brockie PJ, Zheng Y, Madsen DM, Maricq AV (2002) Decoding of Polymodal Sensory Stimuli by Postsynaptic Glutamate Receptors in *C. elegans*. Neuron 36:933–944.

Mellman I (1996) Endocytosis and molecular sorting. Annu Rev Cell Dev Biol 12:575–625.

Mello C, Fire A (1995) DNA transformation. Methods Cell Biol 48:451–482.

Mello CC, Kramer JM, Stinchcomb D, Ambros V (1991) Efficient gene transfer in *C.elegans*: extrachromosomal maintenance and integration of transforming sequences. EMBO J 10:3959–3970.

Melo AA, Hegde BG, Shah C, Larsson E, Isas JM, Kunz S, Lundmark R, Langen R, Daumke O (2017) Structural insights into the activation mechanism of dynamin-like EHD ATPases. Proceedings of the National Academy of Sciences 201614075.

Miller KG, Alfonso A, Nguyen M, Crowell JA, Johnson CD, Rand JB (1996) A genetic selection for *Caenorhabditis elegans* synaptic transmission mutants. Proc Natl Acad Sci USA 93:12593–12598.

Monteiro MI, Ahlawat S, Kowalski JR, Malkin E, Koushika SP, Juo P (2012) The kinesin-3 family motor KLP-4 regulates anterograde trafficking of GLR-1 glutamate receptors in the ventral nerve cord of *Caenorhabditis elegans*. Mol Biol Cell 23:3647–3662.

Murayama T, Maruyama IN (2013) Decision making in *C. elegans* chemotaxis to alkaline pH: Competition between two sensory neurons, ASEL and ASH. Communicative & Integrative Biology 6:e26633.

Naslavsky N, Caplan S (2005a) C-terminal EH-domain-containing proteins: consensus for a role in endocytic trafficking, EH? Journal of Cell Science 118:4093–4101.

Naslavsky N, Caplan S (2005b) C-terminal EH-domain-containing proteins: consensus for a role in endocytic trafficking, EH? Journal of Cell Science 118:4093–4101.

Nonet ML, Saifee O, Zhao H, Rand JB, Wei L (1998) Synaptic Transmission Deficits in *Caenorhabditis elegans* Synaptobrevin Mutants. J Neurosci 18:70–80.

Nuttley WM, Harbinder S, van der Kooy D (2001) Regulation of Distinct Attractive and Aversive Mechanisms Mediating Benzaldehyde Chemotaxis in *Caenorhabditis elegans*. Learn Mem 8:170–181.

Pant S, Sharma M, Patel K, Caplan S, Carr CM, Grant BD (2009) AMPH-1/Amphiphysin/Bin1 functions with RME-1/Ehd1 in endocytic recycling. Nature Cell Biology 11:1399–1410.

Park D, O'Doherty I, Somvanshi RK, Bethke A, Schroeder FC, Kumar U, Riddle DL (2012) Interaction of structure-specific and promiscuous G-protein–coupled receptors mediates small-molecule signaling in *Caenorhabditis elegans*. PNAS 109:9917–9922.

Park EC, Glodowski DR, Rongo C (2009) The Ubiquitin Ligase RPM-1 and the p38 MAPK PMK-3 Regulate AMPA Receptor Trafficking. PLoS ONE 4:e4284.

Park M (2004) Recycling Endosomes Supply AMPA Receptors for LTP. Science 305:1972–1975.

Pawson T (2004) Specificity in Signal Transduction: From Phosphotyrosine-SH2 Domain Interactions to Complex Cellular Systems. Cell 116:191–203.

Piggott BJ, Liu J, Feng Z, Wescott SA, Xu XZS (2011) The Neural Circuits and Synaptic Mechanisms Underlying Motor Initiation in *C. elegans*. Cell 147:922–933.

Polo S, Confalonieri S, Salcini AE, Fiore PPD (2003) EH and UIM: Endocytosis and More. Sci STKE 2003:re17–re17.

Ramachandran R, Schmid SL (2008) Real-time detection reveals that effectors couple dynamin's GTP-dependent conformational changes to the membrane. The EMBO Journal 27:27–37.

Rankin CH, Beck CD, Chiba CM (1990) *Caenorhabditis elegans*: a new model system for the study of learning and memory. Behav Brain Res 37:89–92.

Rapaport D, Auerbach W, Naslavsky N, Pasmanik-Chor M, Galperin E, Fein A, Caplan S, Joyner AL, Horowitz M (2006) Recycling to the Plasma Membrane is Delayed in EHD1 Knockout Mice: Delayed Recycling in EHD1 Knockout Mice. Traffic 7:52–60.

Remy J-J, Hobert O (2005) An Interneuronal Chemoreceptor Required for Olfactory Imprinting in *C. elegans*. Science 309:787–790.

Roayaie K, Crump JG, Sagasti A, Bargmann CI (1998a) The Gα protein ODR-3 mediates olfactory and nociceptive function and controls cilium morphogenesis in *C. elegans* olfactory neurons. Neuron 20:55–67.

Roayaie K, Crump JG, Sagasti A, Bargmann CI (1998b) The Gα Protein ODR-3 Mediates Olfactory and Nociceptive Function and Controls Cilium Morphogenesis in *C. elegans* Olfactory Neurons. Neuron 20:55–67.

Robertson H (2006) The putative chemoreceptor families of *C. elegans*. WormBook.

Rongo C (2013) Going Mobile: AMPA Receptors Move Synapse to Synapse In Vivo. Neuron 80:1339–1341.

Rongo C, Kaplan JM (1999) CaMKII regulates the density of central glutamatergic synapses in vivo. Nature 402:195.

Rongo C, Whitfield CW, Rodal A, Kim SK, Kaplan JM (1998) LIN-10 is a shared component of the polarized protein localization pathways in neurons and epithelia. Cell 94:751–759.

Sambongi Y, Nagae T, Liu Y, Yoshimizu T, Takeda K, Wada Y, Futai M (1999) Sensing of cadmium and copper ions by externally exposed ADL, ASE, and ASH neurons elicits avoidance response in *Caenorhabditis elegans*. Neuroreport 10:753–757.

Sambrook J, Fritsch EF, Maniatis T (1989) Molecular cloning: a laboratory manual. Molecular cloning: a laboratory manual. Cold Spring Harbor, N.Y: Cold Spring Harbor Laboratory Press.

Sandvig K, Kavaliauskiene S, Skotland T (2018) Clathrin-independent endocytosis: an increasing degree of complexity. Histochem Cell Biol 150:107–118.

Sato T, Iwano T, Kunii M, Matsuda S, Mizuguchi R, Jung Y, Hagiwara H, Yoshihara Y, Yuzaki M, Harada R, Harada A (2014) Rab8a and Rab8b are essential for several apical transport pathways but insufficient for ciliogenesis. J Cell Sci 127:422–431.

Schackwitz WS, Inoue T, Thomas JH (1996) Chemosensory Neurons Function in Parallel to Mediate a Pheromone Response in *C. elegans*. Neuron 17:719–728.

Scholey J (2007) The sensory cilia of *Caenorhabditis elegans*_Revised. WormBook.

Sengupta P, Chou JH, Bargmann CI (1996) odr-10 encodes a seven transmembrane domain olfactory receptor required for responses to the odorant diacetyl. Cell 84:899–909.

Shah C, Hegde BG, Morén B, Behrmann E, Mielke T, Moenke G, Spahn CMT, Lundmark R, Daumke O, Langen R (2014) Structural Insights into Membrane Interaction and Caveolar Targeting of Dynamin-like EHD2. Structure 22:409–420.

Shao Y, Akmentin W, Toledo-Aral JJ, Rosenbaum J, Valdez G, Cabot JB, Hilbush BS, Halegoua S (2002) Pincher, a pinocytic chaperone for nerve growth factor/TrkA signaling endosomes. J Cell Biol 157:679–691.

Sharma M, Naslavsky N, Caplan S (2008) A Role for EHD4 in the Regulation of Early Endosomal Transport. Traffic 9:995–1018.

Sheng M, Sala C (2001) PDZ Domains and the Organization of Supramolecular Complexes. Annual Review of Neuroscience 24:1–29.

Shi A, Liu O, Koenig S, Banerjee R, Chen CC-H, Eimer S, Grant BD (2012) RAB-10-GTPase–mediated regulation of endosomal phosphatidylinositol-4,5-bisphosphate. Proc Natl Acad Sci U S A 109:E2306–E2315.

Shipman SL, Herring BE, Suh YH, Roche KW, Nicoll RA (2013) Distance-Dependent Scaling of AMPARs Is Cell-Autonomous and GluA2 Dependent. J Neurosci 33:13312–13319.

Stricker NL, Huganir RL (2003) The PDZ domains of mLin-10 regulate its trans-Golgi network targeting and the surface expression of AMPA receptors. Neuropharmacology, Post-translational modifications of protein structure and synaptic function 45:837–848.

Taniguchi Gun, Uozumi T, Kiriyama K, Kamizaki T, Hirotsu T (2014) Screening of Odor-Receptor Pairs in *Caenorhabditis elegans* Reveals Different Receptors for High and Low Odor Concentrations. Sci Signal 7:ra39–ra39.

Taniguchi G., Uozumi T, Kiriyama K, Kamizaki T, Hirotsu T (2014) Screening of Odor-Receptor Pairs in *Caenorhabditis elegans* Reveals Different Receptors for High and Low Odor Concentrations. Science Signaling 7:ra39–ra39.

Tobin DM, Madsen DM, Kahn-Kirby A, Peckol EL, Moulder G, Barstead R, Maricq AV, Bargmann CI (2002) Combinatorial expression of TRPV channel proteins defines their sensory functions and subcellular localization in *C. elegans* neurons. Neuron 35:307–318.

Traub LM (2009) Clathrin Couture: Fashioning Distinctive Membrane Coats at the Cell Surface. PLOS Biology 7:e1000192.

Troemel ER, Chou JH, Dwyer ND, Colbert HA, Bargmann CI (1995) Divergent seven transmembrane receptors are candidate chemosensory receptors in *C. elegans*. Cell 83:207–218.

Troemel ER, Kimmel BE, Bargmann CI (1997) Reprogramming chemotaxis responses: sensory neurons define olfactory preferences in *C. elegans*. Cell 91:161–169.

Troemel ER, Sagasti A, Bargmann CI (1999) Lateral signaling mediated by axon contact and calcium entry regulates asymmetric odorant receptor expression in *C. elegans*. Cell 99:387–398.

Tsushima H, Malabarba MG, Confalonieri S, Senic-Matuglia F, Verhoef LGGC, Bartocci C, D'Ario G, Cocito A, Di Fiore PP, Salcini AE (2013) A Snapshot of the Physical and Functional Wiring of the Eps15 Homology Domain Network in the Nematode. PLoS ONE 8:e56383.

Van Dyke RW (1996) Acidification of lysosomes and endosomes. Subcell Biochem 27:331–360.

Vidal B, Aghayeva U, Sun H, Wang C, Glenwinkel L, Bayer EA, Hobert O (2018) An atlas of *Caenorhabditis elegans* chemoreceptor expression. PLOS Biology 16:e2004218.

Wang Z, Edwards JG, Riley N, Provance DW, Karcher R, Li X, Davison IG, Ikebe M, Mercer JA, Kauer JA, Ehlers MD (2008) Myosin Vb Mobilizes Recycling Endosomes and AMPA Receptors for Postsynaptic Plasticity. Cell 135:535–548.

Ward JD (2015) Rapid and Precise Engineering of the *Caenorhabditis elegans* Genome with Lethal Mutation Co-Conversion and Inactivation of NHEJ Repair. Genetics 199:363–377.

White JG, Southgate E, Thomson JN, Brenner S (1986) The structure of the nervous system of the nematode *Caenorhabditis elegans.* Philosophical Transactions of the Royal Society of London B, Biological Sciences 314:1–340.

Wong PC, Pardo CA, Borchelt DR, Lee MK, Copeland NG, Jenkins NA, Sisodia SS, Cleveland DW, Price DL (1995) An adverse property of a familial ALS-linked SOD1 mutation causes motor neuron disease characterized by vacuolar degeneration of mitochondria. Neuron 14:1105–1116.

Wu Z, Makihara S, Yam PT, Teo S, Renier N, Balekoglu N, Moreno-Bravo JA, Olsen O, Chédotal A, Charron F, Tessier-Lavigne M (2019) Long-Range Guidance of Spinal Commissural Axons by Netrin1 and Sonic Hedgehog from Midline Floor Plate Cells. Neuron 101:635-647.e4.

Yamada K, Hirotsu T, Matsuki M, Kunitomo H, Iino Y (2009) GPC-1, a G Protein γ-Subunit, Regulates Olfactory Adaptation in *Caenorhabditis elegans*. Genetics 181:1347–1357.

Yap CC, Winckler B (2012) Harnessing the Power of the Endosome to Regulate Neural Development. Neuron 74:440–451.

Yap CCC, Lasiecka ZM, Caplan S, Winckler B (2010) Alterations of EHD1/EHD4 Protein Levels Interfere with L1/NgCAM Endocytosis in Neurons and Disrupt Axonal Targeting. Journal of Neuroscience 30:6646–6657.

Ying G, Rainey MA, Solomon A, Parikh PT, Gao Q, Band V, Band H (2007) Shared as well as distinct roles of EHD proteins revealed by biochemical and functional comparisons in mammalian cells and *C. elegans.* BMC cell biology 8:3.

Yoshida K, Hirotsu T, Tagawa T, Oda S, Wakabayashi T, Iino Y, Ishihara T (2012) Odour concentration-dependent olfactory preference change in *C. elegans*. Nat Commun 3:739.

Zagotta WN, Siegelbaum SA (1996) Structure and function of cyclic nucleotide-gated channels. Annu Rev Neurosci 19:235–263.

Zerial M, McBride H (2001) Rab proteins as membrane organizers. Nature reviews Molecular cell biology 2:107–117.

Zhang C, Zhao N, Chen Y, Zhang D, Yan J, Zou W, Zhang K, Huang X (2016) The Signaling Pathway of *Caenorhabditis elegans* Mediates Chemotaxis Response to the Attractant 2-Heptanone in a Trojan Horse-like Pathogenesis. J Biol Chem 291:23618–23627.

Zheng N, Jeyifous O, Munro C, Montgomery JM, Green WN (2015) Synaptic activity regulates AMPA receptor trafficking through different recycling pathways. eLife 4:e06878.

Zheng Y, Brockie PJ, Mellem JE, Madsen DM, Maricq AV (1999) Neuronal Control of Locomotion in *C. elegans* Is Modified by a Dominant Mutation in the GLR-1 Ionotropic Glutamate Receptor. Neuron 24:347–361.

Zou W, Cheng H, Li S, Yue X, Xue Y, Chen S, Kang L (2017) Polymodal Responses in *C. elegans* Phasmid Neurons Rely on Multiple Intracellular and Intercellular Signaling Pathways. Sci Rep 7.